UCLA
UCLA Electronic Theses and Dissertations

Title

Decreased Reelin Expression and Organophosphate Pesticide Exposure Alters Mouse Behavior and Brain Morphology

Permalink

https://escholarship.org/uc/item/8s20k06d

Author

Mullen, Brian Romney

Publication Date

2014

Peer reviewed|Thesis/dissertation

eScholarship.org Powered by the California Digital Library
University of California

UNIVERSTIY OF CALIFORNIA

Los Angeles

Decreased Reelin Expression and Organophosphate Pesticide Exposure Alters Mouse Behavior and Brain Morphology

A thesis in partial satisfaction

of the requirements for the degree Master of Science

in Physiological Science

by

Brian Romney Mullen

2014

© Copyright by

Brian Romney Mullen

2014

ABSTRACT OF THE THESIS

Decreased Reelin Expression and Organophosphate Pesticide Exposure Alters Mouse Behavior and Brain Morphology

by

Brian Romney Mullen

Masters of Science in Physiological Science

University of California, Los Angeles, 2014

Professor Patricia Emory Phelps, Co-Chair

Professor Ellen M. Carpenter, Co-Chair

Genetic and environmental factors are both likely to contribute to neurodevelopmental disorders, including autism spectrum disorders. In this study, we examined the combinatorial effect of two factors thought to be involved in autism – reduction in the expression of the extracellular matrix protein reelin and prenatal exposure to an organophosphate pesticide, chlorpyrifos oxon on mouse behavior and brain morphology. Mice with either reduced reelin expression or prenatal exposure to chlorpyrifos oxon exhibited subtle changes in ultrasound vocalization, open field behavior, social interaction, and repetitive behavior. Paradoxically, mice exposed to both variables often exhibited a mitigation of abnormal behaviors, rather than

increased behavioral abnormalities as expected. We also identified specific differences in males and females in response to both of these variables. In addition to behavioral abnormalities, we identified anatomical alterations in cell positioning and organization in the olfactory bulb, piriform cortex, hippocampus, and cerebellum in adolescent mice. As with our behavioral studies, anatomical alterations also appeared to be ameliorated in the presence of both variables. Examination of adult brains showed that there are no obvious changes in cell position in the cortex, hippocampus, and cerebellum, and no loss of cellular subtypes. However, there were specific effects on dendritic spines in both the cortex and hippocampus, suggesting alterations in synaptic connectivity. Western blot analysis shows that prenatal exposure to chlorpyrifos oxon transiently increases reelin protein expression in mouse embryos, but that by adulthood, reelin protein levels are decreased, providing a possible biochemical explanation for our findings. While these observations support an interaction between reelin expression and CPO exposure, our results suggest a complexity to this interaction beyond an additive effect of individual phenotypes.

The thesis of Brian Romney Mullen is approved.

Stephanie Ann White

Patricia Emory Phelps, Committee Co-Chair

Ellen M Carpenter, Committee Co-Chair

Table of Contents

Chapter 1: Introduction..... 1

Chapter 2: Decreased Reelin Expression and Organophosphate Pesticide Exposure Alters Mouse Behavior and Adolescent Brain Morphology

Introduction ……. 13

Materials and Methods 17

Results 22

Discussion 34

Tables and Figures 38

References 51

Chapter 3: Lasting Effects due to Decreased Reelin Expression and Prenatal Organophosphate Pesticide Exposure on Adult Brain Morphology

Introduction ……. 59

Materials and Methods 63

Results 68

Discussion 76

Tables and Figures 80

References 100

Chapter 4: Overall Discussion 108

List of Tables and Figures

Chapter 2

Table 2.1: Effects on litters derived from vehicle or CPO implanted dam …… 38

Figure 2.1: Timeline and mouse breeding scheme ……..……39

Figure 2.2: Embryonic biochemical effects …….…….. 41

Figure 2.3: Number and duration of ultrasonic vocalization ……..... 42

Figure 2.4: Open field behavior ……... 43

Figure 2.5: Social interaction behavior…….……..... 44

Figure 2.6: Marble burying behavior …….…….……..... 45

Figure 2.7: ß-galactosidase expression for Olfactory Bulb ……..……..... 46

Figure 2.8: ß-galactosidase expression for Piriform Cortex ……... 47

Figure 2.9: ß-galactosidase expression for Neocortex ……....48

Figure 2.10: ß-galactosidase expression for Hippocampus ……49

Figure 2.11: ß-galactosidase expression for Cerebellum ……50

Chapter 3

Figure 3.1: Repetitive behavior of wild type and reelin heterozygous mouse ……...80

Figure 3.2: Adult reelin western blot …….…….. 81

Figure 3.3: CPO effect on interneurons in adult Neocortex ……...……. 82

Figure 3.4: CPO effect on interneurons in adult Hippocampus ……..... 84

Figure 3.5: Pyramidal cell hippocampal cell distribution …….. 86

Figure 3.6: CA1 pyramidal cells complexity …….. 88

Figure 3.7: Dendritic spine characterization of CA1 Pyramidal Cells ...…… 89

Figure 3.8: Classification of hippcampal dendritic spines …… 90

Figure 3.9: Volumetric effects on adult Cerebellum …….. 92

Figure 3.10: Dendritic spine characterization of Purkinje cells ……..... 93

Figure 3.11: Classification of Purkinje cell spine ……94

Table 3.1: Summary table of dendritic spine analysis……96

Supplementary table 3.1: Statistics for hippocampus spine analysis ……97

Supplementary table 3.2: Statistics for cerebellum spine analysis …… 98

List of Acronyms

ACh, Acetylcholine

AChE, Acetylcholine Esterase

nAChR, Nicotinic Acetylcholine Receptors

ADHD, Attention Deficient/Hyperactivity Disorders

ApoER2, Apolipoprotein E Receptor 2

ASD, Autism Spectrum Disorders

CNS, Central Nervous System

CPO, Chlorpyrifos-oxon

DNMT, DNA methyl transferase

Dab1, Disabled 1

ECM, Extracellular Matrix

EPL, Extra plexiform layer

GAD67, Glutamic Acid Decarboxylase 67

GC, Granule cell alayer

Gl, Glomerular Layer

GrO, Granule cell layer

IPL, Internal plexiform layer

M, Mitral cell layer

ML, Molecular layer

MC, Motor Cortex

NMDA, N-methyl-d-aspartate

OP, Organophophate Pesticide

PCL, Purkinje cell layer

PON1, Paraoxonase 1

RELN/ Rl, Reelin

SS, Somatosensory cortex

SZ, Schizophrenia

UTR, Untranslated Region

VLDLR, Very-Low Density lipoprotein receptor

Acknowledgements

First and foremost I would like to thank Ellen Carpenter for her continual assistance and guidance. A wonderful mentor and a role model that I admire greatly. I would like to thank the continual support and assistance from both the Carpenter and Phelps' labs; specifically Elvira Khialeeva, Andrew Vosko, and Rana Khankan for their help and availability to trouble shoot experiments. I would like to thank the many undergraduates that I worked closely with to build this dataset: Casssandra Gonzalez, Kimberly Bui, Andrew Chiu, Alec Chiu, Joan Chou, Brennan Ross, Daniel Hoffman, Daewoong Kim, and Kiona Coleman.

I thank the Intellectual Developmental and Disabilities Research Center (IDDRC) for the use of core microscopes and computers to accomplish this work. I thank Donna Crandall for assistance with figure preparation and Dorwin Birt for the training and technical support.

I thank the UCLA behavioral testing core facility, specifically Ravikumar Ponnusamy, for help with behavioral testing.

Funding for these studies was provided by grants from Autism Speaks! and pilot project funding from NICHD P50-HD055784 to EMC.

Chapter 1

Introduction

Many researchers believe that neuropsychological disorders have both genetic and environmental components that influence onset, duration and intensity of pathology. However, increasing evidence shows how environmental insults during critical times of development can have drastic long-term effects on the nervous system (Marco et al., 2011). This gene-environment interaction is the prevailing theory behind the etiology of many neuropsychiatric disorders.

One such genetic component, *reelin (RELN),* has been implicated in several developmental disorders. Patients with schizophrenia (SZ), autism spectrum disorders (ASD), bipolar disorder, and major depressive disorders have decreased transcription of reelin (Impagnatiello et al., 1998; Fatemi et al., 2000; Fatemi et al., 2002; Guidotti et al., 2000; Fatemi, et al., 2005). In addition to the decreases in expression levels, two other points of evidence show a genetic connection with these disorders. First, the 7q22 genetic locus where *RELN* is located has been associated with both ASD and SZ in a variety of genetic linkage studies (Bacchelli & Maestrini, 2006; Allen & Walsh, 1999; Rice & Curran, 2001; D'Arcangelo et al., 2006; Wedenoja et al., 2008; Ekelund et al., 2000). Second, direct screening for mutations in *RELN* shows an increased risk of developing a disorder. Two separate families show single nucleotide muation within *RELN* disposes females to a higher risk of SZ (Shifman et al., 2008; Kuang et al., 2014). Studies have found evidence that some ASD patient families were associated with long variants of GGC or CGG repeats in the 5' UTR; however, other studies did not find these repeats (Serajee et al., 2006; Li et al., 2004; Devin et al., 2004; Dutta et al., 2007).

Reelin is a secreted extracellular matrix (ECM) protein fundamental for the normal development of cortical layering (Ogawa et al., 1995; D'Arcangelo et al., 1999). During development, reelin causes phosphorylation of the downstream cytosolic adaptor protein

disabled 1 (dab1) by binding to its receptors Apolipoprotein E Receptor 2 (ApoER2), Very-low-density-lipoprotein Receptor (VLDLR). Through these pathways, it stabilizes cytoskeletal infrastructure and inhibits neuronal migration (Hiesberger et al., 1999; D'Arcangelo et al.,1999). In addition to its important role in development, reelin expression persists through adulthood and is secreted by granule cells in the cerebellum and by glutamic acid decarboxylase 67 (GAD67)-positive interneurons in olfactory bulb, cortex, and hippocampus (Ramos-Moreno et al., 2006; Pesold et al., 1998). In adulthood, reelin is maintained in areas of high synaptic plasticity, leading to the theory that reelin may modulate synaptic connectivity. Reelin plays an important role in dendritic spine morphology by assisting in stabilizing spines and in synaptic transmission by modulating NMDA receptor trafficking (Weeber et al., 2002; Niu et al., 2008; Chen et al., 2005). Studies have shown that the infusion of reelin into the lateral ventricles in adult tissue improves cognition, plasticity and hippocampal spine formation, whereas the blocking of reelin signaling in the lateral entorhinal cortex inhibits spatial memory (Rogers et al., 2011; Stranahan et al., 2011). Interestingly, mutations in RELN have been associated with decreases in working memory amongst patients with SZ (Wedenoja et al., 2008).

Given the heritability of neuropsychiatric disorders, there is strong evidence for genetic involvement. However, in monozygotic twin studies, few disorders have complete penetrance of behavioral phenotypes. In twin studies, the concordance rates within SZ and ASD patients are around 50% and 60%, respectively (Tsuang, 2000; Hallmayer et al., 2011). Since complete penetrance of behavioral phenotypes seen in developmental disorders is not reported within genetically identical twins, other components such as environmental and epigenetic factors must play a role within the onset and prevalence of the disorders. There is strong evidence that maternal infection during pregnancy may influence both SZ and ASD pathology within the fetus (Patterson, 2011; Atladóttir et al., 2010; Brown et al., 2011). Heavy metal toxins have been implicated in ASD progression (DeSoto and Hitlan, 2010). Antiepileptic drugs that are taken while the mother is pregnant are also correlated with higher rates of ASD and ADHD (Cohen et

al., 2013; Christensen et al., 2013). Organophosphate pesticides (OP) are currently being investigated in their role with ASD pathology (Shelton et al., 2012). One commonly used OP throughout agricultural communities within the United States is Chlorpyrifos-Oxon (CPO) and one study showed a positive correlation to higher numbers of ASD patients among those that work with OP within California agricultural communities (Roberts et al., 2007).

OP exposure at specific time points and under certain conditions influences susceptibility for developmental disorders. Many OPs are serine protease inhibitors that function by blocking activity of acetylcholine esterase (AChE), potentially changing the regulation of cholinergic systems. Typically, OPs are hydrolyzed by paraoxonase 1 (PON1), an enzyme whose role is to detoxify organophosphorous compounds. Thus, low levels of OP may be cleared rapidly and exposure has little effect on normal adults (Costa et al., 2005). However, mutations or changes in PON1 activity may affect the rate of OP clearance and influence progression of the disorders. Some studies have shown that ASD patients have a reduced amount of PON1 activity and may be more susceptible to OP exposure (Paşca et al., 2008). Even if there is no genetic mutation or change in activity, humans are susceptible to OP exposure during perinatal periods. Human neonates have been shown to have 4-5 times lower levels of PON1 than adults (Cole et al., 2003). Although little is known about human fetal PON1 levels, fetal mice show around 14 times lower levels of PON1 activity than their dams (Cole et al., 2014).

OPs have been seen to interact with reelin signaling cascades as seen through the paradoxical restoration of neural and drug induced behaviors within mice deficient in reelin protein (Laviola et al., 2006). This amelioration of behavior shows a potential interaction between organophosphates and the reelin signaling cascade giving rise to two theoretical mechanisms of interactions. This interaction can only be present when PON1 activity levels are reduced, such as with a mutation or during early stages of development. The first theoretical mechanism is that reelin has serine protease capabilities and that OPs can directly affect reelin biochemistry. One lab showed that reelin was able to cleave through ECM proteins, such as

laminin, and had a structure similar to serine protease. This result led them to hypothesize that reelin's serine protease activity may play a role within cortical development through assisting cellular movement through the ECM (Quattrocchi et al., 2002). However, more recent publications have biochemically altered the hypothesized proteolytic site within the reelin protein and showed that reelin does not have serine protease capabilities (Kohno and Hattori, 2010). Thus, this theory does not have much traction within the field.

The second hypothesis is that high levels of organophosphates may influence central cholinergic systems, thus resulting in epigenetic changes that influence gene expression, such as *reelin*. It has been shown that inefficient PON1 activity and high levels of OP lead to drastic changes in central cholinergic pathways (Shelton et al., 2012). OPs block AChE activity leading to a potentiation of acetylcholine (ACh), which results in abnormal cell division and differentiation, and possibly cell death through neurotoxicity (Slotkin, 2004). These high levels of OP may effect nicotinic acetylcholine receptor (nAChR) distribution, ultimately leading to epigenetic and molecular changes within the system. Activation of nAChR by nicotine increases methylation of promoter regions by DNA methyltransferase (DNMT) in GAD67-positive cells, causing a down regulation of GAD67 and Reelin (Grayson and Guidotti, 2013). This is more problematic when long CpG nucleotide repeats exist in the promoter region. Based on this evidence, Perisco and Bourgeron (2006) proposed an environment x gene x gene interaction where CPO exposure to a *reelin* mutation with a "long" GGC repeat in animals deficient in PON1 could potentially be a animal model for ASD. Adding to this hypothesis, recent studies have shown that nicotine administration to male heterozygous reelin mice restores reelin and GAD67 protein levels to those seen in wild type animals (Romano et al., 2013). This suggests that nAChR activation modulates genetic expression of reelin and GAD67. The cholinergic toxicity during critical times of neural development could influence the way that the circuits are modulated and regulate protein synthesis, affecting reelin expression levels.

Based upon the points of evidence stated above, Keller and Perisco (2003) hypothesized that *reelin* deficiency in combination with prenatal organophosphate exposure during critical time of development within males could be a pathogenic model for ASD. In this study, we investigate behavior and anatomical changes due to the individual reduction of reelin or prenatal CPO exposure, and to the combinatorial effect of both factors. The first goal of this study is to determine if ASD-like behaviors are exhibited within the mouse model and what factor(s) influence these behaviors. The second goal is to determine how each factor affects morphological changes within adolescent cortical and cerebellar lamination and adult cellular organization, specifically dendritic spine structure. The final goal is to help elucidate the biochemical changes that may influence reelin expression. The benefits of this study would provide a better understanding of the role that each factor has within ASD pathology and potentially to help identify molecular targets for therapies that may alleviate behavioral symptoms seen in ASD patients.

References

Allen, K., & Walsh, C. (1999). Genes that regulate neuronal migration in the cerebral cortex. Epilep. Res. 36: 143-154.

Atladóttir, H. O., Thorsen, P., Østergaard, L., Schendel, D. E., Lemcke, S., Abdallah, M., Parner, E. T. (2010). Maternal infection requiring hospitalization during pregnancy and Autism Spectrum Disorders. J Autism Dev Disord 40:1423–1430

Bacchelli, E., & Maestrini, E. (2006). Autism spectrum disorders: molecular genetic advances. Am. J. Med. Genet. C Semin. Med. Genet., 142: 13-23.

Brown, A. S., Oatterson, P. H. (2011). Maternal infection and schizophrenia: Implications for prevention. Schizophr Bull 37: 284-290.

Chen, Y., Beffert, U., Ertunc, M., Tang, T. S., Kavalali, E. T., Bezprozvanny, I., Herz, J. (2005). Reelin modulates NMDA recetpor activity in cortical neurons. J. Neurosci. 25:8209-8217

Christensen, J., Grønborg, T. K., Sørensen, M. J., Schendel, D., Parner, E. T., Pedersen, L. H., Vestergaard, M. (2013). Prenatal valproate exposure and risk of Autism Spectrum Diorders and childhood Autism. JAMA 309:1696-1703

Cohen, M. J., Meador, K. J., Browning, N., May, R., Baker, G. A., Clayton-Smith, J., Kalayjian, L. A., Kanner, A., Liporace, J. D., Pennel, P. B., Priviteral, M., Loring, D. W. (2013). Fetal antiepilieptic drug exposure: Adaptive and emotional/behavioral functioning at age 6 years. Epilepsy & Behavior 29:308-315

Cole, T. B., Jampsa, R. L., Walter, B. J., Arndt, T. L., Richter, R. J., Shih, D. M., Tward, A., Lusis, A. J., Jack, R. M., Costa, L. G., Furlong, E. (2003) Expression of human paraoxonase (PON1) during development. Pharmacogenetics 13: 357-364

Cole, T. B., Li, W., Co, A. L., Hay, A. M., MacDonald, J. W., Bammler, T. K., Farin, F. M., Costa, L. G., Furlong, C. E. (2014). Repeated gestational exposure of mice to chlorpyrifos oxon is associated with paraoxonase 1 (PON1) modulated effects in maternal and fetal tissues. Toxicol. Sci. doi:10.1093/toxsci/kfu144

Costa, L. G., Vitalone, A., Cole, T. B., Furlong, C. E. (2005) Modulation of paraoxonase (PON1) activity. Biochem. Pharmacology 69:541-550

D'Arcangelo, G. (2006). Reelin mouse mutants as model of cortical development disorders. Epilep. Behav., 8: 81-90.

D'Arcangelo, G., Homayouni, R., Keshvara, L., Rics, D., Sheldon, M., Curran, T. (1999). Reelin is a ligand for lipoprotein receptors. Neuron 24: 471-479.

DeSoto, M. C. and Hitlan, R. T. (2010) Sorting out the spinning of autism: heavy metals and the question of incidence. Acta Neurobiol Exp 70: 165-176

Devin, B., Bennet, P., Dawson, G., Figlewicz, D., Grigorenko, E., McMahon, W., Minshew, N., Pauls, D., Smith, M., Spence, M. A., Rodier, P. M., Stodgell, C., Schellenberg, G. D. (2004). Alleles of a reelin CGG repear do not convey liability to autism in a sample from the CPEA network. Am. J. Med. Genet. B Neuropsychiatr. Genet 126: 46-50.

Dutta, S., Guhathakurta, S., Sinha, S., Chatterjee, A., Ahmed, S., Ghosh, S., Gangopadhyay, P. K., Singh, M., Usha, R. (2007). Reelin gene polymorphisms in the Indian population: a possible paternal 5'UTR-CGG-repeat-allele effect on autism. Am J. Med Genet. B. Neuropsychiatr. Genet, 144: 106-112.

Ekelund, J., Lichtermann, D., Hovatta, I., Ellonen, P., Suvisaari, J., Terwilliger, J. D., Juivonen, H., Varilo, T., Arajärvi, R., Kokko-Sahin, M., Lönnqvist, J., Peltonen, L. (2000) Genome-

wide scan for schizophrenia in the Finnish population: Evidence for a locus on chromosome 7q22. Human Mol. Genetics 9:1049-1057

Fatemi, S. H., Earle, J. A., McMenomy T (2000) Reduction in reelin immunoreactivity in hippocampus of subjects with schizophrenia, bipolar disorder and major depression. Molecular Psychiatry 5: 654-663

Fatemi, S. H., Snow, A .V., Stary, J. M., Araghi-Niknam, M., Reutiman, T. J., Lee, S., Brooks, A. I., and Pearce, D. A. (2005). Reelin signaling is impaired in autism. Biol. Psychiat. 57:777-787.

Fatemi, S. H., Stary, J. M., and Egan, E. A. (2002). Reduced blood levels of reelin as a vulnerability factor in pathophysiology of autistic disorder. Cell. Mol. Neurobiol. 22:139-152.

Grayson, D. R. and Guidotti, A. (2013) The dynamics of DNA methylation in Schizophrenia and related psychiatric disorders. Neuropsychopharmacology 38:138-166

Guidotti, A., Auta, J., Davis, J., Gerevini, V., Dwivedi, Y., Grayson, D., Impagnatiello, F., Pandey, G., Pesold, C., Sharma, R., Uzunov, D., Costa, E. (2000). Decrease in reelin and glutamic acid decarboxylase67 (GAD67) expression in schizophrenia and bipolar disorder. JAMA Psych , 57: 1061-9.

Hallmayer, J., Cleveland, S., Torres, A., Phillips, J., Cohen, B., Torigoe, T., Miller, J., Fedele, A., Collins, J., Smith, K., Lotspeich, L., Croen, L. A., Ozonoff, S., Lajonchere, C., Grether, J. K., Risch, N. (2011) Genetic heritability and shared environmental factors among twin pairs with Autism. JAMA Psych. 68:1095-1102

Hiesberger, T., Trommsdorff, M., Howell, B., Goffinet, A., Mumby, M., Cooper, J., Herz, J. (1999). Direct binding of Reelin to VLDL receptor and ApoE receptor 2 induces tyrosine phosphorylation of disabled-1 and modulates tau phosphorylation. Neuron , 24: 481-489.

Impagnatiello, F., Guidotti, A. R., Pescold, C., Dwivedi, Y., Caruncho, H., Pisu, M. G., Uzunov, D. P., Smalheier, N. R., Davis, J. M., Pandey, G. N., Pappas, G. D., Tueting, P., Sharma, R. P., Costa, E. (1998) A decrease of reelin expression as a putative vulnerability factor in schizophrenia. Proc. Natl. Acad. Sci. USA 95:15718-15723

Kuang, W. J., Sun, R. F., Zhu, Y. S. Li, S. B. (2013). A new single-nucleotide mutation (rs363719) of the reelin (RELN) gene associated with schizophrenia in female Chinese Han. Genet. Mol. Res. 10:1650-1658

Keller, F., and Persico, A. M. (2003). The neurobiological context of autism. Mol. Neurobiol. 28:1-22.

Kohno, T., Hattori, M. (2010) Re-evaluation of Protease Activity of Reelin. Biol. Pharm. Bull. 33:1047-1049

Laviola, G., Adriani, W., Gaudino, C., Marino, R., and Keller, F. (2006). Paradoxical effects of prenatal acetylcholinesterase blockade on neuro-behavioral development and drug-induced sterotypies in reeler mutant mice. Psychopharmacology 187:331-344.

Li, J., Nguyen, L., Gleason, C., Lotspeich, L., Spiker, D., Risch, N., Myers, R. M. (2004). Lack of evidence for an association between WNT2 and RELN polymorphisms and autism. Am. J. Med. Genet. B Neuropsychiatr. Genet, 126:51-57.

Marco, E. M., Macri, S., Laviola, G. (2011) Critical age windows for neurodevelopmental psychiatric disorders: Evidence from animal models. Neurotox. Res. 19:286-307

Niu, S., Yabut, O., D'Arcangelo, G. (2008) The reelin signaling pathway promotes dendritic spine development in hippocampal neurons. J. Neurosci. 28:10339-10348

Ogawa, M., Miyata, T., Nakajima, K., Yoguy, K., Seiko, M., Ikenaka, K., Yamamoto, H., Mikoshiba, K. (1995). The reeler gene-associated antigen on Cajal-Retius neurons is a crucial molecule for laminar organization of cortical neurons. Neuron, 14:890-912.

Paşca, S. P., Dronca, E., Nemeş, B., Kaucsár, T., Endreffy, E., Iftene, F., Benga, I., Cornean, R., Dronca, M. (2008) Paraoxonase 1 activies and polymorphisms in autism spectrum disorders. J. Cell. Mol. Med. 14:600-607

Patterson, P. H. (2011) Maternal Infections and immune involvement in autism. Trends in Mol. Medicine 17: 389-394

Persico, A. M., and Bourgeron, T. (2006). Searching for ways out of the autism maze: genetic, epigenetic, and environmental clues. Trends Neurosci. 29: 349-358

Pesold, C., Impagnatiello, F., Pisu, M., Uzunov, D., Costa, E., Guidotti, A., Caruncho, H. J. (1998). Reelin is preferentially expressed in neurons synthesizing γ-aminobutyric acid in cortex and hippocampus of adult rats. PNAS , 95 :3221-3226.

Quattrocchi, C. C., Wannenes, F., Persico, A . M., Ciafré, S. A., D'Arcangelo, G., Farace, M. G., and Keller, F. (2002) Reelin is a serine protease of the extracellular matrix. J. Biol. Chem. 277:303–309.

Ramos-Moreno, T., Galazo, M., Porrero, C., Martínez-Cerdeño, V., Clascá, F. (2006). Extracellular matrix molecules and synaptic plasticity: immunomapping of intracellular and secreted Reelin in the adult rat brain. European J of Neurosci , 23:401-22.

Rice, D., Curran, T. (2001). Role of reelin signaling pathway in central nervous system development. Annu. Rev. Neurosci., 24:1005-1039.

Rogers, J. T., Rusiana, I., Trotter, J., Zhao, L., Donaldson, E., Pak, D. T. S., Babus, L. W., Peters, M., Banko, J. L., Chavis, P., Rebeck, G. W., Hoe, H., Weeber, E. J. (2011) Reelin supplementation enhances cognitive ability, synaptic plasticity, and dendritic spine densities. Learn. Mem. 15:558-564

Roberts, E. M., English, P. B., Grether, J. K., Windham, G. C., Somberg, L., & Wolff, C. (2007). Maternal residence near agricultural pesticide applications and autism spectrum disorders among children in the California Central Valley. Environmental health perspectives, 115:1482–1489. doi:10.1289/ehp.10168

Romano, E., Fuso, A., & Laviola, G. (2013). Nicotine restores Wt-like levels of reelin and GAD67 gene expression in brain of heterozygous reeler mice. Neurotox Res , 24:205-215.

Serajee, F., Zhong, H., & Mahbubul Huq, A. (2006). Association of reelin gene polymorphisms with autism. Genomics, 87:75-83.

Shelton, J. F.; Hertz-Picciotto, I., Pessah, I. N. (2012). Tipping the balance of Autism risk: Potential mechanisms linking pesticides and autism. Environ Health Perspective 120: 994-951

Shifman, S., Johannesson, M., Bronstein, M., Chen, S. X., Collier, D. A., Craddock, N. J., Kendler, K. S., Li, T., O'Donovan, M., O'Neill, F. A., Owen, M. J., Walsh, D., Weinberger, D. R., Sun, C., Flint, J., Darvasi, A. (2008) Genome-wide association indentifies a common varinant in the reelin gene that increases the risk of schizophrenia only in women. PLOS Genetics 4:e28-e28 DOI: 10.1371/journal.pgen.0040028

Slotkin, T. (2004). Cholinergic systems in brain development and disruption by neurotoxicants: nicotine, environmental tobacco smoke, organophosphates. Tox. and Applied Pharm.198:132-151

Stranahan, A. M., Salas-Vega, S., Jiam, N. T., Gallagher, M. (2011) Interference with reelin signaling in the lateral entorhinal cortex impairs spatial memory. Neurobio. of Learning and Memory 96:150-155

Tsuang, M. (2000) Schizophrenia: genes and enviroment. Biol. Psychiatry 47:210-220

Wedenoja, J., Loukola, A., Tuulio-Henriksson, A., Paunio, T., Ekelund, J., Silander, K., Varilo, T., Heikkilä, K., Suvisaari, J., Paronen, T., Lönnqvist, J., Peltonen, L. (2008) Replication of linkage on chromosome 7q22 and association of the regional Reelin gene with working memory in schizophrenia families. Mol. Psychiatry 13:673-684

Weeber, E. J., Beffert, U., Jones, C., Christian, J. M., Förster, E., Sweatt, J. D., Herz, J. (2002) Reelin and ApoE receptor cooperate to enhance hippocampal synaptic platicity and learning. J. Bio. Chem. 277:39944-39952

Chapter 2

Decreased Reelin Expression and Organophosphate Pesticide Exposure Alters Mouse Behavior and Adolescent Brain Morphology

Introduction

The heritability of neurodevelopmental disorders including autism spectrum disorders (ASDs) suggests a strong genetic component to these diseases and a number of contributing genes have been identified (Persico and Bourgeron, 2006; Abrahams and Geschwind, 2008). However, a variety of environmental factors may also predispose genetically vulnerable individuals to develop ASDs and other neurodevelopmental disorders (Herbert, 2010). From the first report of maternal infection contributing to schizophrenia (Murray et al., 1992), environmental perturbations including infection and immune dysfunction, altered levels of neurotransmitters, neuropeptides and growth factors, hormonal alterations, obstetric complications, and exposure to exogenous agents including medications and illicit drugs, metals, and environmental pollutants have been suggested as predisposing factors in neurodevelopmental disorders including schizophrenia, autism, and attention deficit hyperactivity disorder (reviewed in Newschaffer et al., 2007). Changes in exposure to these environmental factors may also contribute to the increased prevalence of these disorders (Herbert, 2010).

In this study, we have examined the behavioral and anatomic effects of combining genetic and environmental factors thought to be potential candidates for involvement in ASDs. Specifically, we have examined the interactions between the *reelin* gene and prenatal exposure to an organophosphate pesticide, an environmental risk factor (Persico and Bourgeron, 2006). Several lines of evidence implicate *reelin* as a candidate gene for ASDs. First, on average, patients with autism have significantly decreased serum levels of reelin protein (Persico et al., 2001; Fatemi et al., 2002). Additional studies demonstrate decreases in reelin protein and mRNA levels in frontal and cerebellar areas of autistic brains as well as alterations in mRNA

expression of VLDLR and Dab1, downstream mediators of reelin signaling (Fatemi et al., 2005). Second, *reelin* is located on chromosome 7q22 and this locus has been associated with autism spectrum disorders in a variety of linkage studies (Abrahams and Geschwind, 2008; Bacchelli and Maestrini, 2006). Third, there are distinct similarities between neuroanatomical alterations observed in *reeler* mutant mice, which carry a naturally occurring deletion mutation in the *reelin* gene (D'Arcangelo et al., 1995), and in some autistic patients (Persico and Bourgeron, 2006). The heterogeneity of autism precludes establishing a concrete set of neuroanatomical phenotypes, but autistic patients show pathological changes including increased cell density, neuronal disorganization and poor lamination in the cerebral cortex, decreased Purkinjie cell number in the cerebellum, increased cell density and reduced neuronal size in the entorhinal cortex, hippocampus, and amygdala and decreased dendritic branching in the hippocampus (Bailey et al., 1998; Pappas et al., 2001; Bauman and Kemper, 2005). Neuroanatomical alterations in *reeler* mutant mice are more pervasive and extreme than those seen in autistic patients but have a number of similarities including lamination defects and neuronal disorganization in the cortex, decreased and disorganized Purkinje cells, cytoarchitectonic disturbances in the hippocampus, and reduced dendritic branching (Rice and Curran, 2001; Niu et al., 2008).

Several lines of evidence suggest pesticide exposure as a contributing environmental factor in neurodevelopmental disorders. A retrospective case-control study in humans suggested a link between increased exposure to organochlorine pesticides and ASDs (Roberts et al., 2007) and organophosphate exposure, as measured by the presence of urinary metabolites, may contribute to ADHD prevalence (Bouchard et al., 2010). Mutations that reduce or inactivate PON1, which encodes an organophosphate inactivator, show significant association with autism in Caucasian-North American families, but not in Italian families (D'Amelio et al., 2005). There is less organophosphate usage in European households compared with North American households, suggesting region-specific gene-environment

interactions. Finally, organophosphate exposure specifically affects the behavior exhibited by *reeler* mutant mice (Laviola et al., 2006), suggesting a direct interaction between pesticide exposure and the activity of the *reelin* gene. Together, these pieces of evidence have led to the hypothesis that prenatal organophosphate exposure can affect cell migration by modulating reelin activity, thus potentially contributing to the neurodevelopmental basis of autism (Keller and Persico, 2003).

To evaluate the effects of possible gene/environment interactions in the development of behaviors and anatomical phenotypes relevant to ASDs, we have exposed heterozygous *reeler* ($Rl^{+/-}$) mice to the active organophosphate chlorpyrifos oxon (CPO) during embryonic development. $Rl^{+/-}$ mice have reduced levels of reelin protein and show subtle but discernible differences in neuroanatomy including decreased density of nitric oxide synthase-expressing cells in the cortex (Tueting et al., 1999), selective reduction in forebrain cholinergic neurons (Sigala et al., 2007), alterations in dendritic spine morphology in the hippocampus (Pappas et al., 2001; Niu et al., 2008), and altered synaptic activity in the brain including decreased GAD67 expression and changes in NMDA receptor expression and activity (Liu et al., 2001; Ventruti et al, 2011; van den Buuse et al., 2012). Behavioral testing suggests minor deficits in reversal learning, but no differences in anxiety or social behavior (Salinger et al., 2003; Podhorna and Didriksen, 2004; Brigman et al., 2006; Laviola et al., 2006; Teixeira et al., 2011). In particular, we sought to determine whether reelin haploinsufficiency coupled with CPO exposure would affect behaviors specifically relevant to ASDs, such as communication and social interaction. We also examined brain morphology to determine if interactions between reelin and CPO would produce discernible changes in brain structure. Our findings suggest that both behavior and brain anatomy are affected individually by reelin haploinsufficiency or by CPO exposure, but that exposure to both variables does not appear to be additive in effect. Exposure to both variables resulted in mitigation of some behavioral and anatomical phenotypes, producing behaviors and anatomy similar to those seen in control animals. This counterbalancing effect suggests that

while genetic and environmental factors both affect brain development, interactions between these variables are not necessarily additive, and in some cases, may mask symptoms caused by one or the other variable. In this regard, fine discrimination may be needed to discern the effects of genetic and environmental variables in neurodevelopmental disorders.

Methods and Materials

Mouse lines and minipump implantation

Reeler mice (B6C3Fe-*a/a-Reln*^{rl}/$^{+}$, referred to in this study as *Rl* mice) were obtained from the Jackson Laboratory (Bar Harbor, ME, USA) and *Dab1*^{exKIneo} mice, in which a *lacZ* reporter gene replaces exon 1 of *Dab1*, were kindly provided by Dr. Brian Howell (Pramatarova et al., 2008). Both lines of mice are maintained on a C57Bl/6 background. For behavioral studies, heterozygous *reeler* (*Rl*$^{+/-}$) female mice were crossed with wild-type males. The initiation of pregnancies was determined by visual inspection for vaginal plugs; the first appearance of a plug was denoted as gestation day (G) 0.5. At G13.5, pregnant females were anesthetized with Isofluorane and implanted with an osmotic minipump (Alzet 1003D, 100µl reservoir) loaded with 6 mg/ml chlorpyrifos oxon (CPO, the active metabolite of the organophosphate pesticide chlorpyrifos, Chem Service, West Chester, PA) dissolved in 1:1 DMSO:phosphate buffered saline or with a vehicle-loaded pump. Females delivered their litters on average on G20. Pups were raised by their mothers to 28 days, then weaned and group housed for the remainder of their testing period. For anatomical studies, *Rl*$^{+/-}$ females were mated with *Dab1*$^{exKIneo+/-}$ males and minipumps were implanted as above. Offspring from all matings were genotyped by PCR as described (D'Arcangelo et al., 1995; Howell et al., 1997; Khialeeva et al., 2011). Animals of each sex were divided into four groups – vehicle-treated *Rl*$^{+/+}$ and *Rl*$^{+/-}$ mice, and CPO-treated *Rl*$^{+/+}$and *Rl*$^{+/-}$ mice, with a minimum of 6 animals per group used for behavioral testing and a minimum of 3 animals per group used for anatomical analysis.

Acetylcholinesterase activity

Acetylcholinesterase activity was measured using a modified Ellman reaction. Heads were harvested from E16.5 embryos, three days after minipump implantation, flash-frozen and stored at -80°C. Frozen heads were homogenized in 0.1M phosphate buffer, centrifuged at 14k rpm for 5 min, and supernatant collected for the assay. Total protein concentration was

determined using a Bradford assay and AChE activity was determined by colorimetric analysis utilizing the QuantiChrom™ Acetylcholinesterase Assay Kit (BioAssay Systems, US) following the manufacturer's instructions. The protein quantification and AChE assays were repeated in triplicate, then the samples were averaged to determine the final results.

Western blotting for reelin protein quantification

Embryonic heads were harvested at E16.5, three days after minipump implantation, flash-frozen and stored at -80ºC . Heads were homogenized in lysis buffer containing 50 mM Tris/HCl, 0.25% (w/v) sodium deoxycholate, 150 mM NaCl, 1 mM EDTA, 1% (w/v) Triton X-100, 0.1% (w/v) SDS, with phosphatase inhibitor cocktail (ZmTech Scientific) containing 1-2% sodium orthovanadate, 1-3% 4-(2-) aminoethyl)benzenesulfonyl fluoride, 1-3% aprotinin, and 1-3% leupeptin. Samples were resolved on 4–12% mini-SDS polyacrylamide gels (Invitrogen) and transferred to Immobilon polyvinylidene difluoride membranes. Blots were blocked with 5% nonfat dry milk in PBS-T (17 mmKH_2PO_4, 50 mmNa_2HPO_4, 1.5 mm NaCl, pH 7.4, and 0.05% Tween 20) for 1 hr at room temperature and then incubated overnight at 4°C in PBS-T plus 5% nonfat dry milk containing primary mouse anti-reelin clone 142 (1:750 dilution) antibodies (Millipore). Relative reelin protein levels in each sample were determined by comparison with ß-actin levels, which were determined by Western blotting as above using mouse anti-ß-actin antibodies (1:10,000, Sigma, 1 hour incubation at room temperature). Protein bands were detected using an ECL 2 kit for reelin and ECL kit for ß-actin (Amersham Pharmacia Biotech), with horseradish peroxidase-conjugated secondary goat anti-mouse antibodies (Cell Signaling Technologies). Relative intensities of the protein bands were quantified by scanning densitometry using ImageJ.

Behavioral testing

Ultrasound vocalization: Mice at postnatal day (P) 7 were separated from their dams and placed into warm soundproof chambers equipped with ultrasonic detectors connected to recording and analysis software (UltraVox, VisualSonics). The number and duration of vocalizations at 70 Hz were recorded during a 10-minute testing period. Male and female mice were assessed separately, with four groups of animals (vehicle-treated $Rl^{+/+}$, CPO-treated $Rl^{+/+}$, vehicle-treated $Rl^{+/-}$, and CPO-treated $Rl^{+/-}$) tested for each sex. The collected data was scrubbed for outliers and statistical significance across the four test groups in each sex was determined using individual t-test comparisons and aggregate ANOVA analysis.

Open field behavior: Mice at P30 were introduced into a 22.5 cm x 22.5 cm clear plexiglass arena and video-recorded for 20 minutes using TopScan (CleverSys Inc.). A central rectangle, occupying 62.6% of the total area was superimposed over the arena profile and animals were scored for the amount of time spent in the center vs. the periphery of the chamber. The number of sniffing events, an exploratory behavior, was also determined for the center of the chamber and the periphery during the recording.

Social interaction: Mice were tested at P30 for social interactions using a three-chambered social interaction apparatus (Crawley, 2004). Prior to testing, animals were habituated for 5 minutes in the apparatus; testing was then conducted in two phases. In the first phase, an age- and sex-matched stranger mouse was introduced under a wire mesh cup in one of the two side chambers, along with an empty mesh wire cup in the other side chamber. The amount of time spent in each chamber was recorded for the test mouse in a 10-minute trial using TopScan (CleverSys Inc.). In the second phase, a novel stranger (Stranger #2) was introduced into the second side chamber under a mesh cup, while the original stranger mouse (Stranger #1) remained in its original position. Again, the amount of time spent in each of the three chambers was recorded for the test mouse. The number of sniffing events in each of the three chambers was also scored.

Marble burying: Marble burying was used as a test of repetitive and perseverative behavior (Thomas et al., 2009). Standard shoebox mouse cages were filled with 4 cm of SaniChip bedding and an array of 20 black glass marbles in a 4x5 arrangement was laid on top of the bedding. Male mice at P60 were introduced to the arena for a 20-minute testing period; at the end of the testing period, the array was photographed and the buried marbles were counted. Marbles were scored as buried if >50% of the marble was covered by bedding. In addition to scoring the number of marbles buried, the activity of the animals was also assessed by scoring for digging behavior for 2 second intervals every 20 seconds throughout the testing period.

Neuroanatomical characterization

In order to visualize cells potentially responsive to reelin signaling, we utilized a *Dab1*^{lacZ} reporter mouse (*Dab1*^{exKIneo}, Pramatova et al., 2008, Khialeeva et al., 2011). In this animal, *Dab1* coding sequences are replaced with a *lacZ* gene. *Dab1* is a downstream mediator of reelin signaling, thus those cells that express the *lacZ* reporter are potentially responsive to reelin signaling. *Dab1*^{exKIneo} male mice were intercrossed with heterozygous *reeler* female mice (*Rl*$^{+/-}$), which were then used for osmotic minipump implantation as described above. CPO- and vehicle treated *Rl*$^{+/+}$ and *Rl*$^{+/-}$ mice that were also heterozygous for the *Dab1*^{exKIneo} allele were collected at P14, perfused with 4% paraformaldehyde, and the brains dissected and fixed by immersion for 4 hours. After fixation, the brains were washed, infiltrated overnight with 30% sucrose, then embedded and frozen in OCT mounting medium (Sukura Finetek). Sections were cut at 30 µm, air-dried, then reacted with X-Gal reaction buffer as previously described (Choe et al., 2006). Selected sections were photographed using a Zeiss Axioskop equipped with a cooled CCD camera; photographs were minimally processed for color balancing using Adobe Photoshop. Densitometry was performed using NIH Image J by creating a column average plot

for each section using profile plot on a weighted grayscale value (RGB 0.30, 0.59, 0.11) assigned to each pixel.

Results

To evaluate the effects of possible gene/environment interactions in the development of behaviors and anatomical phenotypes relevant to ASDs, we have examined mice that express reduced levels of reelin protein and were exposed to organophosphate pesticides during a period of active cortical development. We used a combination of biochemical analysis, to assess acetylcholinesterase activity and the levels of reelin protein, behavioral analysis, to assess phenotypes relevant to ASD, and anatomical analysis, to assess changes in the organization and anatomy of olfactory, cortical, and cerebellar regions. A schematic outline of the experimental design is provided in Fig. 2.1. All mice were provided with exposure to either CPO or to a vehicle control at E13.5 – E16.5. This corresponds to a time of robust cortical development in mice when reelin signaling is known to be active, and has also been used in prior studies (e.g. Laviola et al., 2006), thus allowing comparison of results across different laboratories. Behavioral testing was performed following a set schedule and in the same order for each cohort of mice, to control for testing or age-related artifacts. Anatomical analysis was performed on mice collected at P14. At P14, cortical and subcortical development is largely complete in mice, eliminating possible artifacts due to immaturity of the brain. In addition, this age was chosen to ensure strong expression of the *Dab1-lacZ* reporter. *Dab1* activity is incrementally decreased postnatally (Keshvara et al., 2002), thus to ensure accurate detection of cells that are likely to be responsive to reelin signaling, anatomical analysis was performed while reporter expression was still strong.

Survival, growth, acetylcholinesterase activity, and reelin protein levels

To determine the prenatal effects of CPO exposure, we first examined the average litters of CPO- treated pups compared to vehicle-treated pups. Prenatal CPO exposure did not have significant effects on litter size, with CPO-treated litters averaging 7.4 pups (n = 9 litters) and vehicle-treated litters averaging 7.5 pups (n = 13 litters). Reelin protein has been reported to be

a serine protease (Quattrocchi et al., 2002) and organophosphate pesticides specifically inhibit serine proteases, therefore we were curious whether prenatal organophosphate exposure might differentially affect *Rl*$^{+/-}$ mice, which have reduced levels of reelin protein, as compared to *Rl*$^{+/+}$ mice. However, we found an approximately equal distribution of *Rl*$^{+/+}$ and *Rl*$^{+/-}$ mice in our litters, with 52% of pups being *Rl*$^{+/+}$ and 48% of pups being *Rl*$^{+/-}$ after CPO treatment and 48% of pups being *Rl*$^{+/+}$ and 52% being *Rl*$^{+/-}$ after vehicle treatment (Table 1). This suggests that prenatal CPO exposure did not differentially affect the survival of *Rl*$^{+/+}$ or *Rl*$^{+/-}$ embryos. We did observe an increased percentage of males in CPO-treated litters (66% male vs. 34% female), however only 67 pups were obtained in total, so this distribution may reflect normal variation in litter composition.

To assess the efficacy of prenatal CPO exposure, we measured acetylcholinesterase activity in embryos. Acetylcholinesterase is a serine protease and serine protease activity is specifically inhibited by organophosphate pesticides. CPO was administered via osmotic minipump for three days beginning at E13.5. This period corresponds to the peak period of neurogenesis and cell migration in the mouse cerebral cortex (Caviness, 1982); thus this window of application is most likely time to affect the development of anatomical alterations relevant to autism. Three days after minipump implantation, we found that baseline AChE activity was slightly higher in *Rl*$^{+/-}$ animals compared to *Rl*$^{+/+}$ animals (Fig. 2.2), similar to results reported for postnatal mice (Laviola et al., 2006). CPO treatment reduced acetylcholinesterase activity in both *Rl*$^{+/+}$ and *Rl*$^{+/-}$ mice to approximately 85% of the starting value, demonstrating that CPO derived from the osmotic minipumps can affect embryonic brain biochemistry. Although reelin activity was not directly tested biochemically, by inference, it should also be affected by CPO exposure (Laviola et al., 2006).

To directly assess the effects of prenatal CPO exposure on reelin protein, we performed Western blotting. Full-length reelin protein is approximately 410 kD; cleavage of the protein yields two major fragments at 330 and 180 kD. As expected, vehicle-treated *Rl*$^{+/-}$ embryos

showed approximately 50% less full-length reelin protein than vehicle-treated *Rl*$^{+/+}$ embryos (Fig. 2). The 330 kD fragment was also reduced approximately 50%, while the 180 kD fragment was reduced, but not to the same extent. CPO treatment of *Rl*$^{+/+}$ embryos did not significantly change the levels of either full-length reelin or of either cleavage fragment. Surprisingly, CPO treatment restored the levels of reelin protein to near wild-type levels in *Rl*$^{+/-}$ embryos, both for full-length protein and for the cleavage fragments. This supports our hypothesis that CPO exerts a protective effect on reelin protein.

Behavioral alterations in response to loss of reelin and to CPO exposure

Three different behavioral measures were used to assess phenotypes relevant to ASD. First, we recorded ultrasound vocalization on mice at P7. Ultrasound vocalization has been reported to peak at P7-P10 in most strains of mice. Empirical observations in our laboratory suggested that the most robust vocalizations were produced at P7 in our mice, therefore we used this age for all additional testing. Mice were then screened for open field behavior and social interaction at P30 and for marble burying and digging behavior at P60. Each cohort of animals was tested at the same ages and following the same schedule.

Ultrasound vocalization: Infant mice emit ultrasonic vocalizations when separated from their dams to elicit pup retrieval, suggesting that these vocalizations play an important role in communication between mothers and their pups. Changes in ultrasound vocalization have also been used to characterize possible mouse models for autism (e.g Scattoni et al., 2009; Young et al., 2010), although unlike human language, mouse ultrasound vocalizations are innate behaviors suggesting that these types of communication are not equivalent (Fischer and Hammerschmidt, 2011). *Rl*$^{+/+}$ and *Rl*$^{+/-}$ pups with and without CPO exposure were assessed for ultrasound vocalization during a brief separation from their dams at P7 (Fig. 2.3).

The number of vocalizations varied significantly across all four groups in both male and female mice by ANOVA analysis (males: $F(3,36)=16.1954$, $p=7.9229\times10^{-7}$; females: $F(3,36)=26.4314$, $p=3.2636\times10^{-9}$). In male mice, both CPO-treated *Rl*$^{+/+}$ mice and vehicle-treated *Rl*$^{+/-}$ mice produced fewer vocalizations than vehicle-treated *Rl*$^{+/+}$ animals (Fig. 2.3A). In contrast, CPO-treated *Rl*$^{+/-}$ mice made more cries than vehicle-treated *Rl*$^{+/+}$ animals. This suggests both individual effects of reduced reelin and CPO exposure and combinatorial effects of the two variables together. In female mice, both CPO-treated *Rl*$^{+/+}$ and *Rl*$^{+/-}$ animals showed significantly reduced vocalizations, while vehicle-treated animals showed similar numbers of vocalizations (Fig. 2.3A). The number of female vocalizations thus seems specifically sensitive to CPO exposure, with no additional effect derived from reduced reelin expression.

Examination of the average duration of vocalizations also showed significance across the four groups by ANOVA analysis (males: $F(3,36)=15.0805$, $p=1.6148\times10^{-6}$; females: $F(3,36)=33.9508$, $p=1.3528\times10^{-10}$). In males, duration of vocalizations was significantly reduced only in CPO-treated *Rl*$^{+/+}$ males (Fig. 2.3B), with no apparent reductions in *Rl*$^{+/-}$ mice. However, duration of vocalization was restored to control levels in CPO-treated *Rl*$^{+/-}$ mice, again suggesting a combinatorial interaction between variables in male mice. In contrast, in female mice, both CPO treatment and loss of reelin expression appeared to reduce the number of vocalizations to levels below that exhibited by vehicle-treated *Rl*$^{+/+}$ animals. In females, combinatorial interactions between reduced reelin and CPO exposure were not apparent, as there was no change in vocal duration between vehicle-treated *Rl*$^{+/-}$ mice and CPO-treated *Rl*$^{+/-}$ mice.

Open field behavior: *Rl*$^{+/+}$ and *Rl*$^{+/-}$ pups with and without CPO exposure were assessed for open field behavior at P30 (Fig. 2.4). For these experiments, mice were introduced to an open field enclosure and allowed to explore for 20 minutes. Mice were scored for the amount of time spent in the center of the chamber vs. the periphery, as well as for sniffing, an exploratory

behavior, in both the center and the periphery of the arena. All groups of male mice spent approximately 60% of their time in the periphery and 40% in the center, with no significant differences between any of the groups (Fig. 2.4A). Most female mice showed a similar spatial distribution, with the exception of CPO-treated *Rl*$^{+/-}$ mice, which showed a small but significant skewing toward more time spent in the center and less time spent in the periphery, when compared with vehicle-treated *Rl*$^{+/+}$ mice. This suggests a possible decrease in anxiety in CPO-treated *Rl*$^{+/-}$ female mice. Similar decreases in anxiety with CPO treatment have been observed previously in mice using an elevated plus maze (Ricceri et al., 2006).

Sniffing behavior in the center and periphery of the arena was quantified by measuring the amount of time engaged in sniffing in each of these areas. Female mice did not show any significant alterations in sniffing in either of the two areas regardless of genotype or treatment, but significant decreases in sniffing in the center of the arena were seen in both CPO-treated *Rl*$^{+/+}$ and vehicle-treated *Rl*$^{+/-}$ male mice; both of these alterations can be interpreted as slight increases in anxiety. However, CPO-treated male *Rl*$^{+/-}$ mice showed sniffing durations that were the same as vehicle-treated *Rl*$^{+/+}$ male mice. This again suggests a combinatorial interaction between reduced reelin and CPO exposure, similar to that observed in male ultrasound vocalization behavior. In summary, both male and female mice showed slight changes in open field behavior in response to either decreasing levels of reelin or to CPO exposure, though by different measures. Females showed a combinatorial effect of both treatments on the distribution of time spent in the center vs. periphery of the arena, while males showed a combinatorial effect of both treatments on sniffing behavior in the center. These results also demonstrate sex-specific changes, with males showing slightly increased anxiety and females showing decreased anxiety.

Social interaction: Social interactions were tested in a three-chamber social interaction apparatus (Crawley, 2004). Two testing paradigms were used. In the first (phase I), the test

mouse was introduced to a single stranger mouse, contained under a wire mesh cup in one of the two side chambers in the apparatus, while the other side chamber contained an empty cup. In this paradigm, the amount of time spent in each of the three chambers, along with the amount of sniffing, was measured. As expected, vehicle-treated *Rl*$^{+/+}$ males and females both showed an increased preference for spending time in the chamber with the stranger mouse and this preference was not significantly altered by either genotype or CPO treatment (Fig. 2.5). Sniffing behavior was also assessed by quantifying the amount of time spent sniffing at the cup containing the stranger mouse and at the empty cup. Males and females both showed an increased preference for sniffing at the stranger mouse. In males, sniffing behavior was not significantly affected by either genotype or CPO treatment, but in females, CPO treatment significantly increased the amount of time spent sniffing at the stranger mouse for both *Rl*$^{+/+}$ and *Rl*$^{+/-}$ mice.

In the second testing paradigm (phase II), a novel stranger mouse was introduced under the previously empty cup and time in each of the chambers and sniffing behavior was recorded for all animals. Both males and females showed a decrease in the amount of time spent with a familiar stranger (Stranger 1) and a concomitant increase in the time spent with a novel stranger (Stranger 2); neither genotype nor CPO treatment affected this distribution. Sniffing at the novel stranger was moderately increased for all males and for most females. However, CPO-treated *Rl*$^{+/+}$ female mice showed the opposite response and sniffed more at the familiar stranger than at the novel stranger, although the differences were not statistically significant. These observations suggest that genotype and CPO treatment had only moderate effects on social behavior, with only significant effects on sniffing behavior in female mice. CPO treatment appears to slightly increase sniffing behavior in female mice in the phase I trials, and to slightly alter sniffing only in *Rl*$^{+/+}$ females in phase II trials.

Marble burying: Marble burying is often used as a measure of anxiety in mice, but recent studies suggest it may be more accurately used as a measure for repetitive and perseverative behaviors (Thomas et al., 2009; Gould et al., 2012), which are some of the core behaviors in ASDs. We examined two behaviors using this assay – the total number of marbles buried at the end of the 20-minute test period and the number of digging events occurring throughout each trial. The total number of marbles buried was affected by genotype, but not by CPO treatment, as elevated levels of marble burying were observed in $Rl^{+/-}$ animals regardless of CPO exposure (Fig. 2.6). T-test comparisons did not identify significant differences between vehicle-treated $Rl^{+/+}$ mice and any other group, but the distribution of marbles buried across all four groups was significant by one-way ANOVA ($F(3,35)=4.263$, $p=0.012$). A moderate increase in digging was also observed in $Rl^{+/-}$ animals, but this increase was not statistically significant (ANOVA: $F(3,35)=2.607$, $p=0.069$).

In summary, our behavioral testing yielded some specific behavioral alterations attributable either to prenatal CPO exposure or to decreased reelin expression. While our model would have predicted an increase in autistic-like behaviors in animals with decreased reelin expression and CPO exposure, the changes we saw were not entirely consistent with this model. Some behaviors seemed sensitive to CPO exposure, while others were somewhat more sensitive to loss of reelin expression. Interestingly, combining CPO exposure and loss of reelin expression seemed to have more of an effect in female mice rather than in male mice. Given the highly increased prevalence of autism in human males, this is surprising. While decreased social interactions were evident in both males and females, they appeared to be differentially induced, with females showing decreased social interactions in response to CPO exposure, while males showed decreased social interactions with decreased reelin expression.

Anatomical alterations in response to loss of reelin and to CPO exposure

Reelin signaling is known to be critically important for the development of layered structures in the brain including the cortex, hippocampus, and cerebellum. We investigated the development of several layered structures that have a particular relevance to autism, including the olfactory bulb, the piriform cortex, the neocortex the hippocampus, and the cerebellum. To identify those cells that are potentially responsive to reelin signaling, and would thus be the cells likely to be affected by changes in reelin expression or activity, we used a *Dab1*^{lacZ} reporter mouse. Dab1 is an intracellular adaptor protein that is phosphorylated in response to reelin signaling, thus its presence is an indicator of those cells that are capable of responding to reelin signaling.

The olfactory system: Olfactory identification has been reported to be impaired in several studies of ASD patients (Suzuki et al., 2003; Bennetto et al., 2007) and impaired olfactory discrimination may provide a categorical tool for identifying sensory subtypes of autism (Lane et al., 2011). We examined the organization of two structures implicated in olfactory reception and information processing, the olfactory bulb and the piriform cortex. In vehicle-treated *Rl*$^{+/+}$ mice, three distinct regions clearly express the *Dab1*^{lacZ} marker in the olfactory bulb – the glomerular layer, the mitral cell layer, and the granule cell layer (Fig. 2.7A). *LacZ* expression outlines the glomeruli, and is found at high levels in both the mitral cell layer and the granule cell layer, with lower *lacZ* expression in the external and internal plexiform layers. Vehicle-treated *Rl*$^{+/-}$ mice and CPO-treated *Rl*$^{+/+}$ and *Rl*$^{+/-}$ mice all retain *Dab1*^{lacZ} expression in these layers, but there are some distinct differences in the distribution of *lacZ* expression. No differences were noted in the glomerular layer, but *Rl*$^{+/-}$ animals, both with and without CPO treatment showed variability in labeling in the granule cell layer, often with an apparent decrease in the intensity of labeling, along with an increase in the thickness of the internal plexiform layer (Fig. 2.7B, D). The mitral cell layer also appears thinner in these animals.

To quantify differences in *lacZ* distribution, we performed a density analysis of *lacZ* expression. To do this, average labeling intensity was calculated from the internal edge of the granule cell layer to the external margin of the external plexiform layer using NIH ImageJ. Density plots were standardized by superimposing the peak of the mitral cell layer from each individual plot and an average density value was calculated for all animals in each genotype and treatment group. Plots from vehicle-treated $Rl^{+/+}$ mice showed tight correlations in the position of the granule cell layer (Fig. 2.7E, asterisk) and the mitral cell layer (Fig. 2.7E, arrow), but some spread of *lacZ* distribution in the external plexiform layer (Fig. 2.7E, bracket). The intensity of mitral cell layer labeling showed increased variability in other treatment conditions, particularly in vehicle-treated $Rl^{+/-}$ animals and in CPO-treated $Rl^{+/+}$ animals (Fig. 2.7F, G). In addition, labeling intensity was highly variable in the granule cell layer, confirming our qualitative observations. Thickness of the inner plexiform layer, defined as the distance from the granule layer peak to the mitral layer peak also increased in CPO-treated $Rl^{+/+}$ animals to 67.33±6.81 µm (n=7) from to 57±1.73 µm (n=3) in vehicle-treated $Rl^{+/+}$ animals. Surprisingly, CPO-treated $Rl^{+/-}$ animals showed a relatively normal intensity profile (Fig. 2.7H). This suggests possible opposing effects of reelin heterozygosity and CPO treatment, resulting in a more normal *lacZ* intensity distribution in CPO-treated $Rl^{+/-}$ mice than in either vehicle-treated $Rl^{+/-}$ mice or CPO-treated $Rl^{+/+}$ mice.

The piriform cortex serves as the first cortical relay station for olfactory input from the mitral cells of the olfactory bulb (Haberly, 2001). The piriform cortex is trilaminar, with a largely cell-free superficial lamina (lamina I), and two cell-dense deeper laminae (Fig. 2.8). Both vehicle-treated and CPO-treated $Rl^{+/-}$ animals showed an increase in the density and width of lamina II, and this cell layer appeared much more pronounced in $Rl^{+/-}$ animals as a result. The distinction between laminae II and III decreased in CPO-treated $Rl^{+/+}$ and the combined width of both laminae increased. A few scattered ß-gal expressing cells were observed in lamina I of

vehicle-treated *Rl*$^{+/+}$ animals, and there was a qualitative increase in the numbers of these cells in both *Rl*$^{+/-}$ and CPO-treated animals. In particular, CPO-treated *Rl*$^{+/+}$ animals had far greater expression of ß-gal in lamina I (Fig. 2.8C).

The neocortex: Reelin signaling has been extensively studied as a factor in neocortical patterning and loss of this signaling leads to altered cell positioning and inverted cortical lamination (reviewed in Rice and Curran, 2001). Moderate neocortical disruptions have also been observed in some autistic patients (Bailey et al., 1998; Casanova et al., 2002), though most studies fail to note any neocortical alterations (e.g. Bauman and Kemper, 2005). Neocortical organization was largely normal in our studies. Vehicle- and CPO-treated mice exhibited essentially normal neocortical layering regardless of genotype. In the somatosensory cortex, ß-gal expression was noted in superficial cortical laminae (laminae II/III) and also in lamina V (Fig. 2.9). Lamina IV was largely free of ß-gal expression. In general, Dab1 expression, as judged by ß-gal expression, was noticeably less pronounced in the neocortex than in the piriform cortex. This suggests several possibilities: that Dab1 expression may be required at earlier stages in the neocortex than in the piriform cortex and thus lacZ expression has dissipated from the neocortex by the postnatal stages examined in this study or that continued Dab1 expression is not required for cortical patterning and maintenance in the postnatal neocortex as it is in the piriform cortex.

The hippocampus: In the absence of reelin signaling, hippocampal layering is significantly altered. Pyramidal cells, which normally form a compact layer in the CA fields, become dispersed dorsally into the stratum oriens, while the granular dentate gyrus becomes extensively disorganized (Caviness and Sidman, 1973; Förster et al., 2006). In our studies, Dab1 ß-gal expression was seen as discrete punctate labeling in a dense layer in the CA pyramidal cell layer (Fig. 2.10). Punctate labeling was evident, but more dispersed in the

stratum oriens, while the radiatum exhibited sparse labeling. Qualitative assessment suggested that there was increased ß-gal expression in the stratum oriens in both vehicle-treated *Rl*$^{+/-}$ animals and in CPO-treated *Rl*$^{+/+}$ animals. To quantify these changes, the stratum oriens was divided into six bins from medial to lateral and the number of ß-gal grains counted in each bin. Vehicle-treated *Rl*$^{+/+}$ animals had ß-gal expression at the highest levels in the three medial bins, while expression substantially decreased in the three more lateral bins (Fig. 2.10E). Vehicle-treated, *Rl*$^{+/-}$ animals showed a similar distribution of expression. In contrast, CPO-treated *Rl*$^{+/+}$ animals showed approximately equal ß-gal distribution across the first four bins, with moderate decreases in expression in the most lateral bins. CPO-treated *Rl*$^{+/-}$ animals also showed relatively equal ß-gal expression across the first four bins. In contrast to all other groups, CPO-treated *Rl*$^{+/-}$ animals showed higher levels of ß-gal expression in the most lateral bin. This suggests a difference in the distribution of Dab1-expressing cells in the stratum oriens in CPO-treated *Rl*$^{+/-}$ animals.

The cerebellum: Reeler mutant mice are known to have cerebellar abnormalities, including lack of distinct lamination and foliation along with displaced Purkinje cells (Bauman and Kemper, 2005). We therefore examined cerebella for changes in either layering or cell placement. We examined both the central vermis and the more lateral ansiform and simple lobules. Dab1-ßgal expression was seen at high levels in Purkinje cells in both regions, and dispersed throughout the molecular layer (Fig. 2.11) in vehicle-treated *Rl*$^{+/+}$ animals. Small amounts of ß-gal expression were also seen in the granule cell layer. There was a clear separation of Purkinje cell expression from ß-gal expression in the molecular layer and expression in the Purkinje cell layer appeared continuous throughout the extent of the folia examined, without significant gaps. Vehicle-treated *Rl*$^{+/-}$ animals exhibited approximately the same distribution of ß-gal, suggesting no apparent changes in cerebellar layering in heterozygous animals. However, CPO treatment in *Rl*$^{+/+}$ animals increased ß-gal expression in

the molecular layer of the lateral lobules, but not in the vermis. To quantify these changes, sections were scored for the levels of ß-gal expression (high, medium, low, using levels equivalent to those seen in the vermis as “high”). Assigning a value of 1 to low, 2 to medium, and 3 to high suggested that vehicle-treated *Rl*$^{+/+}$ animals had an average expression of 2±0 (n=3). Levels were decreased on average in vehicle-treated *Rl*$^{+/-}$ animals (1.375±0.48, n=4), increased in CPO-treated *Rl*$^{+/+}$ animals (2.625±0.48, n=4), and seen at wild-type levels in CPO-treated *Rl*$^{+/-}$ animals (2.07±0.73, n=7). While vehicle-treated *Rl*$^{+/+}$ and *Rl*$^{+/-}$ animals and CPO-treated *Rl*$^{+/+}$ animals had fairly consistent levels of ß-gal expression in the lateral lobes, expression was much more variable in CPO-treated *Rl*$^{+/-}$ animals. This suggests some moderate changes in cerebellar layering specifically in the more lateral lobes.

In summary, our anatomical studies made use of a Dab1-lacZ reporter mouse to visualize all cells potentially responsive to reelin signaling. Anatomical studies have been conducted on *Rl*$^{+/-}$ animals and reveal subtle phenotypes in cell placement and dentritic arborization (Niu et al., 2008). However, all prior studies have relied on examining only specific cell types. Our current study provided a method to perform a survey of potentially all cell populations responsive to reelin signaling. We selected several brain regions known to be affected by disruptions in reelin signaling and assessed the organization of Dab1-expressing cells in these regions. We demonstrate subtle alterations in cell layering and positioning stemming from either reduced reelin expression or CPO exposure, but we found no evidence for combinatorial interactions between these variables leading to increased brain alterations.

Discussion

Our study demonstrates clear but modest changes in behavior and brain anatomy as a result of either decreased reelin expression or CPO exposure. Based on the identification of decreased reelin expression and organophosphate pesticide exposure as possible contributing factors to ASD (Abrahams and Geschwind, 2008; Keller and Persico, 2003), we examined mouse behaviors representative of the three key arenas in ASD – communication, social interaction, and restricted and repetitive behaviors. We found subtle alterations in each of these three behaviors. Some of the alterations, such as increased marble burying, appeared to be directed by genotype alone, while others, such as ultrasound vocalization and social interaction, could be altered by either decreased reelin or by exposure to CPO. Additionally, male and female mice often responded differently to these factors. Curiously, we failed to find an additive detrimental effect of decreased reelin combined with CPO exposure on either mouse behavior or brain anatomy. In fact, we often observed the opposite result – combining decreased reelin and CPO exposure mitigated the effects of either factor alone.

Prior studies have demonstrated a functional interaction between reelin and organophosphate exposure, but the mechanisms for this interaction remain unclear. CPO exposure may have several effects on brain development. Exposure to lethal doses of CPO produces acute neurotoxicity, which likely stems from inhibition of acetylcholinesterase, producing a cholinergic crisis due to synaptic accumulation of acetylcholine and the hyperstimulation of postsynaptic muscarinic and nicotinic receptors (Flaskos, 2012). However, exposure to sublethal doses of CPO also produces neurodevelopmental toxicity, though the mechanisms for this effect are less clear. Sublethal CPO exposure generates stable adducts on tyrosine and serine, altering the function of many proteins, though not in a predictable fashion. In one study, chronic exposure to low levels of CPO altered the structure of microtubules and affected the complement of microtubule-associated proteins (Jiang et al., 2010). These effects have the potential to alter cytoskeletal structure and to affect the migratory ability of developing

neurons. Reelin also has known cytoskeletal effects, with disruption of the reelin signaling pathway resulting in hyperphosphorylation of tau, disturbing interactions with microtubules and destabilizing the cytoskeleton (Heisberger et al., 1999). If both reelin signaling and CPO exposure converge on the cytoskeleton, then we might expect that introduction of these two variables would produce more pronounced alterations in cell migration and brain anatomy. However, this does not appear to be the case in our studies. Alternatively, CPO may affect the structure and stability of reelin itself. Secreted reelin undergoes two cleavage events to produce three fragments (Lambert de Rouvroit et al., 1999; Jossin et al., 2007); as reelin is cleaved, its signaling ability diminishes (Kohno et al., 2009). The enzyme(s) responsible for these cleavages have not yet been identified, but preliminary evidence suggests the involvement of proprotein convertase 2 or ADAM (a disintegrase and metalloprotease) family members (Kohno et al., 2009; Hisanaga et al., 2012). It is possible that CPO may affect the function of these enzymes to inhibit the cleavage of reelin, thus potentially increasing the pool of full-length reelin; this possibility is consistent with our Western blotting results. In this case, animals with decreased reelin levels may have partial restoration of reelin signaling activity in the presence of CPO, at least to levels that allow generation of normal anatomical organization.

A prior study has also demonstrated specific behavioral changes in heterozygous reeler mice embryonically exposed to CPO (Laviola et al., 2006), but similar to our study, the results were also paradoxical. In Laviola et al., the number of ultrasound vocalizations was decreased in CPO-treated $Rl^{+/+}$ mice and increased in CPO-treated $Rl^{+/-}$ mice. Additionally, scopolamine- and amphetamine-induced locomotion was decreased in CPO-treated $Rl^{+/+}$ animals and increased in CPO-treated $Rl^{+/-}$ animals. While we did not test scopolamine- or amphetamine-induced locomotion, our ultrasound vocalization studies showed similar effects to those seen by Laviola et al., with CPO treatment decreasing ultrasound vocalization in WT mice and increasing it in $Rl^{+/-}$ male mice. However, in female mice, the number of ultrasound vocalizations was not affected by changes in reelin expression, as both vehicle-treated $Rl^{+/+}$ and

Rl$^{+/-}$ animals showed similar numbers of vocalizations. In contrast, CPO treatment significantly decreased the number of vocalizations in both *Rl*$^{+/+}$ and *Rl*$^{+/-}$ females.

Additional behavioral tests also showed paradoxical results, with distinct differences between males and females. Open field testing showed no difference in center vs. periphery time distribution in males, but did show decreased sniffing in the center of the arena in both CPO-treated *Rl*$^{+/+}$ mice and vehicle-treated *Rl*$^{+/-}$ mice, while CPO-treated *Rl*$^{+/-}$ mice showed no significant differences from vehicle-treated *Rl*$^{+/+}$ animals. Both CPO-treated *Rl*$^{+/+}$ and vehicle-treated *Rl*$^{+/-}$ female mice showed modest, but not significantly different time distribution, while CPO-treated *Rl*$^{+/-}$ female mice showed a possible additive effect of both phenotypes and demonstrated a preference for the center of the arena. In contrast, no sniffing differences were noted in any treatment condition in female mice. Social interactions were largely indistinguishable from control animals in both males and females, though a slight but significant increase in sniffing at stranger mice was demonstrated by CPO-treated *Rl*$^{+/+}$ and *Rl*$^{+/-}$ females, suggesting that this behavior is modulated by CPO treatment and not by reelin genotype. In contrast, marble burying appeared to be affected solely by genotype in male mice, with no effect of CPO treatment. These results suggest a complex effect of decreases in reelin expression and CPO treatment on behaviors related to ASDs.

Anatomical substrates for ASDs have been poorly defined in humans, likely due to the high variability of the disorder. By using a *Dab1*^{lacZ} reporter mouse, we were able to identify brain regions that are potentially responsive to reelin signaling, by virtue of their expression of *Dab1*. Identifying brain structures that are altered in response to changes in genetic or environmental factors may represent a first step toward identifying possible anatomical substrates of ASDs. Reelin signaling has been widely recognized as a critical signal in establishing cortical layers, with *reeler* mutant mice exhibiting inverted cortical layering (reviewed in Rice and Curran, 2001). Surprisingly, decreased reelin expression and/or CPO exposure failed to induce measurable cortical alterations, at least in terms of cell populations

expressing *Dab1*. It is possible that individual cell populations might be mispositioned even in the absence of gross abnormalities, but confirmation of this possibility in the future will require immunohistochemical studies using cell-specific markers.

Unlike the cortex, layering and cell positioning alterations were observed in the olfactory bulb, hippocampus, and cerebellum. These alterations tended to take the form of more diffuse ß-gal expression in specific cell layers (e.g. in the olfactory bulb), and decreased segregation between identified laminae (e.g in the pyriform cortex). Additionally, we observed mispositioned *Dab1*-expressing cells, e.g. the extra cells present in lamina I of the pyriform cortex, the extra cells in molecular layer of the cerebellum, and altered distribution of cells in the stratum oriens in the hippocampus. These changes are subtle and could likely only be visualized using a reporter gene system as we have done. Similar changes might be difficult to detect using imaging studies on human patients; this may be one reason why anatomic substrates of ASDs have to date gone largely undetected. While we have identified alterations in regional layering and cell positioning, it remains to be seen what specific cell types are affected by reduced reelin expression and/or CPO exposure.

In summary, our findings show measurable effects of reducing reelin expression or early exposure to an organophosphate pesticide, but little exacerbation of phenotypes when both variables are combined. These results do not support the interaction of the reelin signaling pathway and organophosphate pesticides in the generation of ASD, but suggest that each factor has the potential to disrupt specific aspects of nervous system function independently and in an opposite fashion. Thus, when combined, phenotypes generated by each variable independently serve to restore behavioral and anatomical alterations in mice. While genetic and environmental factors are widely thought to act in concert to generate neurodevelopmental disorders, the specific combination of decreased reelin gene expression and CPO exposure appear not to function together in mice to generate the behavioral or anatomical changes similar to those appearing in ASD in humans.

	Total pups	Number of litters	Average litter size	Males	Females	+/+	+/-
Vehicle-treated	98	13	7.5	51 52%	47 48%	47 48%	51 52%
CPO-treated	67	9	7.4	44 66%	23 34%	35 52%	32 48%

Table 2.1: Number of litters and pups derived from vehicle-implanted or CPO-implanted dams.

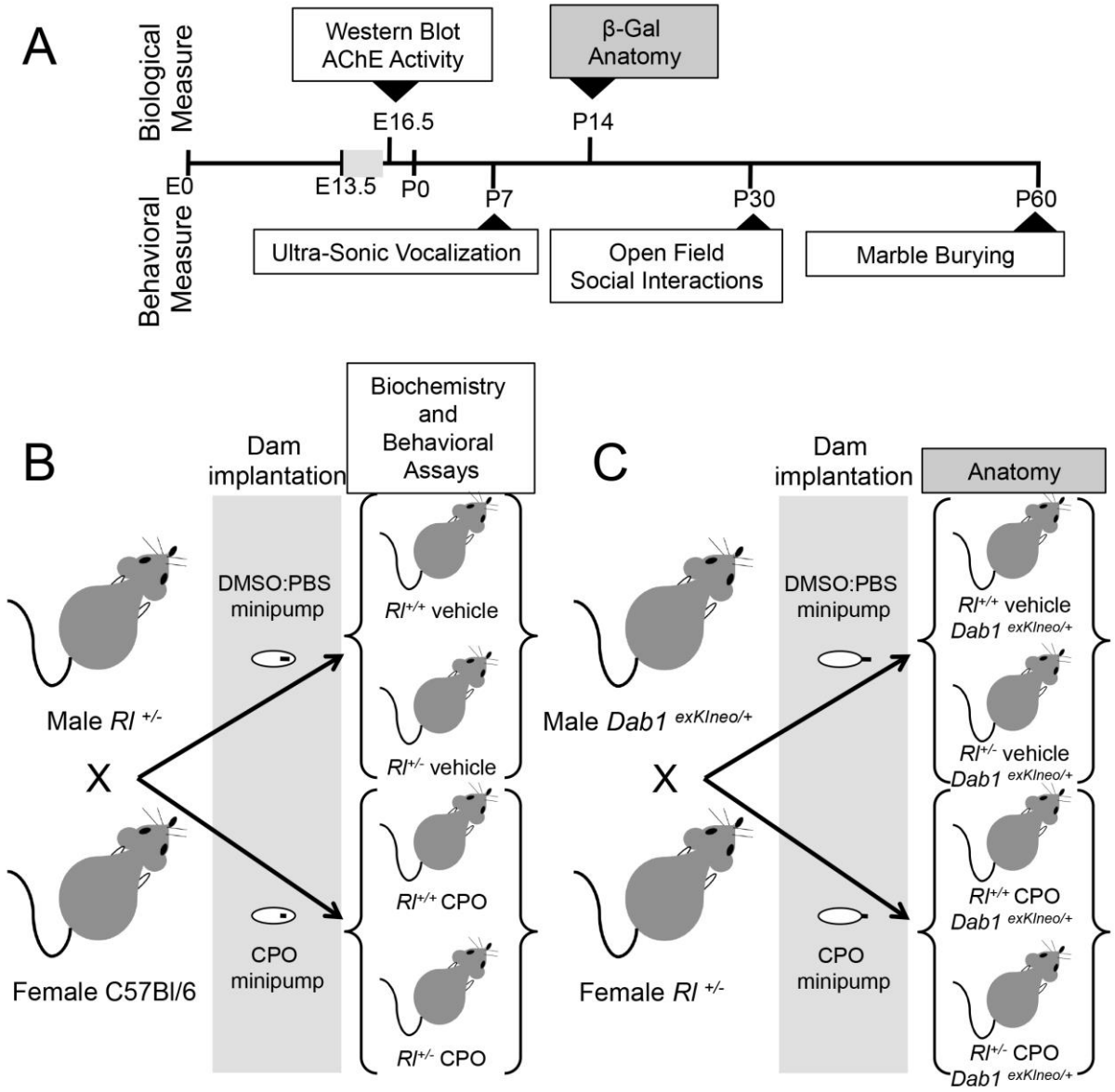

Figure 2.1: Timeline (A) and mouse breeding scheme (B, C) for data presented in this study. Minipumps were implanted at E13.5 and were active for 3 days (gray box in A). Embryos were collected at E16.5 for AChE activity analysis and for Western blotting. Behavioral testing was conducted from P7 to P60, with ultrasound vocalization tested at P7, open field behavior and social interactions tested at P30 and marble burying tested at P60. Mice used for behavioral testing were generated by intercrossing *Rl*$^{+/-}$ males and C57Bl/6 females (B). Mice used for anatomical analysis were generated by intercrossing male *Dab1*$^{exKIneo/+}$ mice with *Rl*$^{+/-}$ females (C). In both breeding schemes, females were implanted with either CPO- or vehicle-loaded

minipumps. The genotypes of offspring used for anatomical and behavioral analysis are illustrated in the brackets in B and C.

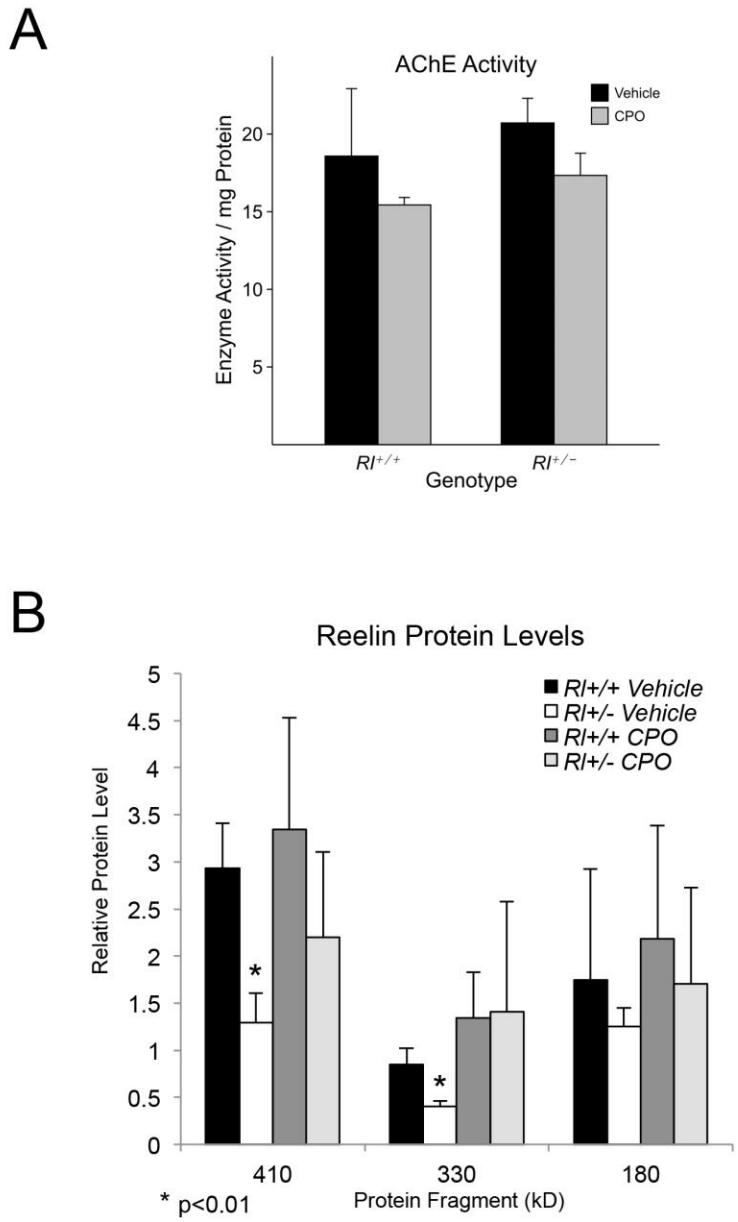

Figure 2.2: Acetylcholinesterase activity (A) and relative levels of reelin protein normalized to ß-acting (B) in E16 mouse brains following three days of prenatal vehicle or CPO treatment.

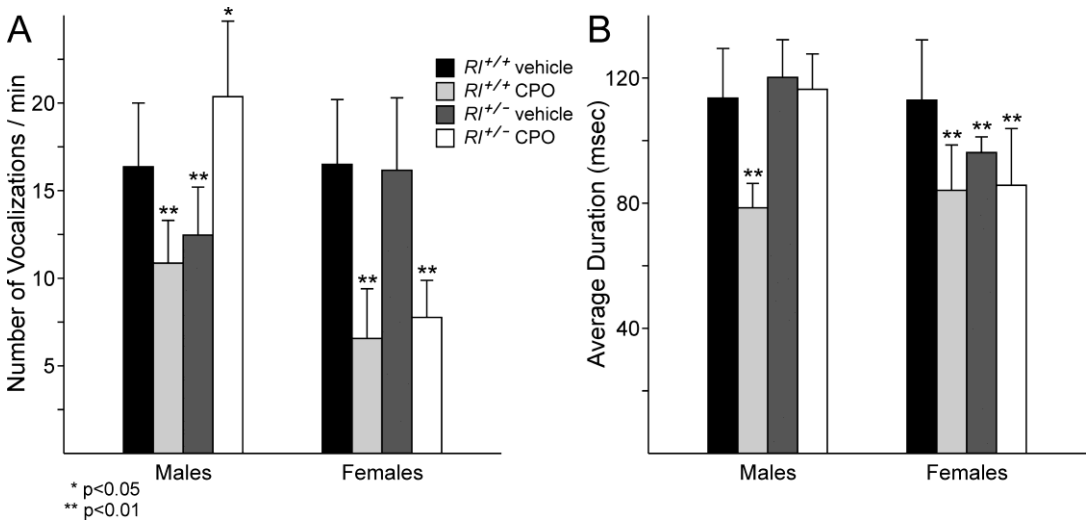

Figure 2.3: Number (A) and duration (B) of ultrasound vocalizations in mice at P7. Statistical significance as determined by t-test comparisons with vehicle-treated *Rl*$^{+/+}$ animals is indicated by asterisks over the appropriate bars.

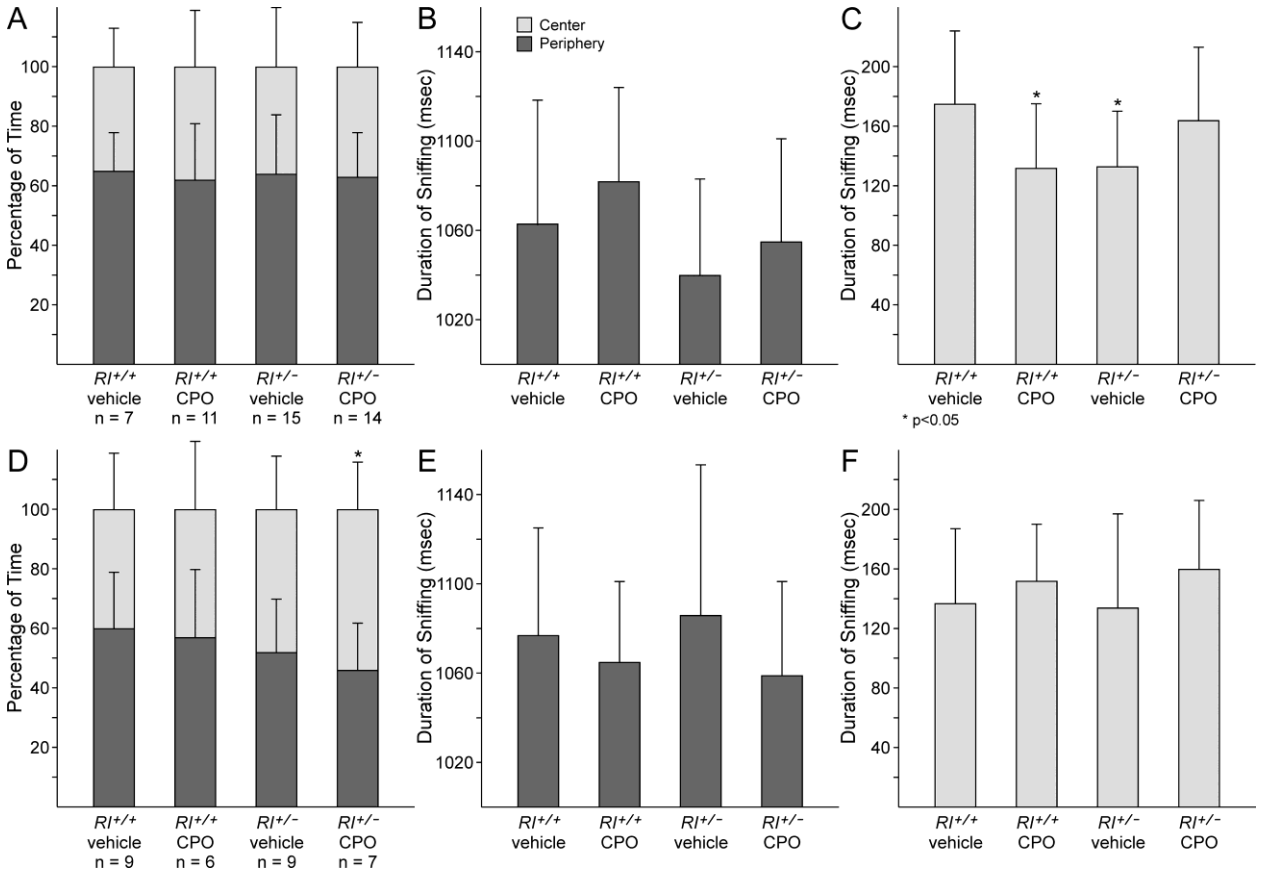

Figure 2.4: Open field behavior. Male (A-C) and female (D-F) mice were scored for time spent in the center vs. the periphery (A, D) and for duration of sniffing in both the periphery (B, E) and the center (C, F). Statistical significance as determined by t-test comparisons with vehicle-treated *RI*$^{+/+}$ animals is indicated by asterisks over the appropriate bars. ANOVA analysis of the time distribution across all four groups did not indicate significance (males: F(3,45)=0.1251, p=0.9448, females: F(3,44)=1.2901,P=0.2896).

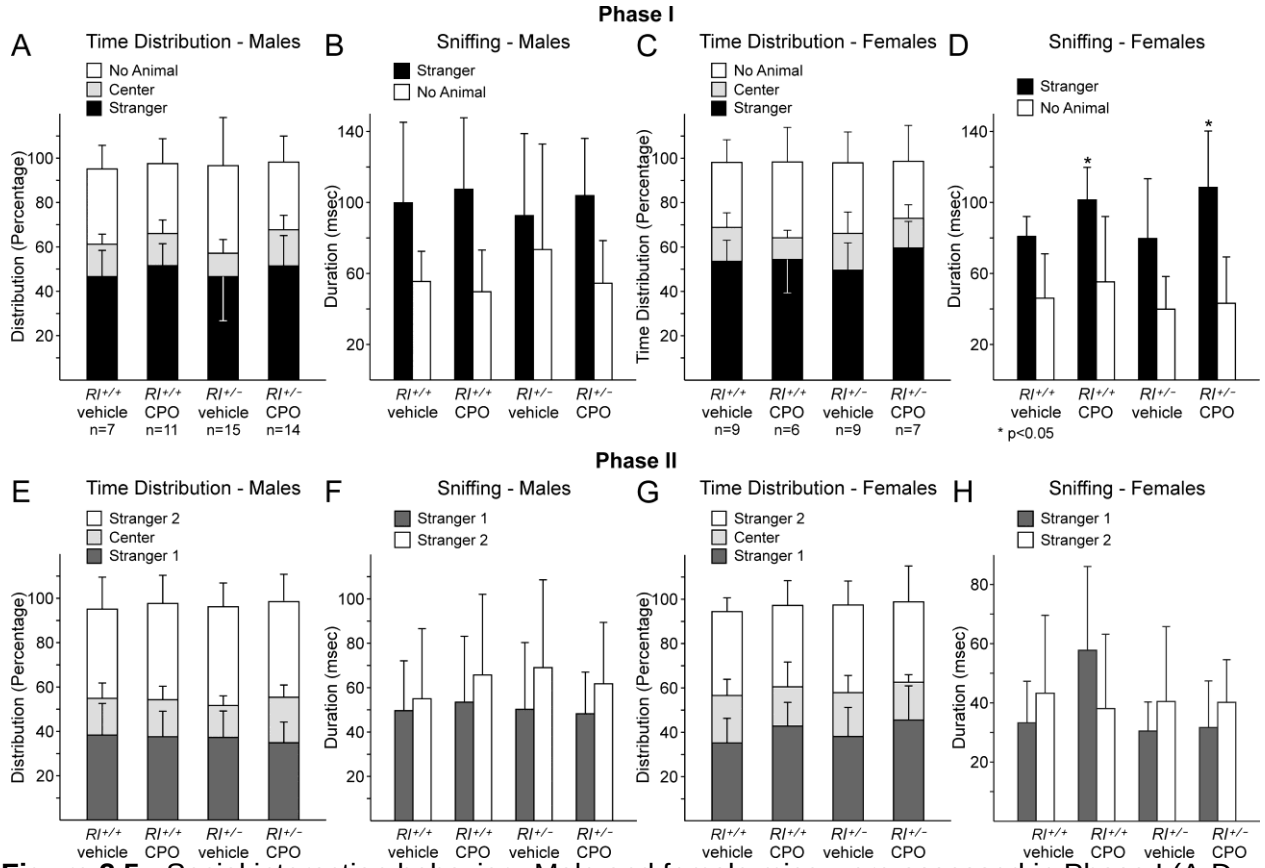

Figure 2.5: Social interaction behavior. Male and female mice were assessed in Phase I (A-D, stranger vs. no stranger) and Phase II (E-H, novel stranger vs. familiar stranger) paradigms. Statistical significance as determined by t-test comparisons with vehicle-treated *RI*$^{+/+}$ animals is indicated by asterisks over the appropriate bars. ANOVA analysis showed no significant change in the time spent with the novel stranger for either Phase I or Phase II (Phase I males: $F(3,43)=0.4010$, $p=0.7530$, Phase I females: $F(3,27)=0.9031$, $p=0.4525$, Phase II males: $F(3,43)=0.2048$, $p=0.8925$, Phase II females: $F(3,27)=0.1341$, $p=0.9389$).

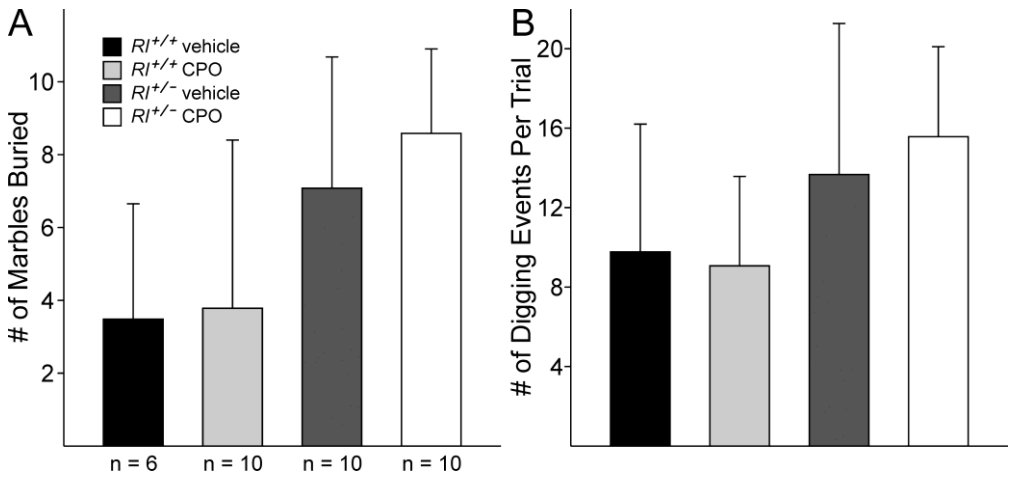

Figure 2.6: Marble burying (A) and digging behavior (B). The marble burying assay was scored for the total number of marbles buried (A) and the number of digging events throughout the trial (B).

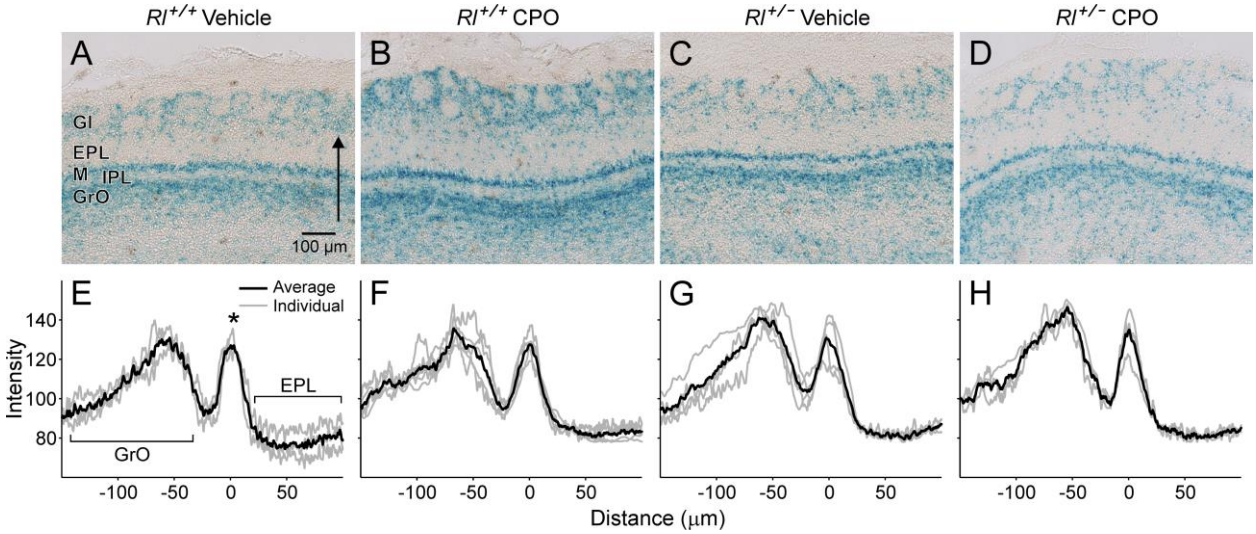

Figure 2.7: ß-galactosidase expression (A-D) and intensity plots (E-H) for the olfactory bulb. The arrow in panel A indicates the span and direction of intensity values plotted in E-H. The asterisk in panel E indicates the position of the mitral cell layer, and the granule cell layer and external plexiform layer are indicated by the brackets. Gl, glomerular layer, EPL, external plexiform layer; M, mitral cell layer; IPL, internal plexiform layer, GrO, graule cell layer.

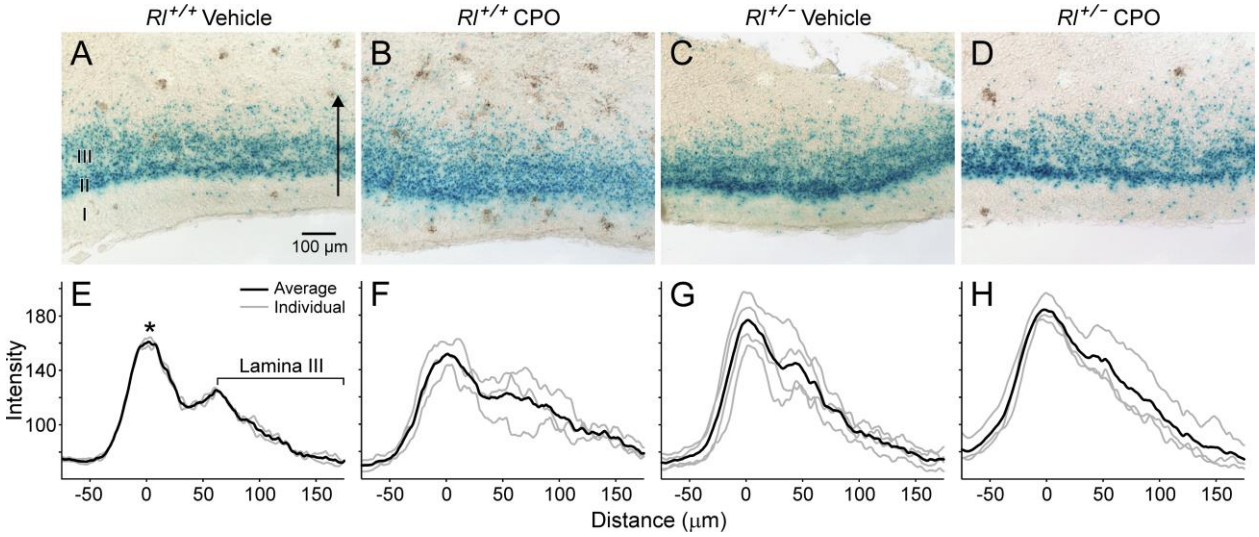

Figure 2.8: ß-galactosidase expression (A-D) and intensity plots (E-H) for the piriform cortex. The arrow in A indicates the span and direction of the intensity plots in E-H. The asterisk in E indicates the position of lamina II and the bracket indicates the position of lamina III. I, II, III, laminae I-III.

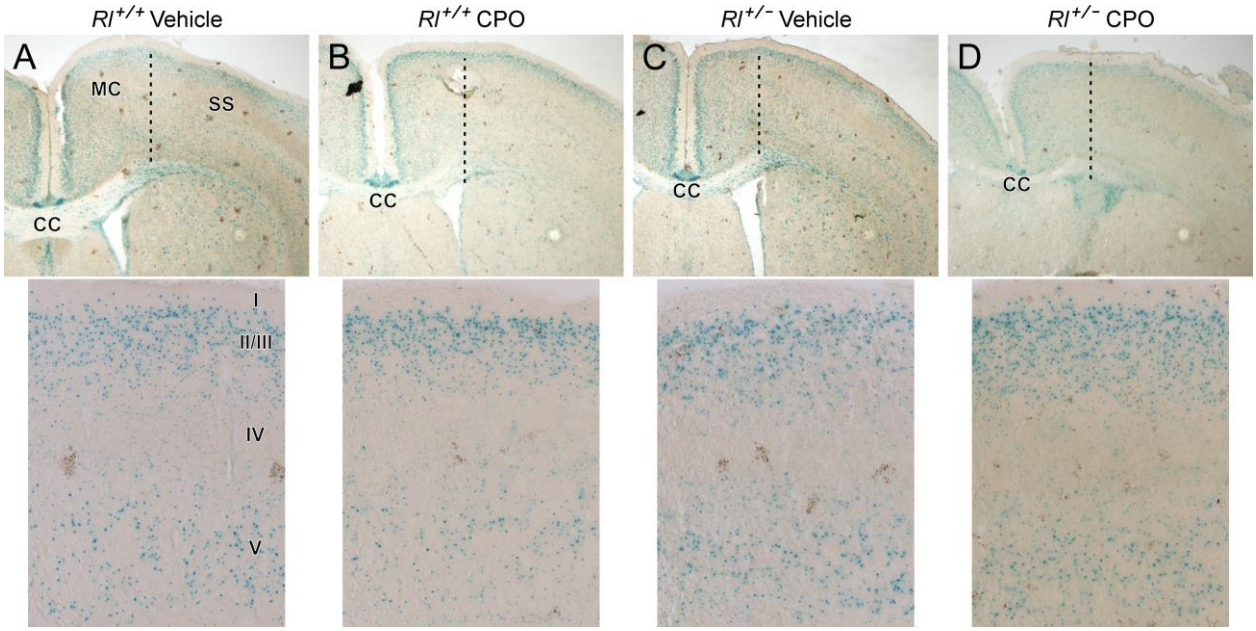

Figure 2.9: A-D, ß-galactosidase expression in the cortex; upper panels are low magnification overviews and lower panels are high magnification views of the somatosensory cortex. The dotted lines in the upper panels indicate the boundary between motor cortex (MC) and somatosensory cortex (SS). The position of the laminae is indicated by roman numerals I, II/III. IV, and V.

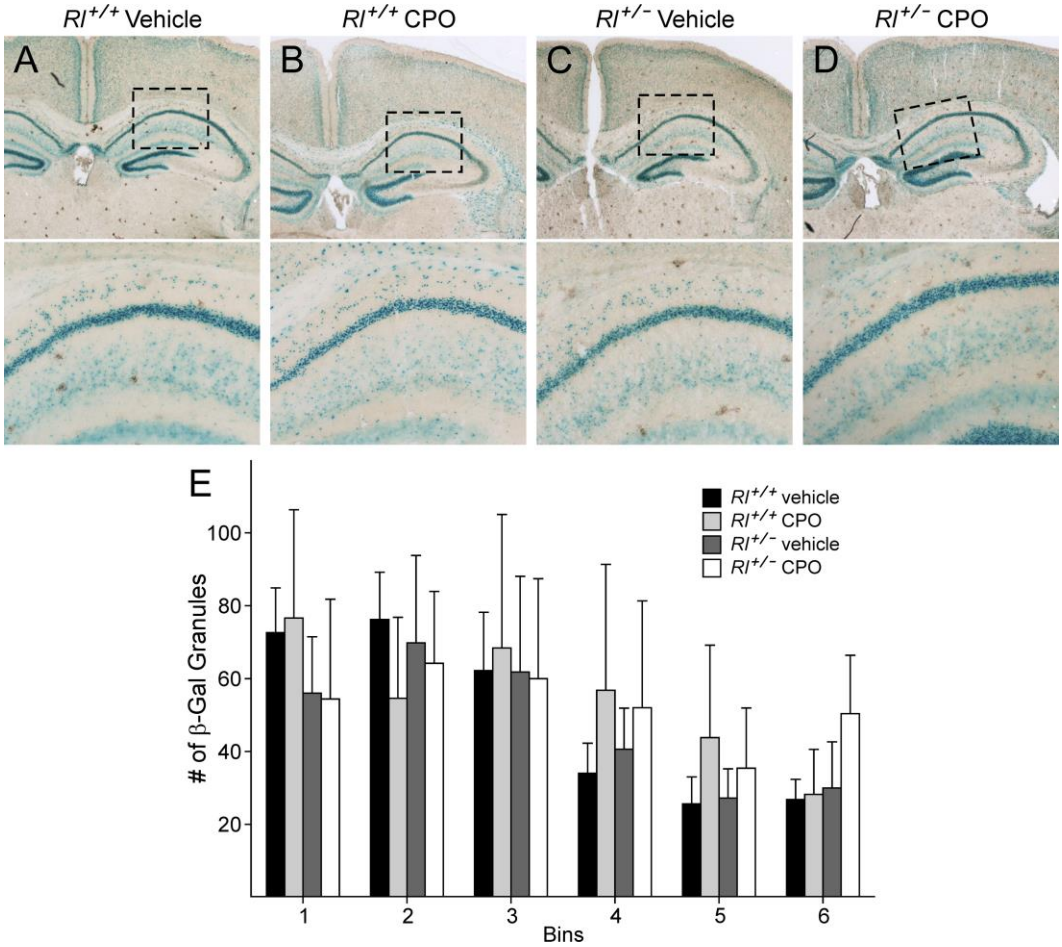

Figure 2.10: ß-galactosidase expression in the hippocampus. A-D, low magnification (upper) and high magnification (lower panels) of the rostral hippocampus. Boxed areas in A-D are illustrated in the lower panels. E, distribution of ß-galactosidase reactivity in the stratum oriens in 6 bins. Bin 1 is the most medial and bin 6 is the most lateral.

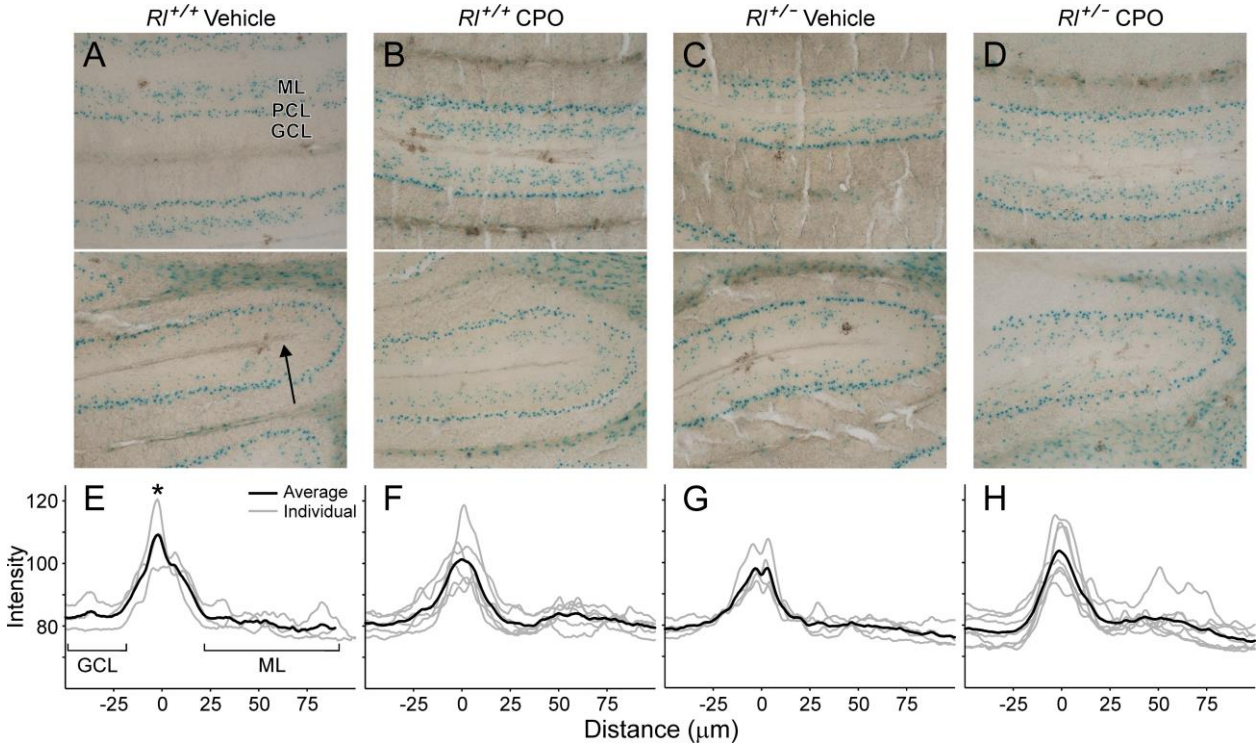

Figure 2.11: A-D, ß-galactosidase expression in the simple (upper) and ansiform (lower) lobules of the vermis of the cerebellum. The arrow in the lower panel of A indicates the span and direction of the intensity plots in E-H. E-H, intensity plots of ß-galactosidase expression in the ansiform lobule. The asterisk in E indicates the position of the Purkinje cell layer, and the position of the granule cell layer and molecular layer are indicated by the brackets. ML, molecular layer, PCL, Purkinje cell layer, GC, granule cell layer

References

Abrahams, B. S., and Geschwind, D. H. (2008). Advances in autism genetics: on the threshold of a new neurobiology. Nat. Rev. Genet. 9: 341-355.

Bacchelli, E., and Maestrini, E. (2006). Autism spectrum disorders: molecular genetic advances. Am. J. Med. Genet. C Semin. Med. Genet. 142C: 13-23.

Bailey, A., Luthert, P., Dean, A., Harding, B., Janota, I., Montgomery, M., Rutter, M. and Lantos, P. (1998). A clinicopathological study of autism. Brain 121: 889-905.

Bauman, M. L. and Kemper, T. L. (2005). Neuroanatomic observations of the brain in autism: a review and future directions. Int. J. Dev. Neurosci. 23: 183-187.

Bennetto, L., Kuschner, E. S., and Hyman, S. L. (2007) Olfaction and taste processing in autism. Biol. Psychiatry 62: 1015-1021.

Betancourt, A. M., Burgess, S. C., and Carr, R. L. (2006). Effect of developmental exposure to chlorpyrifos in the expression of neurotrophin growth factors and cell-specific markers in neonatal rat brain. Toxicol. Sci. 92: 500-506.

Bouchard, M. F., Bellinger, D. C., Wright, R. O., and Weisskopf, M. G. (2010). Attention-deficit/hyperactivity disorder and urinary metabolites of organophosphate pesticides. Pediatrics. 125: e1270-1277.

Brigman, J. L., Padukiewicz, K. E., Sutherland, M. L., and Rothblat, L. A. (2006). Executive functions in the heterozygous reeler mouse model of schizophrenia. Behav. Neurosci. 120: 984-988.

Casanova, M. F., Buxhoeveden, D. P., Switala, A. E., and Roy, E. (2002). Minicolumnar pathology in autism. Neurology 58: 428-432.

Caviness, V. S., Jr. (1982). Neocortical histogenesis in normal and reeler mice: a developmental study based on [3H]thymidine autoradiography. Brain Res. 256: 293-302.

Caviness, V. S., Jr., and Sidman, R. L. (1973). Retrohippocampal, hippocampal, and related structures of the forebrain in the reeler mutant mouse. J. Comp. Neurol. 147: 235-254.

Crawley, J. N. (2004). Designing mouse behavioral tasks relevant to autistic-like behaviors. Ment. Retard. Dev. Disabil. Res. Rev. 10: 248-258.

D'Amelio, M., Ricci, I., Sacco, R., Liu, X, D'Agruma, L., Muscarella, L. A., Guaarnieri, V., Militerni, R., Bravaccio, C., Elia, M., Schneider, C., Melmed, R., Trillo, S., Pascucci, T., Puglisi-Allegra, S., Reichelt, K.-L., Macciardi, F., Holden, J. J. A., and Persico, A. M. (2005). Paroxonase gene variants are associated with autism in North America, but not in Italy: possible regional specificity in gene-environment interactions. Mol. Psychiat. 10: 1006-1016.

D'Arcangelo, G., Miao, G. G., Chen, S. C., Soares, H. D., Morgan, J. I., and Curran, T. (1995). A protein related to extracellular matrix proteins deleted in the mouse mutant reeler. Nature 374: 719-723.

Fatemi, S. H., Snow, A .V., Stary, J. M., Araghi-Niknam, M., Reutiman, T. J., Lee, S., Brooks, A. I., and Pearce, D. A. (2005). Reelin signaling is impaired in autism. Biol. Psychiat. 57:777-787.

Fatemi, S. H., Stary, J. M., and Egan, E. A. (2002). Reduced blood levels of reelin as a vulnerability factor in pathophysiology of autistic disorder. Cell. Mol. Neurobiol. 22: 139-152.

Fischer, J., and Hammerschmidt, K. (2011). Ultrasonic vocalizations in mouse models for speech and socio-cognitive disorders: insights into the evolution of vocal communication. Genes Brain. Behav. 10: 17-21.

Flaskos, J. (2012). The developmental neurotoxicity of organophosphorus insecticides: a direct role for the oxon metabolites. Toxicol. Lett. 209: 86-93.

Förster, E., Jossin, Y., Zhao, S., Chai, X., Frotscher, M., and Goffinet, A. M. (2006). Recent progress in understanding the role of Reelin in radial neuronal migration, with specific emphasis on the dentate gyrus. Eur. J. Neurosci. 23: 901-909.

Gould, G. G., Seillier, A., Weiss, G., Giuffrida, A., Burke, T. F., Hensler, J. G., Rock, C., Tristan, A., McMahon, L. R., Salazar, A., O'Connor, J. C., Satsangi, N., Satsangi, R. K., Gu, T. T., Treat, K., Smolik, C., and Schultz, S. T. (2012). Acetominophen differentially enhances social behavior and cortical cannabinoid levels in inbred mice. Prog. Neuropsychopharmacol. Biol. Psychiatry 38: 260-269.

Haberly. L. B. (2001). Parallel-distributed processing in olfactory cortex: new insights from morphological and physiological analysis of neuronal circuitry. Chem. Senses 26: 551-576.

Heisberger, T., Trommsdorff, M., Howell, B. W., Goffinet, A., Mumby, M. C., Cooper, J. A., and Herz, J. (1999). Direct binding of Reelin to VLDL receptor and ApoE receptor 2 induces tyrosine phosphorylation of disable-1 and modulates tau phosphorylation. Neuron 24: 481-489.

Herbert, M. R., (2010). Contributions of the environment and environmentally vulnerable physiology to autism spectrum disorders. Curr. Op. Neurol. 23: 103-110.

Hisanaga, A., Morishita, S., Suzuki, K., Sasaki, K., Koie, M., Kohno, T., and Hattori, M. (2012). A dinintegrin and metalloproteinase with thrombospondin motifs 4 (ADAMTS-4) cleaves Reelin in an isoform-dependent manner. FEBS Lett., July 20, epub ahead of print.

Howell, B. W., Hawkes, R., Soriano, P., and Cooper, J. A. (1997). Neuronal position in the developing brain is regulated by mouse disabled-1. Nature 389: 733-737.

Jiang, W., Duysen, E. G., Hansen, H., Shlyakhtenko, L., Schopfer, L. M., and Lockridge, O. (2010). Mice treated with chlorpyrifos or chlorpyrifos oxon have organophosphorylated tubulin in the grain and disrupted microtubule structures, suggesting a role for tubulin in neurotoxicity associated with exposure to organophosphorus agents. Toxicol. Sci. 115: 183-193.

Jossin, Y., Gui, L., and Goffinet, A. M. (2007). Processing of Reelin by embryonic neurons is important for function in tissue but not in dissociated cultured neurons. J. Neurosci. 27: 4243-4252.

Keller, F., and Persico, A. M. (2003). The neurobiological context of autism. Mol. Neurobiol. 28:1-22.

Keshvara, L., Magdaleno, S., Benhayon, D., and Curran, T. (2002). Cyclin-dependent kinase 5 phosphorylated disabled-1 independently of Reelin signaling. J. Neurosci. 22: 4869-4877.

Khialeeva, E., Lane, T. F., and Carpenter, E. M. (2011). Disruption of reelin signaling alters mammary gland morphogenesis. Development 138: 767-776.

Kohno, S., Kohno, T., Nakano, Y., Suzuki, K., Ishii, M., Tagami, H., Baba, A., and Hattori, M. (2009). Mechanism and significance of specific proteolytic cleavage of Reelin. Biochem. Biophys. Res. Commun. 380: 93-97.

Lambert de Rouvroit, C., de Bergeyck, V., Cortvrindt, C., Bar, I., Eeckhout, Y., and Goffinet, A. M. (1999). Reelin, the extracellular matrix protein deficient in Reeler mutant mice, is processed by a metalloproteinase. Exp. Neurol. 156: 214-217.

Lane, A. E., Dennis, S. J., and Geraghty, M. E. (2011). Brief report: Further evidence of sensory subtypes in autism. J. Autism Dev. Disorders 41: 826-831.

Laviola, G., Adriani, W., Gaudino, C., Marino, R., and Keller, F. (2006). Paradoxical effects of prenatal acetylcholinesterase blockade on neuro-behavioral development and drug-induced sterotypies in reeler mutant mice. Psychopharmacology 187: 331-344.

Liu, W. S., Pesold, C., Rodriguez, M. A., Carboni, G., Auta, J., Lacor, P., Larson, J., Condie, B. G., Guidotti, A., and Costa, E. (2001). Down-regulation of dendritic spine and glutamic acid decarboxylase 67 expressions in the reelin haploinsufficient heterozygous reeler mouse. Proc. Natl. Acad. Sci. USA. 98: 3477-3482.

Murray, R. M., Jones, P., O'Callaghan, E., Takei, N., and Sham, P. (1992). Genes, viruses and neurodevelopmental schizophrenia. J. Psychiatr. Res. 26: 225-235.

Newschaffer, C. J., Croen, L. A., Daniels, J., Giarelli, E., Grether, J. K., Levy, S. E., Mandell, D. S., Miller, L. A., Pinto-Martin, J., Reaven, J., Reynolds, A. M., Rice, C. E., Schendel, D., and Windham, G. C. (2007). The epidemiology of autism spectrum disorders. Annu. Rev. Public Health 28: 235-58.

Niu, S., Yabut, O., and D'Arcangelo, G. (2008). The reelin signaling pathway promotes dendritic spine development in hippocampal neurons. J. Neurosci. 28: 10339-10348.

Pappas, G. D., Kriho, V., and Pesold, C. (2001). Reelin in the extracellular matrix and dendritic spines of the cortex and hippocampus: a comparison between wild-type and heterozygous reeler mice by immunoelectron microscopy. J. Neurocytol. 30: 413-425.

Persico, A. M., and Bourgeron, T. (2006). Searching for ways out of the autism maze: genetic, epigenetic, and environmental clues. Trends Neurosci. 29: 349-358.

Persico, A. M., D'Agruma, L., Maiorano, N., Totaro, A., Militerni, R., Bravaccio, C., Wassink, T.H., Schneider, C., Melmed, R., Trillo, S., Montecchi, F., Palermo, M., Pascucci, T., Puglisi-Allegra, S., Reichelt, K.L., Conciatori, M., Marino, R., Quattrocchi, C.C., Baldi, A., Zelante, L., Gasparini, P., Keller, F.; Collaborative Linkage Study of Autism. (2001) Reelin gene alleles and haplotypes as a factor predisposing to autistic disorder. Mol. Psychiatry. 6:150-159.

Podhorna, J., and Didriksen, M. (2004). The heterozygous reeler mouse: behavioural phenotype. Behav. Brain Res. 153: 43-54.

Pramatarova, A., Chen, K., and Howell, B. W. (2008). A genetic interaction between the APP and Dab1 genes influences brain development. Mol. Cell. Neurosci. 37: 178-186.

Riccieri, L., Venerosi, A., Capone, F., Cometa, M. F., Lorenzini, Pl, Fortuna, S., and Calamandrei, G. (2006). Developmental neurotoxicity of organophosphorus pesticides: fetal and neonatal exposure to chlorpyrifos alters sex-specific behaviors at adulthood in mice. Toxicol. Sci. 93: 105-113.

Rice, D. S., and Curran, T. (2001). Role of the reelin signaling pathway in central nervous system development. Annu. Rev. Neurosci. 24: 1005-1039.

Roberts, E. M., English, P. B., Grether, J. K., Windhan, G. C., Somberg, L, and Wolff, C. (2007). Maternal residence near agricultural pesticide applications and autism spectrum disorders among children in the California central valley. Environ. Health Perspect. 115: 1482-1489.

Scattoni, M. L., Crawley, J., and Ricceri, L. (2009). Ultrasonic vocalizations: a tool for behavioral phenotyping of mouse models of neurodevelopmental disorders. Neurosci. Biobehav. Rev. 33: 508-515.

Salinger, W. L., Ladrow, P., and Wheeler, C. (2003). Behavioral phenotype of the reeler mutant mouse: effects of *Reln* gene dosage and social isolation. Behav. Neurosci. 117: 1257-1275.

Sigala, S., Zoli, M., Palazzolo, F., Faccoli, S., Zanardi, A., Mercuri, N. B., and Spano, P. (2007). Selective disarrangement of the rostral telencephalic cholinergic system in heterozygous reeler mice. Neuroscience 144: 834-844.

Suzuki, Y., Critchley, H., D., Rowe, A., Howlin, P., and Murphy, D. G. (2003). Impaired olfactory identification in Asperger's syndrome. J. Neuropsychiatry Clin. Neurosci. 15: 105-107.

Teixeira, C. M., Marin, E. D., Sahun, I., Masachs, N. Pujadas, L., Corvelo, A., Bosch, C., Rossi, D., Martinez, A., Maldonado, R., Dierssen, M., and Soriano, E. (2011). Overexpression of reelin prevents the maifestation of behavioral phenotypes related to schizophrenia and bipolar disorder. Neuropsychopharmacology 36: 2395-2405.

Thomas, A., Burant, A., Bui, N., Graham, D., Yuva-Paylor, L. A., and Paylor, R. (2009). Psychopharmacology 204: 361-373.

Tueting, P., Costa, E., Dwivedi, Y., Guidotti, A., Impagnatiello, F., Manev, R., and Pesold, C. (1999). The phenotypic characteristics of heterozygous reeler mouse. NeuroReport 10: 1329-1334.

van den Buuse, M., Halley, P., Hill, R., Labots, M., and Martin, S. (2012). Prog Neuropsychopharmacol. Biol Psychiatry 37: 237-246.

Ventruti, A., Kazdoba, T. M., Niu, S., and D'Arcangelo, G. (2011). Reelin deficiency causes specific defects in the molecular composition of the synapses in the adult brain. Neuroscience 189: 32-42.

Young, D. M., Schenk, A. K., Yang, S. B., Jan, Y. N., and Jan, L. Y. (2010). Altered ultrasonic vocalizations in a tuberous sclerosis mouse model of autism. Proc. Natl. Acad. Sci., USA 107: 11074-11079.

Chapter 3

Decreased Reelin Expression and Organophosphate Pesticide Exposure Affect Adult Brain Morphology

Introduction

Many neuropsychiatric disorders are hypothesized to be due to both genetic and environmental factors. Strong evidence of a genetic component is shown by the heritability of these disorders (Abrahams and Geschwind, 2008). Researchers have begun to identify a number of genetic factors that may influence the progression of neuropsychiatric disorders (Persico and Bourgeron, 2006; Petronis, 2004). Although genes play a major role, there are also a variety of environmental risk factors that may influence these disorders. Examples of environmental risks include maternal infection during pregnancy that correlates with higher rates of schizophrenia (SZ) and Autism Spectrum Disorders (ASD) (Murray et al., 1992) and consumption of antiepileptic drugs during pregnancy increases the risk of ASD and Attention Deficient/Hyperactivity Disorder (ADHD) (Cohen et al., 2013; Christensen et al., 2013). External pollutants such as pesticides, urban air pollution, and heavy metal toxins have been implicated in progression of neuropsychiatric disorders including ASD (Shelton et al., 2012; Freire et al., 2010; DeSoto and Hitlan, 2010).

Although the combination of genetic and environmental factors is the basis for many neuropsychiatric disorders, their exact etiology is poorly understood. As a result, many researchers now assess the cell types and molecular systems that are affected within these developmental disorders, in an attempt to define the cellular and molecular underpinnings of the behavioral manifestations (Maloney et al., 2013). Both postmortem and MRI studies report changes in anatomical regions of susceptibility for these disorders, yet results from these studies are contradictory. For example, some researchers report a decrease in cerebellar size in ASD patients (Courchesne et al., 2001), while other studies found an increase in cerebellar size (Harden et al., 2001). Despite the effect on cerebellar volume changes, Purkinje cells are

known to be susceptible to cell death in the ASD patients (Kern, 2003). Alterations in dendritic spine morphology also are observed, leading to a growing consensus among researchers that ASD and SZ are diseases of the synapse (Penzes et al., 2011).

In the current study, we examined the effects of two potential contributing factors to neuropsychiatric disorders – reduced expression of the secreted signaling protein reelin, and prenatal exposure to an organophosphate pesticide, chlorpyrifos oxon (Laviola et al., 2006; Mullen et al., 2013) – on brain anatomy and cellular morphology. Decreased reelin expression was implicated in multiple neuropsychiatric and degenerative disorders including ASD, schizophrenia, and depression (Guidotti et al., 2000; Fatemi et al., 2005; Chow et al., 2012). Reelin signaling causes phosphorylation of the intracellular adaptor protein disabled 1 (Dab1), leading to a cascade of events that results in stabilization of cytoskeletal proteins. Reelin is a protein of interest to developmental disorders given its high expression during development and its essential role in the proper lamination of cortical and subcortical structures (D'Arcangelo et al., 1995; Hiesberger et al., 1999; Bock et al., 2003). In adult brain, granule cells in the cerebellum and interneurons in olfactory bulb, basal ganglion, cortex, and hippocampus express reelin (Alacatara et al., 1998; Ramos-Moreno et al., 2006; Pesold et al., 1998). Reelin expression is maintained in areas that show high levels of synaptic plasticity, leading researchers to the theory that reelin is important for dendritic spine maturation. These observations implicate reelin as an active participant in the maintenance of synaptic connection and as a factor in the changing plasticity of circuitry within the adult brain (Niu et al., 2008). Some notable differences are reported in heterozygous *reeler* mice ($Reln^{rl/+}$) that express reduced levels of reelin protein. $Reln^{rl/+}$ mice have decreased glutamate decarboxylase 67 (GAD67) expression and decreased dendritic spine density similar to that seen in schizophrenic patients (Liu et al., 2001; Guidotti et al., 2000).

The second factor that we examined is Chlorpyrifos-oxon (CPO), the active metabolite of a common organophosphate pesticide, chlorpyrifos (Whyatt et al., 2002). Studies have

correlated an increase in ASD incidence with prevalence of CPO use in rural California farming communities (Roberts et al., 2007). CPO is a serine protease inhibitor that blocks the effects of acetylcholine esterase and potentiates acetylcholine, disrupting normal neuronal signal regulation. Prenatal exposure to CPO at critical times of development leads to abnormal cell division and cell death due to neurotransmitter toxicity (Slotkin, 2004). Prenatal CPO exposure in male but not female rats causes biochemical changes leading to anhedonia, a phenotype of major depressive disorders (Aldridge et al., 2005). In addition, perinatal CPO administration leads to reduced reelin expression in adolescent rats (Betancourt et al., 2006). During active CPO exposure, however, reelin protein levels are increased in mice (Mullen et al., 2013).

Laviola et al. (2006) first reported an interaction between Reelin and CPO. They reported amelioration of motor and drug-induced behaviors in mice deficient in reelin protein when combined with prenatal CPO exposure. We repeated some of their behavioral tests, verified their amelioration effect ultrasonic vocalizations. In addition, we observed amelioration of anatomical lamination in adolescent animals, where reelin haploinsufficiency tended to increase distance between laminated structures and prenatal CPO decreased distance between laminations, the combination of both insults showed phenotypes more similar to wild type animals (Mullen et al., 2013). Now we further investigate this interaction effect in adult mice, reporting the effects on biochemistry and anatomy of either reelin haploinsufficiency, prenatal CPO exposure, or the combinatorial effect of the two factors. We focused on brain areas where adult reelin levels are established - the neocortex, hippocampus, and cerebellum. We show that prenatal CPO causes a decrease in adult reelin levels as seen in many neuropsychiatric disorders. While the gross anatomical organization of the brain is largely unchanged in *Reln*$^{rl/+}$, reduced reelin expression and CPO exposure cause alterations in dendritic spine morphology in both the hippocampus and cerebellum. We demonstrate that reduced reelin alone is sufficient to decrease overall spine density and to affect one specific class of spines, the mushroom spines. While we found that CPO exposure alone does not affect spine density, but does

increase the ratio of immature to mature spines. The combination of reduced reelin and CPO exposure appears to generate a phenotype highly similar to CPO exposure alone, suggesting that prenatal CPO exposure is sufficient to alter dendritic spine morphology throughout life and that this effect may be independent of protein levels.

Material and Methods

Mouse lines and minipump implantation

Behavioral data presented in Chapter 3 are from Reeler mice (B6C3Fe-a/a-*Reln*$^{rl/+)}$ originally obtained from the Jackson Laboratory (Bar Harbor, ME, U.S.A.) and maintained by interbreeding *Reln*$^{rl/+}$ mice. Animals used for behavioral studies were not subjected to osmotic minipump implantation nor exposed to vehicle or CPO.

Minipump implantation, Golgi staining, Nissl staining, DAPI staining, and Western blotting were performed as described in Chapter 2. Minipumps were implanted into pregnant C57Bl/6 dams at E13.5, following mating with *Reln*$^{Rl/+}$ male mice. Anatomical and biochemical studies were performed on brains collected from mice at P90.

To determine the effects of CPO on interneuron populations, male GAD67 $^{GFP\ +/-}$ C57Bl/6 mice (Tamamaki et al., 2003) were crossed with heterozygous female *reeler orleans (Reln*$^{rl\text{-}Orl/+}$*)* BALB/C mice (gift of Dr. PE Phelps, UCLA; Abadesco et al., 2014). *Reln*$^{rl\text{-}Orl/+}$ produce 50% normal reelin, and 50% mutated protein that is manufactured but not secreted (de Bergeyck et al., 1997). Pregnant mice were implanted with an osmotic mini-pump loaded with 6 mg/ml of the organophosphate pesticide (CPO) or a vehicle control at 13 days of gestation. E13 was chosen because it is the time that interneurons migrate out to the cerebral cortex and hippocampus (E11.5-E16.5) and therefore would allow CPO to act during cortical and hippocampal development (Anderson et al., 2001). Neonates were visually assessed for the expression of the GFP protein using UV illumination at P1-3. Genotype of the *reeler Orleans* allele was determined using PCR as described in Hammond et al. (2006).

Repetitive behavior assessment

Marble burying: Standard shoebox mouse cages were filled with 4 cm of SaniChip bedding and an array of 20 black glass marbles in a 4×5 arrangement was laid on top of the bedding. Mice at P60 were introduced to the arena for a 20-min testing period; at the end of the

testing period, the array was photographed and the buried marbles were counted. Marbles were scored as buried if bedding covered >50 % of the marble. In addition to scoring the number of marbles buried, the activity of the animals was also assessed by scoring for digging behavior for 2 s intervals every 20 s throughout the testing period ($Reln^{+/+}$ Male N=10; $Reln^{+/+}$ Female, N=4; $Reln^{rl/+}$ Male, N=10; $Reln^{rl/+}$ Female, N=9). Marble burying was used as a test of repetitive and perseverative behavior (Thomas et al., 2009).

Nest Construction: Mice at age P60 ($Reln^{+/+}$ Male N=7; $Reln^{+/+}$ Female, N=4; $Reln^{rl/+}$ Male, N=5; $Reln^{rl/+}$ Female, N=8) were placed into a shoebox cage by themselves with 0.5 cm of SaniChip bedding to cover the floor and given a 5.0 cm bedding nestlet. After a 30 min testing period, the bedding height was recorded from the base of the nestlet to the highest bedding fragment. After 24 hours, a photograph of the nest was taken, the height of the nestlet was reassessed, and the untouched nestlet material was weighed. Nest construction was scored based on the parameters established by Deacon (2012).

Hindlimb standing, grooming, and sniffing: Mice age P60 were placed into a new clean shoebox cage with the standard 0.5 cm of SaniChip bedding to cover the floor of the cage and video recorded for 10 min (*Reln*$^{+/+}$ Male N=10; *Reln*$^{+/+}$ Female, N=4; *Reln*$^{rl/+}$ Male, N=10; *Reln*$^{rl/+}$ Female, N=9). The recordings were then scored for the amount of time that the mouse spent grooming, the number of sniffing events and the number of times the mouse stood up on its hind legs.

<u>Western blot for reelin protein fragments</u>

Adult brains were rapidly dissected out of P90 animals (*Reln*$^{+/+}$ Veh N=2; *Reln*$^{+/+}$ CPO, N=4; *Reln*$^{rl/+}$ Veh, N=4; *Reln*$^{rl/+}$ CPO, N=4). One hemisphere was collected for Western blots and the neocortex and hippocampus were isolated; the remaining hemisphere and cerebellum were used for Golgi analysis (see below). The tissue for Western blots was flash frozen in dry ice-ethanol bath and stored at -80 ˚C. Tissue was homogenized and processed with the same

anti-protease cocktail as previously described. Protein bands were resolved as described in Chapter 2.

Histology

Golgi Stain: Individual brain hemispheres and cerebella were stained utilizing an FD Rapid GolgiStain Kit (FD NeuroTechnologies #PK401A). The brains were placed into the Golgi-Cox solution for 2 weeks at room temperature, protected from the light. The cerebella were sagittally sectioned and the cerebral hemispheres were coronally sectioned at 200µm on a vibratome to ensure the visualization of complete and intact cells. Sections were collected in PBS buffer then mounted on subbed glass microscope slides. After mounting, the sections were reacted with the silver-mercury solutions provided within the kit and cover slipped utilizing Permount (Fisher SP15-500).

Analysis: Sholl analysis was performed on camera lucida drawings made of CA1 pyramidal cells (total n=86 cells, N=14 animals: *Reln*$^{+/+}$ Veh: n=21, *Reln*$^{+/+}$ CPO: n=21, *Reln*$^{rl/+}$ Veh: n=23, *Reln*$^{rl/+}$ CPO: n=21). The first Sholl ring was placed 50 µm from the center of the cell body; subsequent rings were placed every 25 µm to a total distance of 300 µm; each ring was scored for the total number of processes that crossed it.

Spine characterization and classification was performed on high magnification z-stack images collected on a Zeiss Apotome microscope in bright field using a 100x oil immersion objective. Classifications of dendritic spines were performed in the hippocampus and cerebellum. In the hippocampus, two dendrites on the CA1 pyramidal cells - the first apical oblique dendrite (AO) closest to the soma and a basal dendrite (Bas) after the first branch point off of the soma - were selected for analysis. The number of animals (N) and number of cells (n) are provided in Supplementary Table 1. In the cerebellum we characterized spines on the distal dendrites of Purkinje cells that were stained in lobules III, IV/V, VI, and VII. The number of animals (N) and number of cells (n) are described within supplementary table 2. All protrusions

off of the dendrites between 30 and 115 µm in length were classified as mushroom, thin, stubby, branched, or filopodial spines following criteria established by Lee et al. (2004). Mushroom spines had discernible stalks and heads, thin spines were longer than mushroom spines without a discernible head, stubby spines were as thick as the head of a mushroom spine, branched spines had a bifurcated stalk and filopodial spines were defined as those thin spines whose width was less than half the width of the dendrite it was protruding from, but longer than the total width of the dendrite. Both total spine length and cross-sectional areas of mushroom heads were measured. The total number of spines examined is presented below and the numbers of mushroom spines assessed in the hippocampus and cerebellum are presented in Supplementary Tables 1 and 2.

Group (N of Animals)	Hippocampus n of cells=96 per dendritic section		Cerebellum – Distal Dendrites N of cells=80 cells per lobe	
	Apical Oblique Dendrite	Basal Dendrite	Anterior Lobe	Posterior lobe
$Reln^{+/+}$ Veh (N=2)	709	897	425	460
$Reln^{+/+}$ CPO (N=4)	500	623	642	616
$Reln^{rl/+}$ Veh (N=4)	608	486	656	665
$Reln^{rl/+}$ CPO (N=4)	526	536	631	719
Total (N=14)	2,343	2,542	2,354	2,460

Image analysis was performed using AxioVision software (Zeiss). Two-way ANOVA and Holm-Sidak post-hoc analysis were performed in Sigma Plot.

Nissl stain: Coronal and sagittal 30 µm sections were collected from P90 mice and stained using standard Nissl histology (*Reln*$^{+/+}$ Veh, N=3; *Reln*$^{+/+}$ CPO, N=4; *Reln*$^{rl/+}$ Veh, N=3; *Reln*$^{rl/+}$ CPO, N=4). Slides were photographed using a Zeiss Axioskop with a cooled CCD camera; quantification and analysis were performed using ImageJ software. Two-way ANOVA and Holm-Sidak post-hoc analysis were performed in Sigma Plot.

Immunofluorescence (IF): Free floating tissue sections of 30 µm coronal neocortex and hippocampus of *Reln*$^{rl\text{-}Orl/+}$ / GAD67 $^{GFP\ +/-}$ Balb/C treated prenatally with either vehicle or CPO were stained with rat anti-Ctip2 (Abcam AB18465; 1:500 dilution), mouse anti-reelin G10 (EMD

Millipore MAB5364; 1:500 dilution), or chicken anti-GFP (Novus NB100-1614; 1:1000 dilution), and counterstained with DAPI. The M1 region of the frontal motor cortex and rostral hippocampus vehicle-treated tissue (N=3) and prenatal CPO treated tissue (N=4) were examined to determine interneuron subtype. The M1 cortex was subdivided into three regions based upon Ctip2 and DAPI staining: layer I, layers II - IV, and layers V – VI. Hippocampi were divided into 3 regions: dentate gyrus, striatum radiatum/striatum moleculare, and striatum pyramidal/striatum oriens/striatum alveus. Images were collected on Zeiss LSM 510 Confocal microscope and assessed in Neurolucida. Two-way ANOVA and Holm-Sidak post-hoc analysis were performed in Sigma Plot.

Results

Behavioral Assessment

We assessed repetitive and perseverative behaviors using marble burying and nest construction tests. Previously we reported that male $Reln^{rl/+}$ showed an increase in marble burying behavior, but did not assess female mice. To further evaluate marble burying in animals with reduced reelin expression, we asked if there is a sex difference. We also determined whether or not both male and female mice showed any other signs of repetitive behavior by assessing grooming, rearing, and sniffing behavior and examined nest building as a measure of a routine task.

In the marble burying test, male and female *Reln*$^{+/+}$ and *Reln*$^{rl/+}$ were scored for the number of marbles that were over 50% buried (out of 20 possible) and the number of observed number of digging moments throughout the 20 min task. The *Reln*$^{rl/+}$ males (n=10) showed a significant increase in the number of marbles buried (Figure 3.1A) when compared with their $Reln^{+/+}$ male littermates (n=10), similar to our previous report (Mullen el al., 2013). Females, however, did not differ by genotype ($Reln^{rl/+}$ n=9; $Reln^{+/+}$ n=4). The numbers of digging moments (Figure 3.1B) were also assessed, but this behavior not differ by sex either.

To evaluate other repetitive behaviors, mice were scored on the amount of time spent grooming (Figure 3.1C), the number of rearing movements (Figure 3.1D), and the number of sniffing events (Figure 3.1E) within a 10 min trial. There were no significant differences in any of these behaviors. Interestingly, the number of sniffing events did not increase within the male $Reln^{rl/+}$ even though the number of marbles buried did increase. Both sniffing events and marble burying are considered exploratory behaviors. Thus, male $Reln^{rl/+}$ do not increase general exploratory behaviors, but only showed a specific increase in the marble burying task.

Nest construction is a routine mouse behavior and alterations in this behavior were used to show the onset of Alzheimer-like symptoms in the Tg2576 mouse model (Deacon, 2012; Deacon et al., 2008). Recently nest building was proposed as a repetitive or compulsive-like

behavior (Angoa-Pérez et al. 2013). We assessed nesting behavior of male and female adult mice by measuring the height of the nest after the mouse is allowed 30 min and 24 hours with a new nestlet (Figure 3.1F). At the 24-hour mark, the nest is given a score on a scale of 5 (0 meaning the nestlet is barely disturbed to 5 being a fully developed nest; Figure 3.1G). There were no significant changes in the nest heights or nesting score.

Reelin expression in adult $Reln^{rl/+}$ animals after prenatal CPO exposure

Western blots were used to assess the effects of prenatal CPO exposure on reelin protein levels in adult cerebral (Figure 3.2A) and hippocampal cortices (Figure 3.2B). Full length reelin protein is approximately 410 kDa and upon protein processing, results in two smaller fragments at 330kDa and 180kDa (Lambert de Rouvroit et al., 1999; Jossin et al., 2007). As expected, overall reelin protein levels were reduced in *Reln*$^{rl/+}$ versus *Reln*$^{+/+}$ mice. Reductions were statistically significant in the neocortex, but not in the hippocampus. Following CPO treatment, significant reductions in both the 410 and 330 kDa bands were noted. Analysis of cortical samples across all four groups showed effects of both genotype and treatment. $Reln^{rl/+}$ mice had reduced levels of both the 410 kDa and 330 kDa bands, while CPO exposure also reduced expression of these two bands. Post-hoc analysis confirmed that all groups, when compared to vehicle-treated $Reln^{+/+}$ animals, showed a significant decrease in reelin protein levels in both 410kDa and 330kDa bands.

CPO effect on GABAergic interneurons

Reelin is known to be expressed preferentially in GABAergic interneurons in the adult neocortex and hippocampus (Alcantara et al., 1998; Pesold et al., 1998). To determine if CPO exposure specifically affected reelin-positive GABAergic interneurons, we compared the effects of CPO and vehicle treated animals on the distribution of these in the Balb/C GAD67$^{GFP/+}$ / $Reln^{Rl\text{-}Orl/+}$ adult mice (Abadesco et al., 2014) implanted with osmotic minipumps loaded with

CPO. The motor cortex was subdivided into three regions. DAPI was used to distinguish the largely cell-free lamina I from the rest of the cortex, Ctip2 was used as a biomarker for lamina V-VI, the remaining cortex was assessed as lamina II-IV. Lamination of the cerebral cortex did not appear to be affected by prenatal CPO exposure.

For further evaluation, interneurons were counted in lamina I (L1), laminae II-IV (LII-IV), and laminae V-VI (LV-VI) at postnatal day 60. Cell density and distribution were quantified to determine three distinct subpopulations of interneurons: 1) GAD67+ (GFP^+ only), 2) GAD67+/Reelin+ (GFP^+, Rl^+), and 3) Reelin+/GAD67- (GFP^-, Rl^+). We assessed the density and distribution of each of these types of cells in vehicle-treated (n=3) and CPO-treated (n=4) animals.

Approximately 60% of the labeled cells within the motor cortex expressed only GAD67 (Figure 3.3C, F). The majority of these neurons were found in LII-IV and LV-VI, with only a few cells in LI. Approximately 33% of the cells are the GAD67 and Reelin+ interneurons (Figure 3.3D, F). The majority of these cells were found in LI, with the remainder distributed across LII-IV and LV-VI. Approximately 9% of labeled cells were Reelin+ only. The largest number of these cells were found in LV-VI, with fewer cells in LII-IV and LI, respectively. Prenatal CPO treatment did not affect the distribution of any of these cell types.

We also investigated the effect of prenatal CPO on the distribution of GAD67 and reelin-expressing interneurons in the hippocampus (Figure 3.4). We divided the hippocampus in four regions based upon anatomical markers: 1) the granular and hilus regions of the dentate gyrus (DG), 2) the stratum moleculares of both dentate gyrus and hippocampus proper (Mol), 3) the strata radiatum and lacunosum (Rad), and 4) the alveus and strata pyramidale and oriens (Py/Or). There were approximately equal numbers of GAD67+ and GAD67+/Reelin+ cells, and significantly fewer Reelin+/GAD67- cells. GAD67+/Reelin+ cells were most abundant in the DG, with fewer cells in the Mol, Rad and Py/Or. In contrast, GAD67+ cells were most abundant in the Py/Or, with fewer cells in the DG and Rad, and very few cells in the Mol. Reelin+/GAD67-

cells were largely seen in the Mol. Prenatal CPO exposure did not affect the distribution of any of these cell types in the hippocampus.

Gross morphology of the hippocampus:

Based on our prior observations of subtle changes in hippocampal organization in adolescent animals with either reduced reelin or CPO exposure (Chapter 2; Mullen et al.,2013), we wondered if there would be any long-term effects in adults. We examined hippocampal lamination using DAPI-stained tissue, plotting histograms of the intensity of staining in the two pyramidal regions CA1 and CA3 in all 4 experimental groups (Figure 3.5A-D). CA1 was not affected by any experimental conditions, but CA3 appeared to have an expansion of the pyramidal cell layer due to CPO exposure. Because some histograms have trailing tails at the base of the peaks, to reduce the ambiguity of where the peak starts/ends we measured the full width at half maximum (FWHM) intensity (Figure 3.5E). CA3 was significantly widened due to prenatal CPO effect ($F_{1,10}$=8.284, p=0.016). Post-hoc analysis showed a significant increase pyramidal layer width in CPO-treated *Reln*$^{rl/+}$ animals ($p<0.05$) and a trend toward significance in CPO-treated *Reln*$^{+/+}$ animals (p=0.09).

We then looked at the complexity of dendritic branching of CA1 pyramidal cells in Golgi-stained sections (Figure 3.6). Camera lucida drawings were prepared for CA1 pyramidal cells (*Reln*$^{+/+}$ Veh: n=21, *Reln*$^{+/+}$ CPO: n=21, *Reln*$^{rl/+}$ Veh: n=23, *Reln*$^{rl/+}$ CPO: n=21) and subjected to Sholl analysis (Figure 3.6A-H). Beginning approximately 75 µm and continuing as far as 300 µm away from the soma, there was a slight but significant decrease in pyramidal cell dendritic complexity due to prenatal CPO exposure in both *Reln*$^{+/+}$ and *Reln*$^{Rl/+}$ animals. Reelin haploinsufficiency alone had no effect on dendritic branching, but prenatal CPO exposure did affect CA1 dendritic complexity.

Dendritic spines in the hippocampus

Previous studies reported that reelin influences dendritic spine maturation and plasticity in hippocampal neurons (Liu et al., 2001; Niu et al., 2008), so we next examined dendritic spines on CA1 pyramidal cells. First, to characterize the effect of each experimental condition on general properties of the dendritic spines, we analyzed total spine density and created probability curves of the dendritic spine lengths found on the apical oblique (AO) and basal dendrites (Bas) (Figure 3.7). Second, we then classified the morphology of each of the spines from both the apical and basal dendrites to further elucidate the effect of each variable (Figure 3.8). Representative images of Golgi stained dendritic spines from each experimental condition are shown in Figure 3.7A. All statistics for these analyses are reported in Supplementary Table 1.

Total spine density decreased significantly on apical oblique dendrites in vehicle-treated *Renl*$^{rl/+}$ animals and slightly on basal dendrites in both vehicle-treated *Reln*$^{rl/+}$ and CPO-treated *Reln*$^{rl/+}$ animals (figure 3.7B), suggesting that reduced reelin expression can affect spine density independently of CPO treatment. This confirms the reduction in dendritic spines previously reported by Niu et al. (2008). Dendritic spines appeared slightly longer on both apical oblique and basal dendrites following CPO treatment (Figure 3.7C, D), while apical oblique spines were slightly shorter in vehicle-treated *Reln*$^{rl/+}$ animals. Combining both reduced reelin and CPO exposure returned spine lengths to normal.

Following the classification established by Lee et al. (2004), we identified dendritic spines as immature (thin, branched or filopodial) or as mature (mushroom or stubby) spines (Figure 3.8). We then asked if the distribution of spine types in the hippocampus was affected by either genetic or prenatal CPO treatment. Thin spines were increased on apical oblique dendrites in CPO-treated *Reln*$^{+/+}$ animals, but were unaffected in all other conditions and on basal dendrites (Figure 3.8A). Branched spines were increased on apical oblique dendrites in CPO-treated *Reln*$^{+/+}$ and CPO-treated *Reln*$^{rl/+}$ animals and on basal dendrites in CPO-treated

Reln$^{+/+}$ animals. Filopodial spines were also increased on apical oblique dendrites in CPO-treated *Reln*$^{+/+}$ and CPO-treated *Reln*$^{rl/+}$ animals and on basal dendrites in vehicle-treated *Reln*$^{rl/+}$ animals and in CPO-treated *Reln*$^{+/+}$ and CPO-treated *Reln*$^{rl/+}$ animals. Thus, all three categories of immature spines appeared to be affected by loss of reelin expression, CPO exposure, or both. Mature stubby spines showed little difference on apical oblique dendrites, although there were slight increases in this spine type in CPO-treated *Reln*$^{+/+}$ animals, and slight decreases in vehicle-treated *Reln*$^{rl/+}$ animals. In contrast, both mushroom spine density and mushroom spine head area were decreased in all treatment groups when compared to vehicle-treated *Reln*$^{+/+}$ animals. Together, these data suggest an increase in immature spines, and a concomitant decrease in at least one category of mature spines.

Gross morphology of the cerebellum

Reelin plays a crucial role within development of the cerebellum, allowing proper migration of Purkinje cells (PC) from midbrain regions out to the rhombic lip (Miyata et al., 1996). Both reelin and Dab1, the intracellular component to the reelin signaling cascade, are expressed in the adult cerebellum (Abadesco et al., 2014), suggesting that reelin signaling may play a role in PC maintenance and circuit formation (Ramos-Moreno et al., 2006; Pesold et al., 1998). It was reported that PC loss occurs in both *Reln*$^{rl/+}$ and CPO-treated *Reln*$^{+/+}$ animals (Hadj-Sahraoui et al., 1996; Biamonte et al., 2009), thus we investigated if a combination of the two factors would affect gross cerebellar organization and PC morphology. We examined Nissl-stained sagittal sections of the cerebellum and quantified cross-sectional area of the lobules in the vermis (Figure 3.9). There were no differences in lobule area and no gross morphological alterations in the Purkinje cell layers (data not shown).

Dendritic spines in the cerebellum

We examined PC distal spiny dendrites (Figure 3.10A) in four different lobules of the cerebellum (III, IV/V, VI, VIII). The anterior lobe, comprised of lobules I-V, is typically associated with information coming from the spinal cord and plays an integral part in sensorimotor systems. The posterior lobe, comprised of lobules VI-IX, receives information primarily from corticopontine pathways associated with higher order cognitive processing (Schmahmann 2013). To understand the role that reelin and CPO may have on dendritic spine morphology, we looked for regional differences in PC spine morphology in these two lobes. We first characterized the total spine density and created probability curves of the dendritic spine lengths found in the anterior and posterior lobes (Figure 3.10). We then classified each of the spines from both the anterior and posterior lobe PC dendrites to determine if there were changes in the distribution of the different spine types (Figure 3.11). All statistics for these analyses are reported in Supplementary Table 2. Representative images of Golgi stained dendritic spines within each experimental condition and lobule are shown in Figure 3.10A.

Total spine density (Figure 3.10B) of anterior lobules showed little difference in between the 4 groups. Spine density was moderately reduced in posterior lobules VI and VIII in vehicle-treated *Reln*$^{rl/+}$, however CPO treatment appeared to restore lobule VI and VIII spine density in *Reln*$^{rl/+}$ to levels similar to vehicle treated *Reln*$^{+/+}$ mice. Probability curves of dendritic spine length suggested a slightly higher probability of shorter spines in the anterior lobe in both vehicle-treated and CPO-treated *Reln*$^{rl/+}$ mice (Figure 3.10C), but no change in spine length in the posterior lobe (Figure 3.10D).

Spine type distribution was also examined in the different lobe and lobules. Thin spines (Figure 3.11A) were reduced to nearly the same extent in both *Reln*$^{rl/+}$ and CPO-treated *Reln*$^{+/+}$ animals in both the anterior and posterior lobes, and the reduction was statistically significant in all but lobule VI. Combining both reduced reelin and CPO exposure did not affect thin spine

distribution in the anterior lobe, but increased thin spine density in the posterior lobe, primarily in lobule VIII. Branched spines (Figure 3.11B) in the anterior lobe seemed to be unaffected either by loss of reelin expression or by CPO exposure. However, in the posterior lobe, CPO treatment increased the number of branched spines in *Reln*$^{rl/+}$ mice to above that seen in *Reln*$^{+/+}$ mice. Filopodial spines (Figure 3.11C) appeared to be the most affected class of spines. CPO treatment dramatically increased the number of filopodial spines in *Reln*$^{+/+}$ animals and decreased reelin expression also increased filopodial spines. In the anterior lobe, CPO exposure appeared to have no effect on spines in *Reln*$^{rl/+}$ mice, while in the posterior lobe, CPO-treated *Reln*$^{rl/+}$ mice had a large increase in filopodial spines, significantly above that seen in *Reln*$^{+/+}$ animals, and above the level seen in *Reln*$^{rl/+}$ mice, suggesting a significant effect of CPO treatment on filopodial spines in the posterior lobe.

Mature spine types appeared to be somewhat less affected than immature spines. *Reln*$^{rl/+}$ mice had mild to moderate increases in stubby spines, primarily in the anterior lobe, while stubby spine density was similar that seen in vehicle-treated *Reln*$^{+/+}$ animals in the posterior lobe (Figure 3.11D). CPO treatment increased stubby spine concentration slightly by itself, but the combination of reduced reelin expression and CPO exposure returned stubby spine density to normal levels. Mushroom spines were increased following CPO treatment in *Reln*$^{+/+}$ animals in all but lobule VIII, while decreased reelin expression appeared to have no independent effect on these spines. Combining reduced reelin and CPO exposure either returned mushroom spine density to normal levels or caused a slight overall reduction in mushroom spine density (Figure 3.11E). Mushroom spine cross-sectional area (Figure 3.11F) also decreased in *Reln*$^{rl/+}$ and CPO-treated animals particularly in the posterior lobe. The greatest decrease was observed in CPO-treated *Reln*$^{rl/+}$ animals (Figure 3.11G, H). Interestingly, mushroom spines appeared larger overall in the posterior lobe than in the anterior lobe (Figure 3.11F).

Discussion

The study reported here demonstrates long-lasting behavioral, biochemical, and anatomical alterations stemming from reduced reelin protein expression and/or embryonic CPO exposure. Our behavioral studies showed an increase repetitive behavior evaluated by the marble burying test in male *Reln*$^{rl/+}$, but not female *Reln*$^{rl/+}$ mice, but no differences in the two other repetitive behavior tests, nest construction and digging. These results suggest a very precise interaction between expressed levels of the *reelin* gene and subsequent effects on behavior, and illustrate the necessity for a thorough examination of the behavioral consequences of genetic status. Reduced reelin expression can affect cellular distribution in the piriform cortex, hippocampus, and cerebellum (Mullen et al., 2013) and the maturity and distribution of dendritic spines in the hippocampus and cerebellum (this study). Either of these alterations might contribute to the observed behavioral changes. Although we did not examine the effect of CPO exposure on this behavior in female mice, our prior study of male mice (Mullen et al., 2013) did not show any additive or ameliorative effects of CPO exposure, leading us to conclude that CPO alone does not affect this behavior.

We also found that embryonic CPO exposure could affect adult levels of reelin protein. In a prior study (Mullen et al., 2013), we demonstrated that both full length and cleaved reelin protein was decreased in embryonic mice, but that CPO exposure paradoxically restored reelin expression to near wild-type levels. In the current study, we examined if these changes in reelin protein were maintained in adult animals. To our surprise, we found that embryonic CPO exposure resulted in a decrease in reelin protein levels in both the cortex and hippocampus in adult *Reln*$^{+/+}$ and *Reln*$^{rl/+}$ mice, and this was not due to a decrease in reelin-expressing interneurons in the adult cortex and hippocampus. In the cortex, both full-length reelin and cleaved fragments were decreased below the levels seen in *Reln*$^{rl/+-}$ mice in CPO-exposed *Reln*$^{rl/+}$mice, while in the hippocampus, CPO exposure did not increase the amount of full-length

or cleaved reelin, as detected in embryonic mice (Mullen et al., 2013). These results suggest that there are substantial long-term biochemical effects resulting from prenatal CPO exposure.

Our failure to see similar results in embryonic animals suggests that these biochemical changes occur slowly, after the period of CPO exposure is completed. Exposure to high levels of CPO produces acute neurotoxicity, likely stemming from a cholinergic crisis stemming from inhibition of AChE (Flaskos, 2012). Lower level exposure of CPO also results in neurodevelopmental toxicity, possibly through alteration of microtubule structure (Jiang et al., 2010), which may alter cell migration during neurodevelopment. Our current study also suggests that prenatal CPO exposure affects dendritic spine morphology and distribution, which may contribute to neurodevelopmental disorders. CPO exposure may interact with the reelin signaling pathway in several ways. First, CPO acts as an ACHE inhibitor, contributing to acute neurotoxicity at high levels of exposure, and the cholinergic system is known to modulate reelin expression. Nicotine, a cholinergic agonist, can restore reelin mRNA levels in *Reln*$^{rl/+}$ mice in several brain regions (Romano et al., 2013). Second, CPO may act directly on reelin itself, by modulating the activity of the enzymes that cleave reelin (Casida and Quistad, 2005), and delayed polyneuropathy has been attributed to exposure to CPO and other organophosphates (Costa, 2006).

Finally, we found significant and lasting effects of reduced reelin expression and CPO exposure on brain morphology. Our prior study found disruptions in gross cellular organization in the olfactory bulb and piriform cortex, the hippocampus, and the cerebellum (Mullen et al., 2013). In the current study, we show region-specific disruptions of hippocampal pyramidal cell distribution, along with significant changes in dendritic spine morphology and distribution. In this study, we found that CPO exposure, but not reduced reelin expression, affected the placement of pyramidal cells in the CA3 region of the hippocampus. Functional studies have suggested that different CA regions subserve different functions in the hippocampus, with cells in the CA1 regions distinctly responsive to spatial information while cells in the CA3 region integrate spatial

and non-spatial information (reviewed in Igarashi et al., 2014). These different functions may result from the different type of neuronal circuitry at play in each region, with recurrent collateral circuitry evident in CA3, and little cellular interconnectivity in CA1 (Lee et al., 2004). Our observation of cell displacement in CA3 might then argue that loss of reelin and/or CPO exposure may affect integration of information in CA3 more strongly than the place recognition modulated by CA1.

Hippocampal cellular complexity and hippocampal and cerebellar dendritic spine morphology and distribution were affected by both reduced reelin expression and CPO exposure, with cellular complexity more strongly affected by reductions in reelin, and dendritic morphology affected in specific regions by CPO exposure. Similar to our previous anatomical studies, combinatorial effects of both reduced reelin and CPO exposure were seen in hippocampal cellular complexity and dendritic spine morphology, with complexity restored and dendritic spine abnormalities partially ameliorated in CPO-exposed $Rl^{+/-}$ animals. Interestingly, there was little evidence of combinatorial interactions on dendritic spine morphology in the cerebellum. Here, CPO exposure alone appeared sufficient to skew the spine profile toward greater representation of immature spines. Our observations suggest an interaction between reduced reelin and CPO exposure in regulating hippocampal cellular morphology, which is more pronounced in apical oblique dendrites, and a singular effect of CPO exposure on cerebellar spines. Prenatal CPO exposure may interfere with spine maturation, possibly through modulation of cholinergic inputs to the hippocampus and cerebellum; manipulation of ACh activity is known to affect synaptic maturation and plasticity (reviewed in Yakel, 2014).

Regardless of their origin, alterations in dendritic spine morphology are widely known to be contributory factors in neurodevelopmental disorders including schizophrenia and ASDs. Our findings point to effects of both loss of reelin and CPO exposure on dendritic spine morphology, although these effects may be quite specific in terms of region or cell type affected. However, this may also provide an explanation for the behavioral deficits observed in our mice,

in which only specific behaviors were found to be altered. Neurodevelopmental disorders, including schizophrenia and ASDs likely stem from multiple factors; characterization of endophenotypes resulting from each contributing factor may thus provide only a partial characterization of a complex disorder.

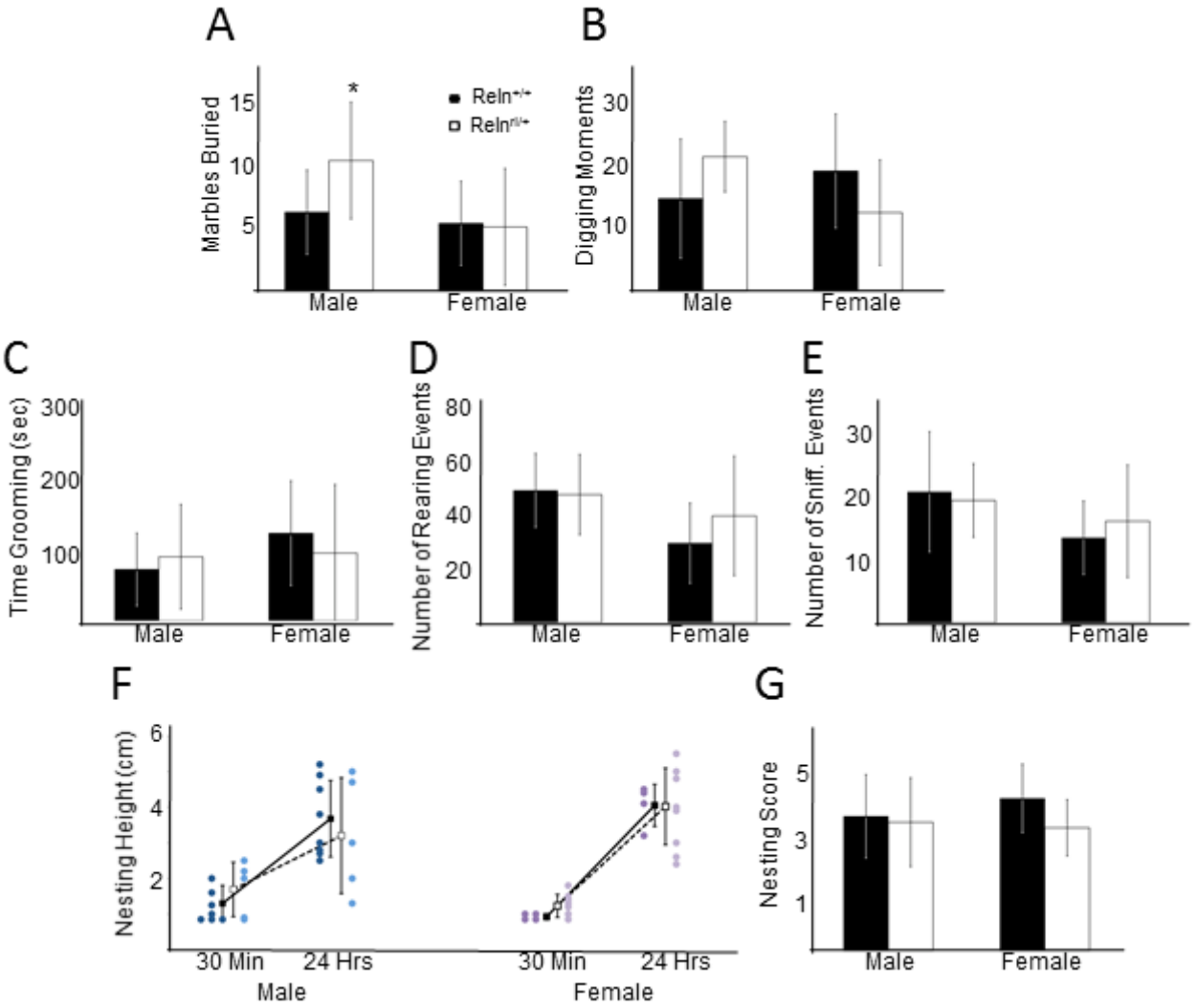

Figure 3.1: Assessment of repetitive behaviors. $Reln^{+/+}$ mice (black bars) and $Reln^{+/rl}$ (white bars) were assessed with marble burying (A) and digging (B); results are divided by sex. Other repetitive measures during a 10 min observation period, grooming (C), number of rearing events on the hindlegs (D), and number of sniffing events (E). Nesting heights with individual points of either male (dark blue: $Reln^{+/+}$; light blue: $Reln^{rl/+}$) or females (dark purple: $Reln^{+/+}$; light purple: $Reln^{+/rl}$) are shown next to mean ± SD (F) taken after 30 min and 24 hrs with were significantly affected, nor the nesting score (G). Bars are representative of mean ± SD. *, $p<0.05$, students' t-test.

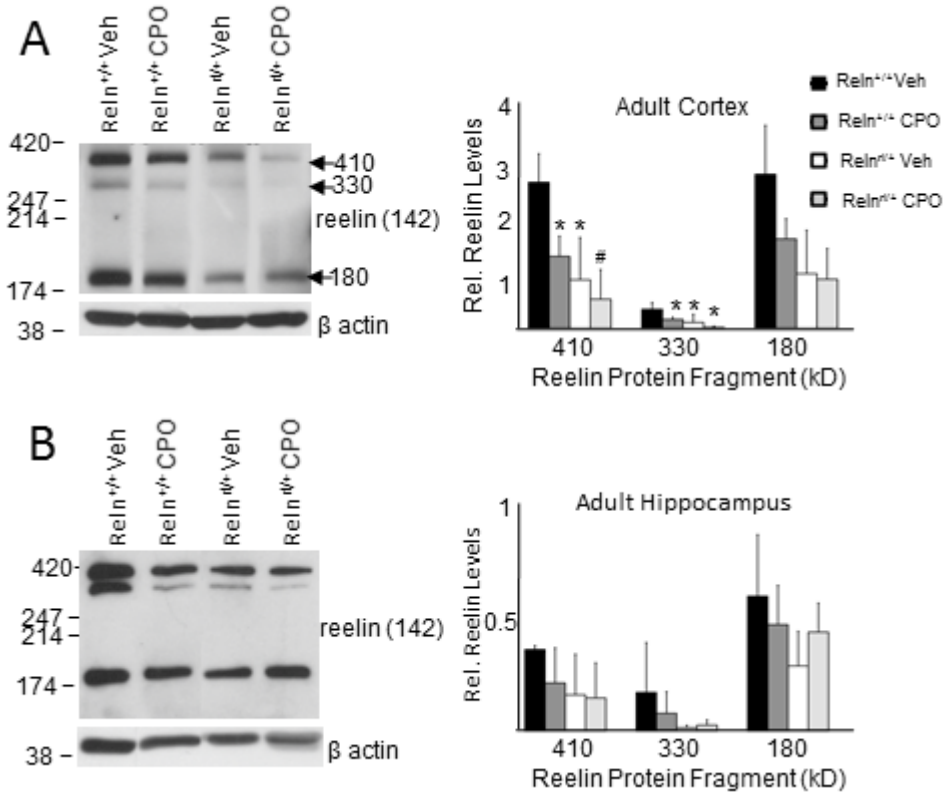

Figure 3.2: Reelin expression in the adult cerebral cortex and hippocampus. Western blots from cortical (A) and hippocampal (B) tissue of *Reln*$^{+/+}$ VEH (Black), *Reln*$^{+/+}$ CPO (Dark Grey), *Reln*$^{rl/+}$ VEH (White), and *Reln*$^{rl/+}$ CPO (Light Grey) mice. Western blotting was resolved using reelin and compared to ß-actin. Three bands (arrows) representing full-length reelin (410 kDa) and two breakdown products (330 kDa and 180 kDa) were observed; each band was independently quantified. Bars are representative of mean ± SD. Statistics were based upon two-way ANOVA. Significance determined based on comparison to vehicle-treated Reln$^{+/+}$ animals (*$p<0.05$, $^{\#}p<0.01$) as calculated by Holm-Sidak post-hoc analysis.

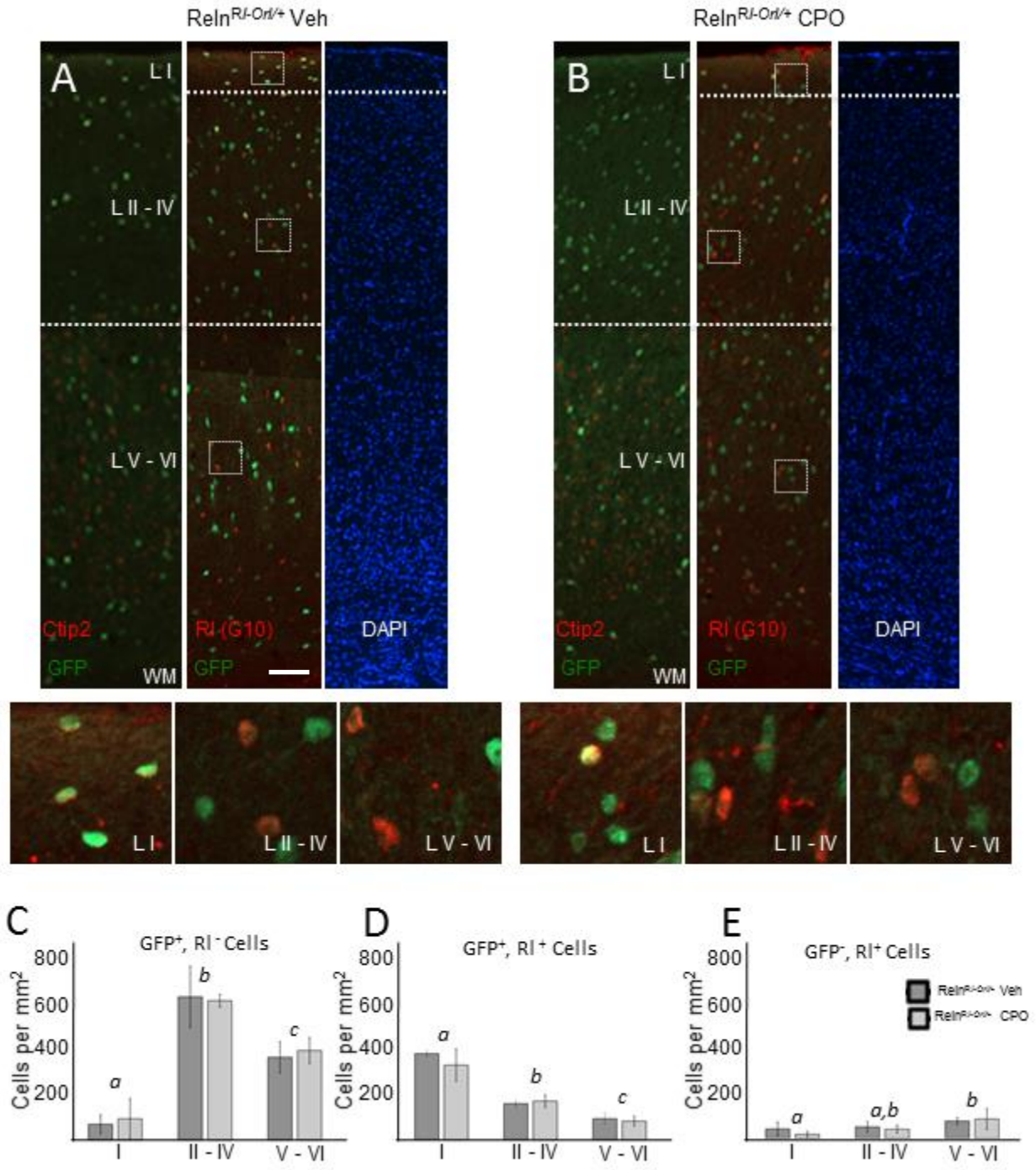

Figure 3.3: Interneuronal expression of reelin (Rl) and GAD67-GFP in the motor cortex. GAD67-GFP and reelin (G10) antibody were used to identify GABAergic interneurons in vehicle (A) and CPO-treated (B) motor cortex of adult mice; Ctip2 labeling demonstrated the position of LV-VI. Interneurons were quantified based upon expression pattern: GFP-positive cells without

reelin expression (GFP+/Rl-; C), GFP-positive cells with reelin expression (GFP+/Rl+; D), and GFP negative cells with reelin expression (GFP-/Rl+; E). Bars are representative of mean ± SD. Laminae with different lowercase letters (*a*, *b*, *c*) are significantly different ($p<0.01$) from one another. Significance was determined by two-way ANOVA. Scale bar= 100 μm

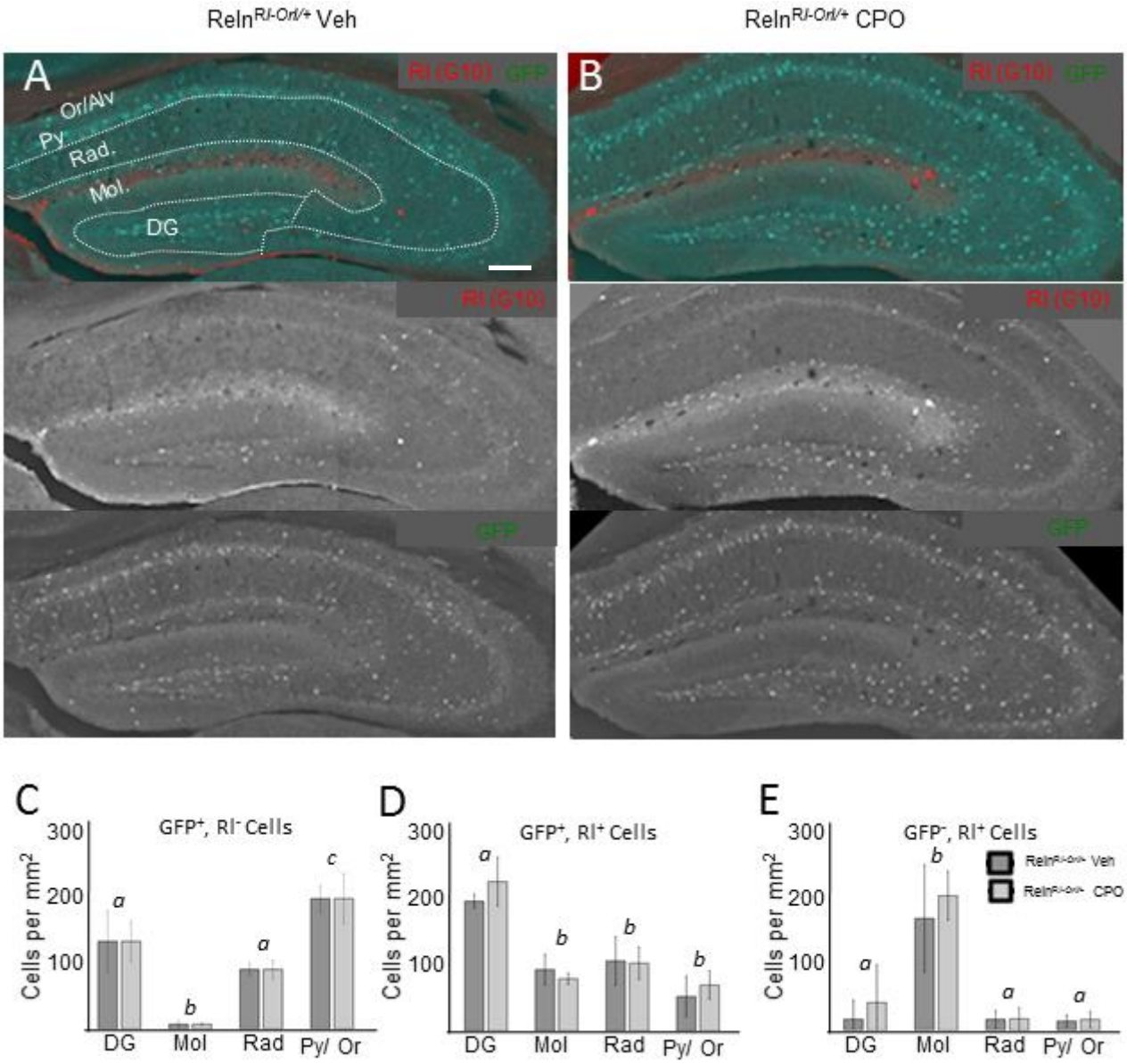

Figure 3.4: Coexpression of reelin and GAD67 in the hippocampus identified reelin-expressing GABAergic interneurons. Vehicle-treated (A) and CPO-treated (B) hippocampi were examined for the coexpression of GAD67-GFP and reelin to identify reelin-expressing GABAergic interneurons. Merged images of reelin (red, Rl) and GFP (green) of the hippocampus and individual channels are represented. Interneurons were quantified based upon expression pattern: GFP positive cells without reelin expression (GFP+/Rl-; C), GFP-positive cells with

reelin expression (GFP+/Rl+; D), and GFP negative cells with reelin expression (GFP-/Rl+; E) within 4 anatomical areas: 1) granule cell and hilus regions of the dentate gyrus (DG); 2) stratum moleculare of both dentate gyrus and hippocampus proper (Mol); 3) strata radiatum and lacunosum (Rad); and 4) alveus, stratums pyramidale and oriens (Py/Or) and Bars are representative of mean ± SD. Anatomical region with different lowercase letters (*a*, *b*, *c*) are significantly different ($p<0.01$) from one another. Significance was determined by two-way ANOVA. Scale bar= 200 μm

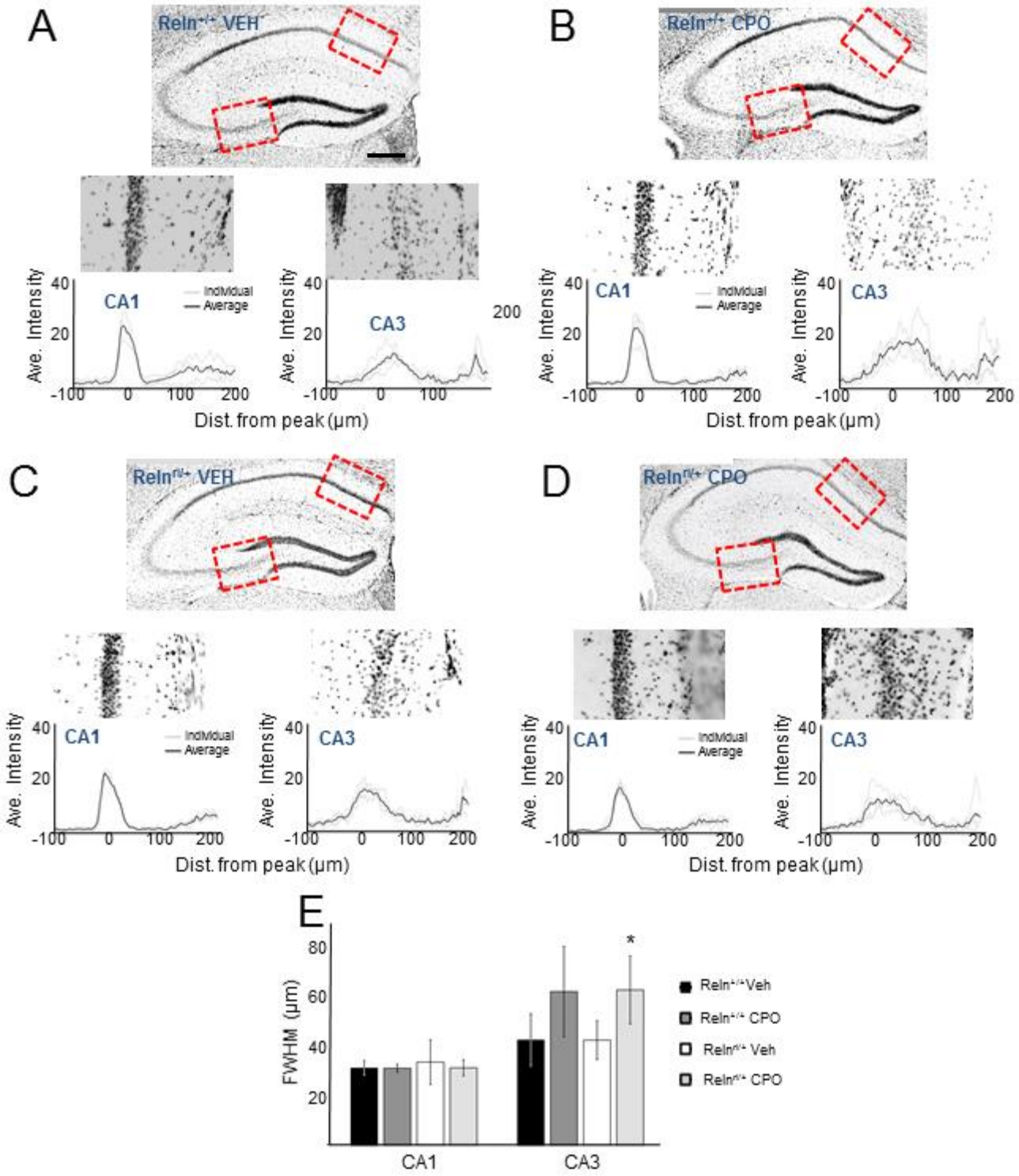

Figure 3.5: Pyramidal cell distribution in CA1 and CA3 in the hippocampus of vehicle-treated *Reln*$^{+/+}$ mice (A), CPO-treated *Reln*$^{+/+}$ mice (B), vehicle-treated *Reln*$^{rl/+}$ (C), and CPO-treated *Reln*$^{rl/+}$ (D) as revealed with DAPI labeling. The black and white pictures are inverted

representations of DAPI fluorescence (white = black; black = blue). Boxed regions were used to create histograms of labeling, with measurements taken across the boxes in the direction of the arrows (A). High magnification of each area is provided. Histograms are group data, where the black line represents the average and grey lines represent individual animals. Quantification (E) of the half width of pyramidal cell layers within each group. Bars are representative of mean ± SD. Statistics were based upon two-way ANOVA. Significance determined based on comparison to *Reln*$^{+/+}$ Veh (*$p<0.05$) as calculated by Holm-Sidak post-hoc analysis. Scale bar= 150 μm

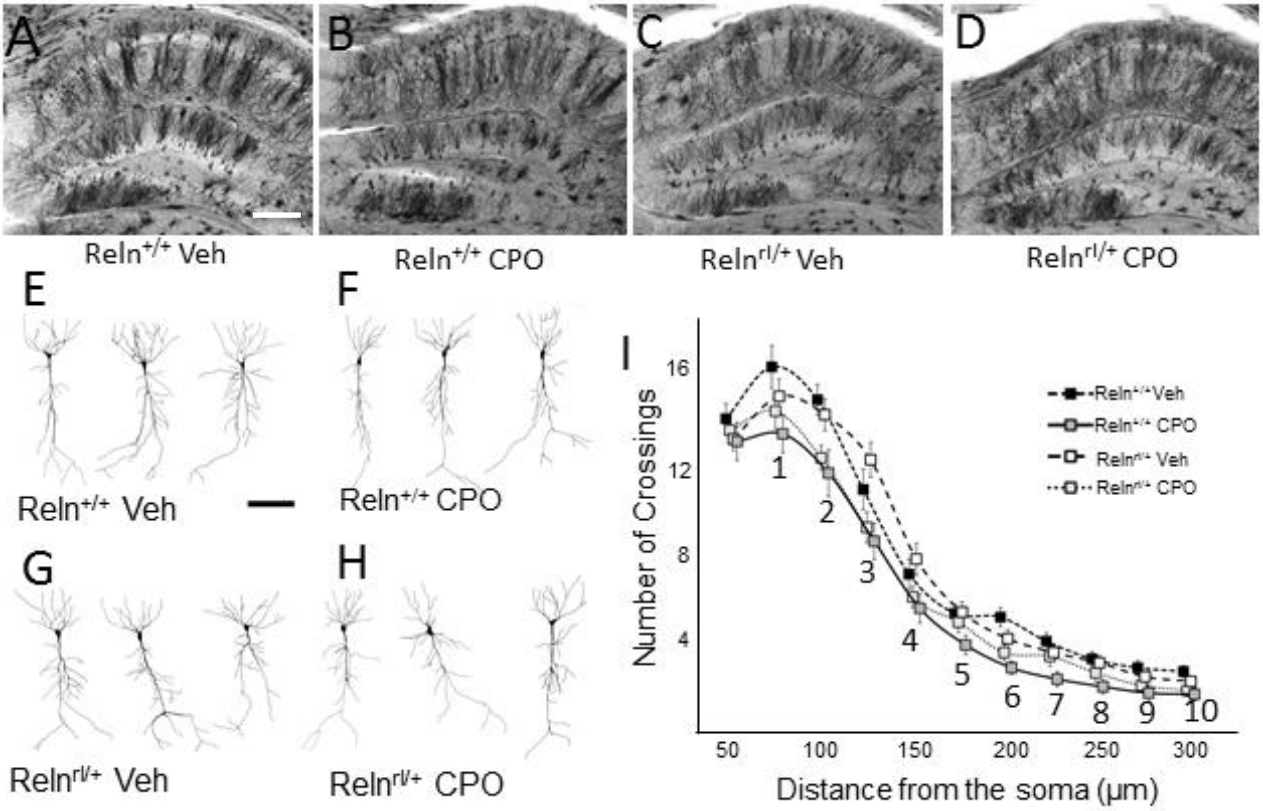

No.	Dist.	F statistic	P value		No.	Dist.	F statistic	P value
1	75µm	$F_{1,82}$=4.700	p=0.033		6	200µm	$F_{1,82}$=14.892	p<0.001
2	100µm	$F_{1,82}$=11.404	p=0.001		7	225µm	$F_{1,82}$=13.287	p=0.013
3	125µm	$F_{1,82}$=11.154	p=0.001		8	250µm	$F_{1,82}$=5.951	p=0.017
4	150µm	$F_{1,82}$=6.371	p=0.014		9	275µm	$F_{1,82}$=6.420	p=0.013
5	175µm	$F_{1,82}$=4.459	p=0.038		10	300µm	$F_{1,82}$=6.894	p=0.010

Figure 3.6: Golgi-stained hippocampi (A-D) and camera lucida drawings (E-H) from all groups: *Reln*$^{+/+}$ Veh (A,E), *Reln*$^{+/+}$ CPO (B,F), *Reln*$^{rl/+}$ Veh (C,G), and *Reln*$^{rl/+}$ CPO (D,H). Sholl analysis (I) Two way ANOVA results are from a main CPO effect: F statistic and p value are reported for each numeric location on the Sholl plot. Sholl analysis is represented by mean ± SE. (A) Scale bar= 150 µm (E) Scale Bar=100 µm

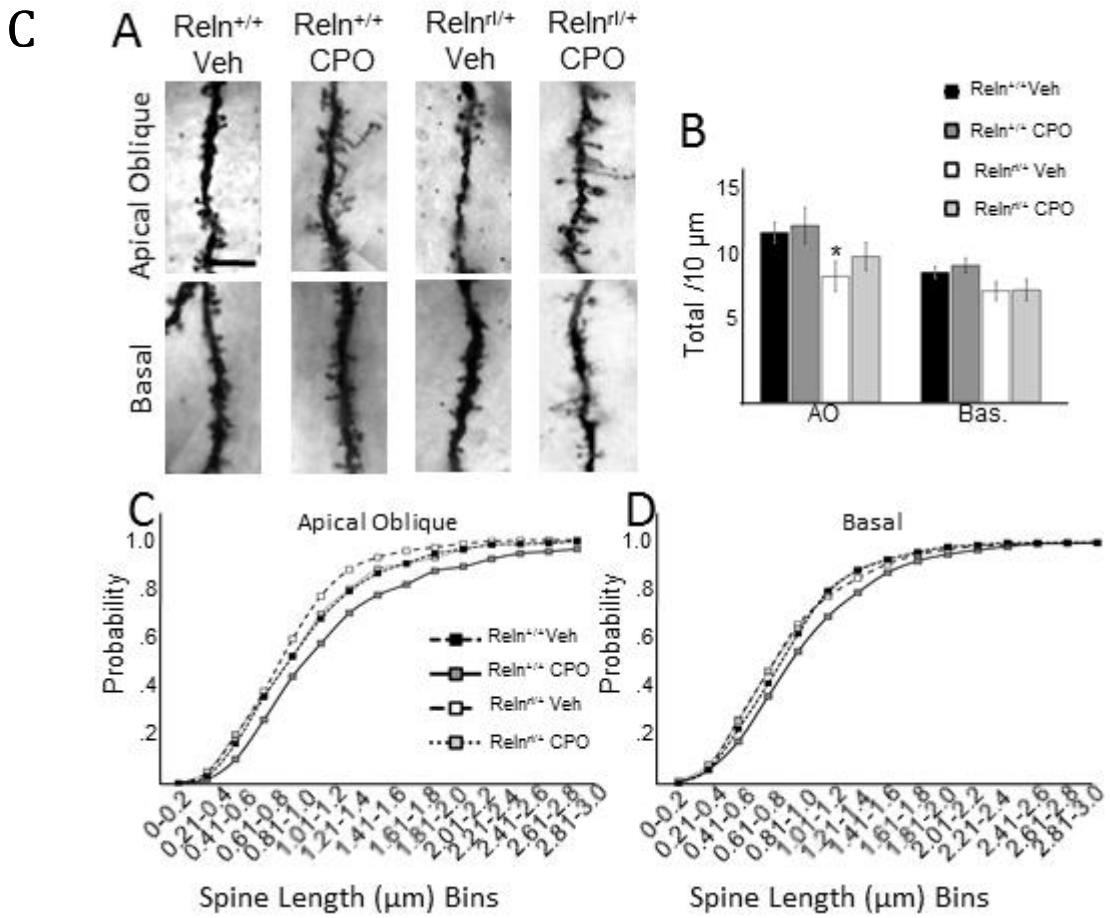

Figure 3.7: Analysis of dendritic spines on CA1 pyramidal cells. Apical oblique and basal dendrites of Golgi impregnated cells (A) were analyzed for total spine density (B) and spine length of apical oblique (C) and basal (D) dendrites. Bars are representative of mean ± SE. Statistics were based upon two-way ANOVA. Significance determined based on comparison to *Reln*$^{+/+}$ Veh (*$p<0.05$) as calculated by Holm-Sidak post-hoc analysis. Scale bar = 5µm

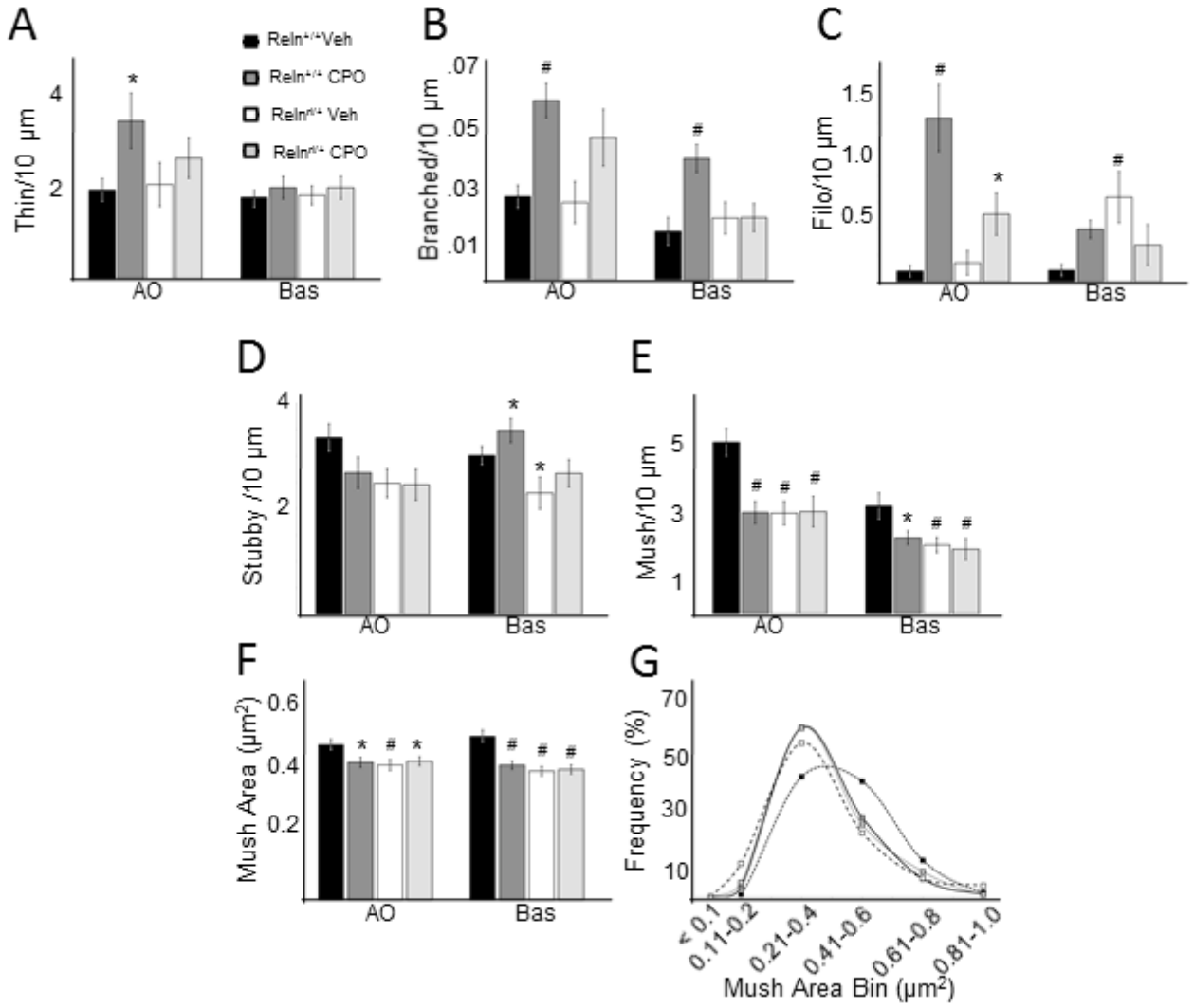

Figure 3.8: Characterization of dendritic spines within each apical oblique (AO) and basal (Bas). Group analysis of vehicle-treated *Reln*$^{+/+}$ mice (black bars), CPO-treated *Reln*$^{+/+}$ mice (dark grey), vehicle-treated *Reln*$^{rl/+}$ (white bars), and CPO-treated Reln$^{rl/+}$ (light grey bars) showing the density of each type of spine per 10µm of dendrite length. Immature spines: thin (A), branched (B), and filopodial (Filo; C); and stable spines: mushroom (D) and stubby (E) were assessed for each dendrite type. Cross sectional areas of mushroom spines (F) are measured and reported in µm^2. Frequencies of spine area are representative of both AO and Bas spine cross sectional area. Bars are representative of mean ± SE. Statistics were based upon two-

way ANOVA. Significance determined based on comparison to *Reln*$^{+/+}$ Veh (* $p<0.05$; # $p<0.01$) as calculated by Holm-Sidak post-hoc analysis.

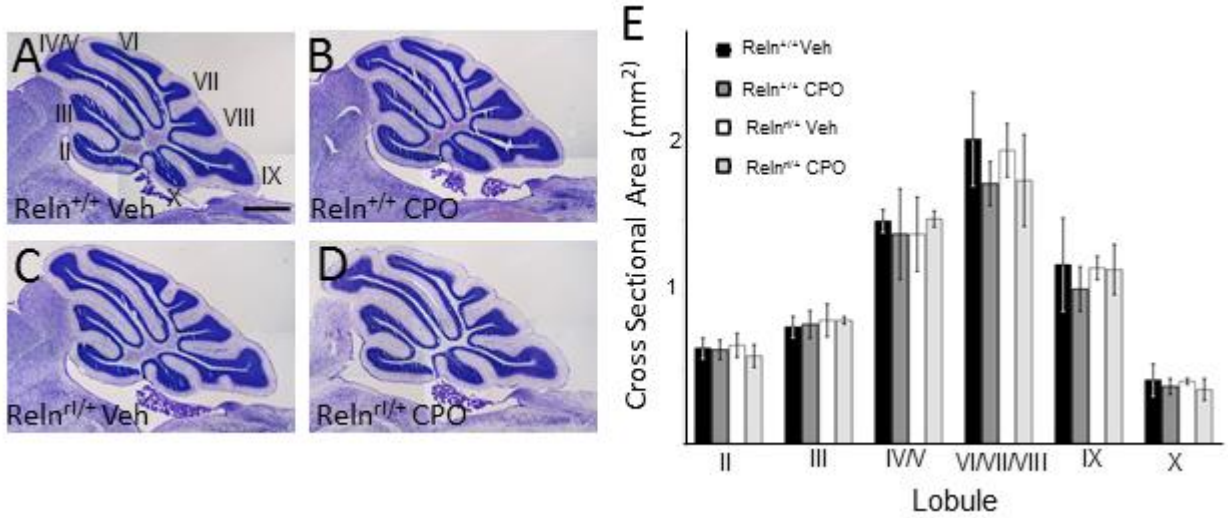

Figure 3.9: Adult cerebellar vermal sections of *Reln*$^{+/+}$ (A,B) and *Reln*$^{rl/+}$ (C,D) exposed prenatally to either vehicle (A,C) or CPO (B,D). Lobules II through X are labeled in A. Cross sectional area of cerebellar lobules was calculated (E). Bars are representative of Mean ± SD. Significance was assessed by two-way ANOVA. No significant variation was found. Scale bar = 1 mm

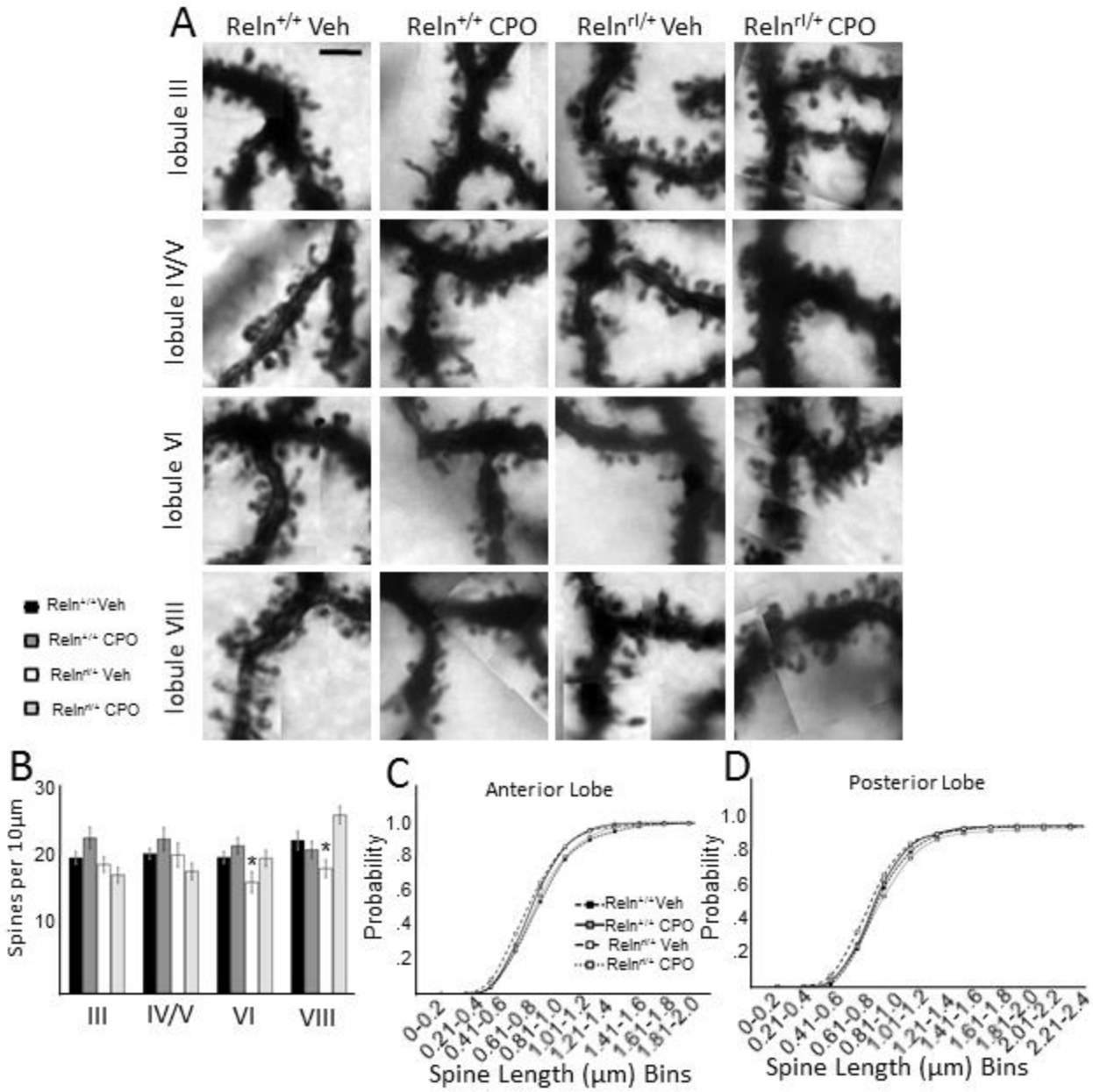

Figure 3.10: Dendritic spine analysis of anterior lobe (lobule III and IV/V) and posterior lobe (lobules VI and VIII) of distal dendrites of Purkinje cells (A). Each lobule was characterized separately overall spine densities (B). Probability of spine length was assessed within the anterior lobe (C) and the posterior lobe (D). Bars are representative of mean ± SE. Statistics were based upon two-way ANOVA. Significance determined based on comparison to $Reln^{+/+}$ Veh (*$p<0.05$) as calculated by Holm-Sidak post-hoc analysis. Scale bar=5µm

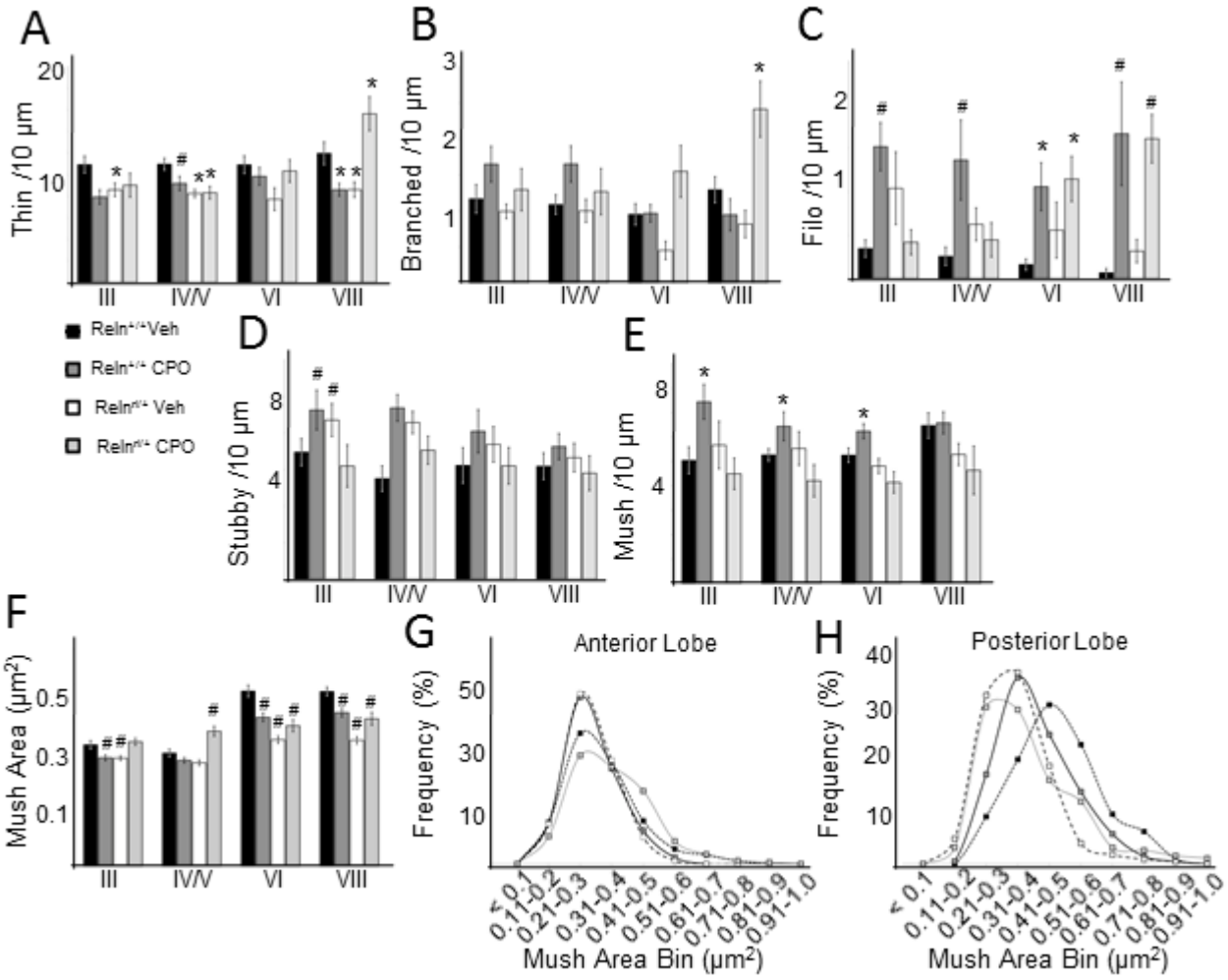

Figure 3.11: Characterization of dendritic spines within each lobule. Group analysis of vehicle-treated *Reln*$^{+/+}$ mice (black bars), CPO-treated *Reln*$^{+/+}$ mice (dark grey), vehicle-treated *Reln*$^{rl/+}$ (white bars), and CPO-treated *Reln*$^{rl/+}$ (light grey bars) reporting the density of each classification of spine type per 10µm of dendritic length. Immature spines: thin (A), branched (B), and filopodial (Filo; C); and stable spines: mushroom (D) and stubby (E) were assessed within each lobule. Cross sectional areas of mushroom spines (F) are measure and reported in µm^2. Frequency of spine area for anterior lobe (G) and posterior lobe (H). Bars are representative of mean ± SE. Statistics were based upon two-way ANOVA. Significance

determined based on comparison to vehicle-treated *Reln*$^{+/+}$ mice (* $p<0.05$; # $p<0.01$) as calculated by Holm-Sidak post-hoc analysis.

Anatomical Structure	Spine Type	Effect		
		CPO	$Reln^{rl/+}$	$Reln^{rl/+}$ x CPO
Hippocampus				
Overall Spine Density		=	↓	↓
Stable	Mushroom	↓↓	↓↓	↓↓
	Area	↓↓	↓↓	↓↓
	Stubby	=	↓	↓
Immature	Thin	↑	=	=
	Branched	↑↑	=	=
	Filopodial	↑↑	=	=
Cerebellum Anterior Lobe				
Overall Spine Density		↑	=	=
Stable	Mushroom	↑↑	=	=
	Area	↓↓	↓↓	↑
	Stubby	↑	↑	=
Immature	Thin	↓	↓	↓
	Branched	=	=	=
	Filopodial	↑↑	=	=
Cerebellum Posterior Lobe				
Overall Spine Density		=	↓	=
Stable	Mushroom	↑	=	↓
	Area	↓↓	↓↓	↓↓
	Stubby	=	=	=
Immature	Thin	↓	↓↓	↑
	Branched	=	↓	↑
	Filopodial	↑↑	=	↑↑

Table 3.1: Summary of dendritic spine analysis. Symbols are changes with respect to *Reln*$^{+/+}$ Veh animals. No change (=), moderately significant increase (↑) or decrease (↓), or highly significant increase (↑↑) or decrease (↓↓).

Supplementary table 1: Two-way ANOVA data chart for dendritic spine analysis of Hippocampus

	Group	N of mice	n of cells	n of spine$	F-statistic, p-value Holm-Sidak Post hoc significant only			
					Branched Spines	**Thin Spines**	**Filopodial Spines**	**Total**
CA1 Apical Oblique	WT Veh	2	12	--	G: $F_{1,45}$=1.099, p=0.300 **T: $F_{1,45}$=15.409, p<0.001** GxT: $F_{1,45}$=0.578, p=0.451 Post hoc: WT VEH vs WT CPO, p<.0.01# HRM VEH vs HRM CPO, p<0.05*	G: $F_{1,45}$=0.567 p=0.455 **T: $F_{1,45}$=5.093, p=0.029** GxT: $F_{1,45}$=1.021, p=0.318 Post hoc: WT VEH vs WT CPO, p<0.05*	**G: $F_{1,45}$=4.547, p=0.038** **T: $F_{1,45}$=7.129, p<0.001** **GxT: $F_{1,45}$=6.382, p=0.015** Post hoc WT VEH vs WT CPO, p<0.01# WT CPO vs HRM CPO, p<0.01#	**G: $F_{1,45}$=6.547, p=0.014** T: $F_{1,45}$=0.849, p=0.362 GxT: $F_{1,45}$=0.196, p=0.660 Post hoc: WT VEH vs HRM VEH, p<0.05*
	WT CPO	3	12	--				
	HRM VEh	3	12	--				
	HRM CPO	3	12	--				
	Total	11	48	--				
					Mushroom Spine	**Stubby spine**	**Cross section Area**	
CA1 Apical Oblique	WT Veh	2	12	120	**G: $F_{1,45}$=7.127, p=0.011** **T: $F_{1,45}$=6.836, p=0.012** **GxT: $F_{1,45}$=7.498, p=0.009** Post hoc: WT VEH vs WT CPO, p<0.01# WT VEH vs HRM VEH, p<0.01#	G: $F_{1,45}$=3.787, p=0.058 T: $F_{1,45}$=1.521, p=0.224 GxT: $F_{1,45}$=1.290, p=0.262	G: $F_{1,544}$=3.529, p<0.061 T: $F_{1,544}$=1.798, p<0.181 **GxT: $F_{1,544}$=4.402, p=0.036** Post hoc: WT VEH vs WT CPO, p<0.05* WT VEH vs HRM VEH, p<0.01#	
	WT CPO	3	12	133				
	HRM VEh	3	12	162				
	HRM CPO	3	12	133				
	Total	11	48	548				

	Group	N of mice	n of cells	n of spine$	F-statistic, p-value Holm-Sidak Post hoc significant only			
					Branched Spines	**Thin Spines**	**Filopodial Spines**	Total
CA1 Basal	WT Veh	2	12	--	G: $F_{1,44}$=1.833, p=0.183 **T: $F_{1,44}$=4.737, p=0.035** **GxT: $F_{1,44}$=4.598, p=0.038** Post hoc: WT VEH vs WT CPO, p<.0.01# WT CPO vs HRM CPO, p<0.05*	G: $F_{1,44}$=0.0205, p=0.887 T: $F_{1,44}$=0.612, p=0.438 GxT: $F_{1,44}$=0.0277, p=0.958	G: $F_{1,44}$=2.751, p=0.104 T: $F_{1,44}$=0.0385, p=0.845 **GxT: $F_{1,44}$=6.602, p=0.014** Post hoc: WT VEH vs HET VEH, p<0.01#	**G: $F_{1,44}$=5.348, p=0.025** T: $F_{1,44}$=0.174, p=0.679 GxT: $F_{1,44}$=0.103, p=0.750
	WT CPO	3	12	--				
	HRM VEh	3	12	--				
	HRM CPO	3	12	--				
	Total	11	48	--				
					Mushroom Spine	**Stubby spine**	**Cross section Area**	
CA1 Basal	WT Veh	2	12	120	**G: $F_{1,44}$=6.478, p=0.015** T: $F_{1,44}$=3.300, p=0.076 GxT: $F_{1,44}$=1.930, p=0.172 Post hoc: WT VEH vs WT CPO, p<0.05* WT VEH vs HET VEH, p<0.01#	**G: $F_{1,44}$=9.587, p=0.003** T: $F_{1,44}$=2.954, p=0.093 GxT: $F_{1,44}$=0.0409, p=0.841 Post hoc: WT VEH vs HET VEH, p<0.05* WT CPO vs HET CPO, p<0.05*	**G: $F_{1,515}$=15.468, p<0.001** **T: $F_{1,515}$=7.278, p=0.007** **GxT: $F_{1,515}$=10.700, p=0.001** Post hoc: WT VEH vs WT CPO, p<0.01# WT VEH vs HRM VEH, p<0.01#	
	WT CPO	3	12	131				
	HRM VEh	3	12	143				
	HRM CPO	3	12	125				
	Total	11	48	519				

$: number of spines are for the cross sectional area only G: Main genotype effect; T: Main treatment effect; GXT: Interaction effect

WT- wild type, HRM – Heterozygous reelin mice, VEH- vehicle, CPO-Chlorpyrifos-oxon

Bold: Significant F statistic; * p<0.05; # p<0.01

Supplementary table 2: Two-way ANOVA data chart for dendritic spine analysis of cerebellum

	Group	N of mice	n of cells	n of spine$	F-statistic, p-value Holm-Sidak Post hoc significant only			
					Branched Spines	**Thin Spines**	**Filopodial Spines**	**Total**
Lobule III-Immature Spines	WT Veh	2	10	--	G: $F_{1,34}$=0.978, p=0.33 T: $F_{1,34}$=3.047, p=0.090 GxT: $F_{1,34}$=0.389, p=0.537	**G: $F_{1,34}$=6.228, p=0.018** T: $F_{1,34}$=0.746, p=0.394 GxT: $F_{1,34}$=1.972, p=0.169 Post hoc: WT VEH vs HET VEH, p<0.05 *	G: $F_{1,34}$=0.923, p=0.344 T: $F_{1,34}$=2.615, p=0.115 **GxT: $F_{1,34}$=5.005, p=0.032** Post hoc: WT VEH vs WT CPO, p<0.01 # WT CPO vs HRM CPO, p<0.05 *	**G: $F_{1,34}$=6.546, p=0.015** T: $F_{1,34}$= 0.310, p=0.581 GxT: $F_{1,34}$=3.184, p=0.083 Post hoc: WT CPO vs HRM CPO, p<0.01 #
	WT CPO	4	10	--				
	HRM VEh	4	10	--				
	HRM CPO	4	10	--				
	Total	14	40	--				
					Mushroom Spine	**Stubby spine**	**Cross section Area**	
Lobule III-Mature Spines	WT Veh	2	10	119	G: $F_{1,34}$=2.651, p=0.113 T: $F_{1,34}$=3.047, p=0.090 **GxT: $F_{1,34}$=0.389, p=0.047** Post hoc: WT CPO vs HRM CPO, p<0.05 *	G: $F_{1,34}$=0.282, p=0.559 T: $F_{1,34}$=2.712, p=0.109 **GxT: $F_{1,34}$=14.223, p<0.001** Post hoc: WT VEH vs WT CPO, p<0.01 # WT VEH vs HRM VEH, p<0.01 # WT CPO vs HRM CPO, p<0.01 #	G: $F_{1,451}$=0.143, p=0.705 T: $F_{1,451}$=0.255, p=0.614 **GxT: $F_{1,451}$=18.925, p<0.001** Post hoc; WT VEH vs HRM VEH, p<0.1# WT VEH vs WT CPO, p<0.01# HRM CPO vs HRM VEH,p<0.01# HRM CPO vs WT CPO, p<0.01#	
	WT CPO	4	10	109				
	HRM VEh	4	10	119				
	HRM CPO	4	10	107				
	Total	14	40	454				

	Group	N of mice	n of cells	n of spine$	F-statistic, p-value Holm-Sidak Post hoc significant only			
					Branched Spines	**Thin Spines**	**Filopodial Spines**	Total
Lobule IV/V-Immature Spines	WT Veh	2	10	--	G: $F_{1,36}$=1.422, p=0.241 T: $F_{1,36}$=3.098, p=0.087 GxT: $F_{1,36}$=0.166, p=0.686	G: $F_{1,36}$=2.112, p=0.155 **T: $F_{1,36}$=6.078, p=0.019** **GxT: $F_{1,36}$=4.257, p=0.046** Post hoc WT VEH vs WT CPO, p<0.01# WT VEH vs HRM VEH, p<0.05*	G: $F_{1,36}$=0.594, p=0.446 T: $F_{1,36}$=1.087, p=0.304 **GxT: $F_{1,36}$=11.374, p=0.002** Post hoc: WT VEH vs WT CPO, p<0.1# WT CPO vs HRM CPO, p<0.01#	G: $F_{1,36}$=2.995, p=0.092 T: $F_{1,36}$=0.00784, p=0.930 GxT: $F_{1,36}$=2.566, p=0.118
	WT CPO	4	10	--				
	HRM VEh	4	10	--				
	HRM CPO	4	10	--				
	Total	14	40	--				
					Mushroom Spine	**Stubby spine**	**Cross section Area**	
Lobule IV/V-Mature Spines	WT Veh	2	10	112	G: $F_{1,36}$=2.478, p=0.124 T: $F_{1,36}$=0.692, p=0.411 **GxT: $F_{1,36}$=5.897, p=0.020** Post hoc: WT VEH vs WT CPO, p<0.05* WT CPO vs HRM CPO, p<0.01#	G: $F_{1,36}$=0.435, p=0.514 T: $F_{1,36}$=0.0113, p=0.916 **GxT: $F_{1,36}$=5.941, p=0.020** Post hoc: WT CPO vs HRM CPO, p<0.05 *	**G: $F_{1,433}$=6.938, p=0.009** **T: $F_{1,433}$=10.986, p<0.001** **GxT: $F_{1,433}$=27.848, p<0.001** Post hoc; HRM CPO vs HRM VEH,p<0.01# HRM CPO vs WT CPO, p<0.01#	
	WT CPO	4	10	106				
	HRM VEh	4	10	113				
	HRM CPO	4	10	105				
	Total	14	40	436				

$: number of spines are for the cross sectional area only G: Main genotype effect; T: Main treatment effect; GXT: Interaction effect

WT- wild type, HRM – Heterozygous reelin mice, VEH- vehicle, CPO-Chlorpyrifos-oxon

Bold: Significant F statistic; * p<0.05; # p<0.01

Supplementary table 2: Two-way ANOVA data chart for dendritic spine analysis of cerebellum

	Group	N of mice	n of cells	n of spine[$]	F-statistic, p-value Holm-Sidak Post hoc significant only			
					Branched Spines	**Thin Spines**	**Filopodial Spines**	**Total**
Lobule VI-Immature Spines	WT Veh	2	10	--	G: $F_{1,35}$=0.840, p=0.840 T:$F_{1,35}$=7.446, p=0.010 **GxT: $F_{1,35}$=7.050, p=0.012** Post hoc: HRM CPO vs HRM VEH, p<0.01[#]	G: $F_{1,35}$=2.068, p=0.159 T: $F_{1,35}$=0.678, p=0.416 GxT: $F_{1,35}$=3.883, p=0.057	G: $F_{1,35}$=0.932, p=0.341 **T: $F_{1,35}$=8.753, p=0.006** GxT: $F_{1,35}$=0.375, p=0.544 Post hoc: WT VEH vs WT CPO, p<0.05	**G: $F_{1,35}$=5.077, p=0.0.31** **T: $F_{1,35}$=4.632, p=0.038** GxT: $F_{1,35}$=0.557, p=0.461 Post hoc: WT VEH vs HRM VEH, p<0.05*
	WT CPO	4	10	--				
	HRM VEh	4	10	--				
	HRM CPO	4	10	--				
	Total	14	40	--				
					Mushroom Spine	**Stubby spine**	**Cross section Area**	
Lobule VI-Mature Spines	WT Veh	2	10	108	**G: $F_{1,35}$=14.551, p<0.001** T: $F_{1,35}$=0.215, p=0.646 **GxT: $F_{1,35}$=6148, p=0.018** Post hoc: WT CPO vs WT VEH, p<0.05* WT CPO vs HRM CPO, p<0.01[#]	G: $F_{1,35}$=0.128, p=0.722 T: $F_{1,35}$=0.110, p=0.742 GxT: $F_{1,35}$=2.132, p=0.153	**G: $F_{1,408}$=32.665, p<0.001** T: $F_{1,408}$=1.488, p=0.223 GxT: $F_{1,408}$=16.193, p<0.001 Post hoc: WT VEH vs WT CPO, p<0.01[#] WT VEH vs HRM VEH, p<0.01[#]	
	WT CPO	4	10	106				
	HRM VEh	4	10	109				
	HRM CPO	4	10	89				
	Total	14	40	412				

	Group	N of mice	n of cells	n of spine[$]	F-statistic, p-value Holm-Sidak Post hoc significant only			
					Branched Spines	**Thin Spines**	**Filopodial Spines**	Total
Lobule VIII-Immature Spines	WT Veh	2	10	--	**G: $F_{1,35}$=7.481, p=0.010** T: $F_{1,35}$=2.937, p=0.095 **GxT: $F_{1,35}$=10.114, p=0.003** Post hoc: HRM VEH vs HRM CPO, p<0.01[#] WT CPO vs HRM CPO, p<0.01[#]	G: $F_{1,35}$=2.658, p=0.112 T: $F_{1,35}$=2.658, p=0.112 **GxT: $F_{1,35}$=21.398, p<0.001** Post hoc: WT VEH vs WT CPO, p<0.05 HRM VEH vs HRM CPO, p<0.01[#] WT VEH vs HRM VEH, p<0.05 WT CPO vs HRM CPO, p<0.01[#]	G: $F_{1,35}$=0772, p=0.783 **T: $F_{1,35}$= 18.094, p<0.001** GxT: $F_{1,35}$=0.202, p=0.656 Post hoc: WT VEH vs WT CPO, p<0.01# HRM VEH vsHRM CPO,p<0.05*	**G: $F_{1,35}$=0.0480, p=0.828** T: $F_{1,35}$=2.469, p=0.125 **GxT: $F_{1,35}$=12.435, p=0.001** Post hoc: HRM VEH vsHRM CPO,p<0.01[#] WT VEH vs HRM VEH, p<0.05* WT CPO vs HRM CPO, p<0.05*
	WT CPO	4	10	--				
	HRM VEh	4	10	--				
	HRM CPO	4	10	--				
	Total	14	40	--				
					Mushroom Spine	**Stubby spine**	**Cross section Area**	
Lobule VIII-Mature Spines	WT Veh	2	10	101	**G: $F_{1,35}$=30.968, p=0.005** T: $F_{1,35}$=0.347, p=0.559 GxT: $F_{1,35}$=0.890, p=0.352 Post hoc: WT CPO vs HRM CPO, p<0.01[#]	G: $F_{1,35}$=0.769 p=0.386 T: $F_{1,35}$=0.0120, p=0.913 GxT: $F_{1,35}$=2.156, p=0.151	**G: $F_{1,35}$=33.723, p<0.001** T: $F_{1,35}$=000852, p<0.977 **GxT: $F_{1,35}$=20.171, p<0.001** Post hoc: WT VEH vs WT CPO, p<0.01[#] HRM VEH vsHRM CPO,p<0.01[#] WT VEH vs HRM VEH, p<0.01[#]	
	WT CPO	4	10	103				
	HRM VEh	4	10	119				
	HRM CPO	4	9	103				
	Total	14	39	426				

[$]: number of spines are for the cross sectional area only G: Main genotype effect; T: Main treatment effect; GXT: Interaction effect
WT- wild type, HRM – Heterozygous reelin mice, VEH- vehicle, CPO-Chlorpyrifos-oxon
Bold: Significant F statistic; * p<0.05; [#] p<0.01

References

Abadesco, A., Cilluffo, M., Yvone, G., Carpenter, E., Howell, B., & Phelps, P. (2014). Novel Disabled-1 expressing neurons identified in adult brain and spinal cord. European J. Neurosci. 39: 579-92.

Abrahams, B. S., and Geschwind, D. H. (2008). Advances in autism genetics: on the threshold of a new neurobiology. Nat. Rev. Genet. 9: 341-355.

Alcantara, S., Ruiz, M., D'Arcangelo, G.D., Ezan, F., de Lecea, L., Curran, T., Sotelo, C., Soriano, E. (1998) Regional and cellular patterns of reelin mRNA expression in the forebrain of developing and adult mouse. J. Neurosci. 18:7779-7799.

Aldridge, J.E., Levin, E., Seidler, F., & and Slotkin, T. (2005). Developmental Exposure of Rats to Chlorpyrifos Leads to Behavioral Alterations in Adulthood, Involving Serotonergic Mechanisms and Resembling Animal Models of Depression. Environ. Health Perspectives 113: 527-31.

Anderson, S.A., Marin, O., Horn, C., Jennings, K., Rubenstein, J.L.R. (2001) Distinct cortical migration from the medial and lateral ganglionic eminences. Development 128:353-363.

Angoa-Pérez, M., Kane, M.J., Briggs, D.I., Francescutti, D.M., Kuhn, D.M. (2013) "Marble burying and nestlet shredding as tests of repetitive, compulsive-like behaviors in mice" J Vis Exp 82: e50978.

Betancourt, A., Burgess, S., & Carr, R. (2006). Effect of Developmental Exposure to Chlorpyrifos on the Expression of Neurotrophin Growth Factors and Cell-Specific Markers in Neonatal Rat Brain . Toxicological Science 92: 500-6.

Biamonte, F., Assenzab, G., Marinoa, R., D'Amelioc, M., Panteria, R., Carusod, D., et al. (2009). Interactions between neuroactive steroids and reelin haploinsufficiency in Purkinje cell survival. Neurobio. of Disease 36: 103-15.

Bock, H., Jossin, Y., Liu, P., Förster, E., May, P., Goffinet, A., et al. (2003). Phosphatidylinositol 3-Kinase Interacts with the Adaptor Protein Dab1 in Response to Reelin Signaling and Is Required for Normal Cortical Lamination. J Biol Chemistry 278: 38772-9.

Casida, J. E., and Quistad, G. B. (2005). Serine hydrolase targets of organophosphorus toxicants. Chemico-Biological Interactions: Proceedings of the VIII International Meeting on Cholinesterases. 157-158: 277-283.

Chow, M., Pramparo, T., Winn, M., Barnes, C., Li, H., Weiss, L., et al. (2012). Age-Dependent Brain Gene Expression and Copy Number Anomalies in Autism Suggest Distinct Pathological Processes at Young Versus Mature Ages. PLOS Genetics 8: 1-14.

Christensen, J., Grønborg, T. K., Sørensen, M. J., Schendel, D., Parner, E. T., Pedersen, L. H., Vestergaard, M. (2013). Prenatal valproate exposure and risk of Autism Spectrum Diorders and childhood Autism. JAMA 309:1696-1703.

Cohen, M. J., Meador, K. J., Browning, N., May, R., Baker, G. A., Clayton-Smith, J., Kalayjian, L. A., Kanner, A., Liporace, J. D., Pennel, P. B., Priviteral, M., Loring, D. W. (2013). Fetal antiepilieptic drug exposure: Adaptive and emotional/behavioral functioning at age 6 years. Epilepsy & Behavior 29:308-315.

Courchesne, E., Karns, C., Davis, H., Ziccardi, R., Carper, R., Tigue, Z., et al. (2001). Unusual brain growth patterns in early life in patients with autistic disorder: An MRI study. Amer Acad of Neurology , 57:245-54.

Costa, L.G. (2006). Current issues in organophosphate toxicology. Clin. Chim. Acta 366: 1-13.

D'Arcangelo, G., Miao, G. G., Chen, S. C., Soares, H. D., Morgan, J. I., and Curran, T. (1995). A protein related to extracellular matrix proteins deleted in the mouse mutant reeler. Nature 374:719-723.

De Bergeyck, V., Nakajima, K., Lambert de Rouvroit, C., Naerhuyzen, B., Goffinet, A., Miyata, T., et al. (1997). A truncated Reelin protein is produced but not secreted in the 'Orleans' reeler mutation (Reln[rl-Orl]). Brain Res Mol Brain Res , 50:85-90.

Deacon, R. (2012). Assessing Burrowing, Nest Construction, and Hoarding in Mice. JOVE , 59: 1-12.

Deacon, R. M., Cholerton, L. L., Talbot, K., Nair-Roberts, R. G., Sanderson, D. J., Romberg, C., Koros, E., Bornemann, K. D., and Rawlins, J. N. (2008). Age-dependent and – independent behavioral deficits in Tg2576 mice. Behav. Brain Res. 189: 126-38.

DeSoto, M. C. and Hitlan, R. T. (2010) Sorting out the spinning of autism: heavy metals and the question of incidence. Acta Neurobiol Exp 70: 165-176.

Fatemi, S., Snow, A., Stary, J., Araghi-Niknam, M., Reutiman, T., Lee, S., et al. (2005). Reelin signaling is impaired in autism. Biol Psychiatry , 57: 777-787.

Freire, C., Ramos, R., Puertas, R., Lopez-Espinosa, M., Julvez, J., Aguilera, I., Cruz, F., Fernandez, M., Sunyer, J., Olea, N. (2010) Association of traffic-related air pollution with cognitive development in children. J. Epidemiol Community Heath 64: 223-228.

Flaskos, J. (2012). The developmental neurotoxicity of organophosphorus insecticides: a direct role for the oxon metabolites. Toxicol. Lett. 209: 86-93.

Guidotti, A., Auta, J., Davis, J., Gerevini, V., Dwivedi, Y., Grayson, D., et al. (2000). Decrease in Reelin and Glutamic Acid Decarboxylase67 (GAD67) Expression in Schizophrenia and Bipolar Disorder. JAMA Psych , 57: 1061-9.

Hadj-Sahraoui, N., Frederic, F., Delhaye-Bouchaud, N., & Mariani, J. (1996). Gender effect on Purkinje cell loss in the cerebellum of the heterozygous reeler mouse. J. Neurogenet. 11: 45-58.

Hammond, V., So, E., Gunnersen, J., Valcanis, H., Kalloniatis, M., & Tan, S. (2006). Layer positioning of Late-Born Cortical Interneurons is dependent on Reelin but not p35 signaling. Journal of Neurosci 26: 1646-55.

Hardan, A., Minshew, N., Harenski, K., & Keshavan, M. (2001). Posterior fossa magnetic resonance imaging in autism. J. Am. Acad. Child Adolesc. Psychiatry 40: 666-672.

Heinrichs, M., Domes, G. (2008) Neuropeptides and social behaviour: effects of oxytocin and vasopressin in humans. Prog. Brain Research 170:337-350

Hiesberger, T., Trommsdorff, M., Howell, B., Goffinet, A., Mumby, M., Cooper, J., et al. (1999). Direct binding of Reelin to VLDL receptor and ApoE receptor 2 induces tyrosine phosphorylation of disabled-1 and modulates tau phosphorylation. Neuron 24: 481-489.

Igarashi, K. M., Hiroshi, T., Moser, E. I., and Moser, M.-B. (2014). Functional diversity along the transverse axis of hippocampal area CA1. FEBS Lett. 588: 2470-2476.

Jiang, W., Duysen, E. G., Hansen, H., Shlyakhtenko, L., Schopfer, L. M., and Lockridge, O. (2010). Mice treated with chlorpyrifos or chlorpyrifos oxon have organophosphorylated tubulin in the grain and disrupted microtubule structures, suggesting a role for tubulin in neurotoxicity associated with exposure to organophosphorus agents. Toxicol. Sci. 115: 183-193.

Jossin, Y., Gui, L., and Goffinet, A. M. (2007). Processing of Reelin by embryonic neurons is important for function in tissue but not in dissociated cultured neurons. J. Neurosci. 27: 4243-4252.

Kern, J. (2003). Purkinje cell vulnerability and autism: a possible etiological connection. Brain and Develop. , 25:377-82

Lambert de Rouvroit, C., de Bergeyck, V., Cortvrindt, C., Bar, I., Eeckhout, Y., and Goffinet, A. M. (1999). Reelin, the extracellular matrix protein deficient in Reeler mutant mice, is processed by a metalloproteinase. Exp. Neurol. 156: 214-217.

Laviola, G., Adriani, W., Gaudino, C., Marino, R., and Keller, F. (2006). Paradoxical effects of prenatal acetylcholinesterase blockade on neuro-behavioral development and drug-induced sterotypies in reeler mutant mice. Psychopharmacology 187: 331-344.

Lee, K.J., Kim, H., Kim, T.S., Park, S., Rhyu, I.J (2004) Morphological analysis of spine shapes of Purkine cell dendrties in the rat cerebellum using high-voltage electron microscopy. Neuosci. Letters 359:21-24.

Liu, W., Pesold, C., Rodriguez, M., Carboni, G., Auta, J., Lacor, P., et al. (2001). Down-regulation of dendritic spine and glutamic acid decarboxylase 67 expressions in the reelin haploinsufficient heterozygous reeler mouse. Proc Natl Acad Sci USA 98: 3477-82.

Maloney, S., Rieger, M., & Dougherty, J. (2013). Identifying Essential Cell Types and Circuits in Autism Spectrum Disorders. Rev Neurobiol 113: 61-96.

Meyer-Lindenberg, A., Domes, G., Kirsch, P., and Heinrichs, M. (2011) Oxytocin and vasopressin in the human brain: social neuropeptides for translational medicine. Nat. Rev. Neurosci. 12: 524-538.

Mullen, B., Khialeeva, E., Hoffman, D., Ghiani, C., & Carpenter, E. (2013). Decreased reelin expression and organophosphate pesticide exposure alters mouse behaviour and brain morphology. ASN NEURO 5: 27-42.

Murray, R. M., Jones, P., O'Callaghan, E., Takei, N., and Sham, P. (1992). Genes, viruses and neurodevelopmental schizophrenia. J. Psychiatr. Res. 26: 225-235.

Niu, S., Yabut, O., & D'Arcangelo, G. (2008). The reelin signaling pathway promotes dendritic spine development in hippocampal neurons. J Neurosci 28: 10339–10348.

Petronis, A (2004) The origin of schizophrenia: genetic thesis, epigenetic antithesis, and resolving synthesis Biol. Psychiatry 55: 965-970.

Persico, A. M., and Bourgeron, T. (2006). Searching for ways out of the autism maze: genetic, epigenetic, and environmental clues. Trends Neurosci. 29: 349-358.

Penzes, P., Cahill, M. J., VanLeeuween, J., & Woolfrey, K. (2011). Dendritic spine pathology in neuropsychiatric disorders. Nature Neurosci. 14: 285-93.

Pesold, C., Impagnatiello, F., Pisu, M., Uzunov, D., Costa, E., Guidotti, A., et al. (1998). Reelin is preferentially expressed in neurons synthesizing γ-aminobutyric acid in cortex and hippocampus of adult rats. PNAS 95: 3221-6.

Ramos-Moreno, T., Galazo, M., Porrero, C., Martínez-Cerdeño, V., & Clascá, F. (2006). Extracellular matrix molecules and synaptic plasticity: immunomapping of intracellular and secreted Reelin in the adult rat brain. European J. Neurosci 23: 401-22.

Roberts, E. M., English, P. B., Grether, J. K., Windhan, G. C., Somberg, L, and Wolff, C. (2007). Maternal residence near agricultural pesticide applications and autism spectrum disorders among children in the California central valley. Environ. Health Perspect. 115: 1482-1489.

Romano, E., Fuso, A., & Laviola, G. (2013). Nicotine Restores Wt-Like Levels of Reelin and GAD67 Gene Expression in Brain of Heterozygous Reeler Mice. Neurotox Res 24: 205-15.

Shelton, J.F.; Hertz-Picciotto, I., Pessah, I.N. (2012). Tipping the balance of Autism risk: Potential mechanisms linking pesticides and autism. Environ Health Perspective 120: 994-951.

Slotkin, T. (2004). Cholinergic systems in brain development and disruption by neurotoxicants: nicotine, environmental tobacco smoke, organophosphates. Tox. and Applied Pharm.198:132-151.

Tamamaki, N., Yanagawa, Y., Tomioka, R., Miyazaki, J., Obata, K., & Kaneko, T. (2003). Green fluorescent protein expression and colocalization with calretenin, parvalbumin, and somatostatin in GAD67-GFP knock-in mouse. J. Comp. Neurol. 467: 60-79.

Thomas, A., Burant, A., Bui, N., Graham, D., Yuva-Paylor, L., & Paylor, R. (2009). Marble burying reflects a repetitive and perseverative behavior more than novelty-induced anxiety. Psychopharmacology 204: 361-73.

Whyatt, R., Camann, D., Kinney, P., Reyes, A., Ramirez, J., Dietrich, J., et al. (2002). Residential pesticide use during pregnancy among a cohort of urban minority women. Environ Health Perspect., 110: 507-514.

Yakel, J. (2014). Nicotinic ACh receptors in the hippocampal circuit; functional expression and role in synaptic plasticity. J. Physiol. 592: 4147-4153.

Chapter 4

Overall Discussion

During the past few years, I have investigated a pathogenic model of autism spectrum disorder (ASD) originally proposed by Keller and Persico (2003). In this model, reduced reelin expression combined with prenatal organophosphate exposure at a critical time in brain development was proposed as a factor that leads to ASD. Within this concluding chapter, I summarize the major findings of this study and propose future directions that may be beneficial to understanding how altered reelin expression and organophosphate pesticide exposure may contribute to neuropsychiatric disorders such as ASD.

Biochemical changes that may influence reelin expression

Reelin expression is reduced in many psychiatric disorders, yet we do not understand how or why this change occurs and whether reduced reelin is causative or correlative with these disorders. Within ASD patients, there seem to be common brain morphological features, such as the cells are smaller and packed more densely in areas such as the hippocampus and amygdala (Kemper and Bauman, 1993). Given that this small dense cell phenotype is typically seen in developing brains, some have suggested that developmental errors occur so that the brain remains in an immature state (Palmen et al., 2004). One theory suggests that dysregulation of proper signaling occurs during critical times of development in ASD patients and can change the genetic expression of the leading to behavioral phenotypes seen in ASD. Evidence of this dysregulation comes from a study that compares post-mortem brains of young and adult ASD patients with those of control groups to identify changes in gene expression profiles (Chow et al., 2012). Within young ASD patients, changes in expression of pathways that influence development of prefrontal cortices, such as those that govern cell number, cortical patterning, and differentiation when compared to their control samples were reported. Comparison between young ASD patients to those of older patients revealed

dysregulation of regulatory signaling, repair, and response pathways. RELN was one of the more severely affected genes, showing a 2.6-fold reduction in expression within adult tissue. Regardless of age, ASD patients' samples were distinguishable from control groups based upon atypical gene expression of developmental processes (Chow et al., 2012). Disruptions within proper cell cycle and signaling during development could effect changes within the regulatory process of proper development and ultimately change the genetic landscape of the patient.

Factors that may contribute to this dysregulation are those that influence the cholinergic pathways. Two facts have led researchers to believe that ASD is influenced by abnormal activity within cholinergic systems during development: 1) disruptions within the cholinergic system delay cortical development and lead to permanent architectural changes that resemble immature organization within the adult brain (Hohmann and Berger-Sweeny, 1998) and 2) ASD patients show decreases in cholinergic receptor distribution in frontal and parietal cortices and within the cerebellum (Perry et al., 2001; Lee et al., 2002). Some researchers have claimed the cholinergic systems should be a primary target for pharmaceutical therapy with ASD patients, given some efficacy in treatment (Deutsch et al., 2010). Reelin deficiency can be ameliorated by targeting the cholinergic system with an agonist, nicotine, which restores reelin protein levels in $Reln^{rl/+}$ male mice to $Reln^{+/+}$ levels (Romano et al., 2013). These findings support the theory that cholinergic pathways influence reelin expression.

In this study, we exposed animals to an organophosphate pesticide that affects the cholinergic pathways through an inhibition of acetylcholine esterase (AChE) during a critical time in neural development. Anti-cholinesterases, such as CPO, affect the regulation of cholinergic pathways, by causing drastic changes to central nervous system development (Shelton et al., 2012). Correlation studies have found a link between this developmental delay leading to ASD pathology and rural communities that have high concentrations of pesticides (Shelton et al., 2014). We found that CPO has a transient effect on reelin expression. While

CPO is present in embryonic mice, reelin expression increases (measured at E16.5, day 3 of exposure); however, the long-term effect of prenatal CPO exposure causes reelin expression to decrease in adults (measured at P90). Interestingly, we showed that prenatal CPO exposure in *Reln*$^{+/+}$ animals caused reelin expression to be reduced to half that of control animals in neocortical tissue, potentially working through the cholinergic pathway leading to epigenetic suppression of reelin (Grayson and Guidotti, 2013). Thus high levels of CPO exposure are sufficient to reduce adult reelin expression to levels seen within neuropsychiatric disorders.

Future studies should investigate the direct effects of CPO on the cholinergic systems to see if there are changes within the expression patterns of the cholinergic markers. Immunohistochemistry should be done to see if there are direct changes to the pre- and post-synaptic cholinergic systems (ie. immunofluorescence against choline-acetyltransferase or nAChR subunits). A study to test if cholinergic agonists, such as nicotine, can restore the CPO induced reduction of reelin would also be of interest. Experiments to determine if CPO exposure causes epigenetic changes within the reelin gene, proposed through the activation of DNA methyltransferase (DNMT) (Grayson and Guidotti, 2013) could provide a possible mechanism.

ASD-like behaviors

Since reelin is decreased in several neuropsychiatric disorders, reelin deficiency is likely to play a role in establishing and maintaining cognitive ability. This idea led to a number of studies assessing the role of reduced reelin expression in animal behavior. Salinger et al. (2003) found that heterozygous reelin mice (*Reln*$^{rl/+}$) have an increased acoustic intensity response and a decreased latency to approach a novel object. In their study, however, there seemed to be no effect on learning, cognition, or repetitive behaviors. Due to extensive reporting on behaviors within *Reln*$^{rl/+}$ mice that showed only subtle differences from *Reln*$^{+/+}$ animals, Salinger et al. (2003) proposed two theories: 1) reelin dosage in mice does not develop

the same behavioral phenotypes as humans, and 2) a “two hit” mechanism may be needed to elicit the same behaviors seen in neuropsychiatric diseases. For this reason, a search for factors that could influence behavior within *Reln*$^{rl/+}$ ensued. Laviola et al. (2006) first reported an interaction effect on the behaviors of *Reln*$^{rl/+}$ when exposed prenatally to CPO.

Typically any mammal detoxifies organophosphorous compounds, such as CPO, using the enzyme paraoxonase1 (PON1), and thus partially protecting against a systemic influence of pesticides. However, during the perinatal periods mammals are susceptible to sub-toxic exposure to CPO that may cause neuropsychiatric behaviors within mice. One study showed that prenatal CPO exposure caused anhedonia, a neuropsychiatric symptom for major depressive disorders (Aldridge et al., 2005). On the other hand, another study looked for deficits in complex cognitive abilities such as learning and motor tasks, but failed to report significant findings with CPO exposure to neonatal *PON1*$^{-/-}$ mice (Cole et al., 2012).

ASD is diagnosed by impaired communication, compromised social interactions, and restricted or repetitive behaviors. Communication measured in our study (Mullen et al., 2013) by ultrasonic vocalizations during the neonatal period was affected by both reelin and prenatal CPO exposure. Additional studies demonstrated differential effects on males and females. In males, either reduced reelin or CPO exposure decreased the number of cries made by P7 pups. In addition, CPO exposure decreased the duration of the vocalizations. When these two factors were combined within the same animal, the number and duration of vocalizations were restored to near-normal levels. This implies that combination of both insults ameliorates the behavioral phenotypes that result from each factor independently. In contrast, reducing reelin expression in females seemed to have a more drastic effect, decreasing both number and duration of cries. The exposure to CPO, on the other hand, did not affect the number of cries, but did decrease the duration. Females did not show an amelioration of the vocalization phenotype when the two insults were paired together.

Social interactions were not affected much by reelin haploinsufficiency, prenatal CPO exposure, or the combination of the two factors. This was surprising given that male *Reln*$^{rl/+}$ have disrupted cortical oxytocin receptors (Liu et al., 2005) and that oxytocin influences social behaviors (Heinrichs and Domes, 2008). Further analysis on the regional expression of oxytocin within *Reln*$^{rl/+}$ mice may assist in understanding the role that oxytocin has on cortical circuits.

Restrictive and repetitive behaviors were measured by a marble burying test and seemed to be influenced by reelin heterozygosity selectively in males. However, when reelin heterozygosity was paired with prenatal CPO, this led to a more pronounced phenotype in adults. Prenatal CPO alone did not seem to affect this behavior in *Reln*$^{+/+}$ animals. Other repetitive behaviors studied, such as grooming and sniffing, in *Reln*$^{rl/+}$ did not differ. Thus, our studies suggest that decreased reelin expression may have only a subtle influence on repetitive behaviors in male mice.

One limitation of this study is that reelin expression was only measured twice at E16.5 and P90. Two additional time points would help establish the progression of the effect that prenatal CPO exposure has on reelin. Given that behaviors will change due to brain biochemistry, assessments of transient changes in signaling molecules, such as with a microarray, should be performed to determine if and when a plateau or stable state is achieved. After understanding this effect, one should plan additional behavioral assessments in accordance within the biochemical time line.

The pairing of reduced reelin and prenatal CPO exposure does not seem to elicit a complete ASD-like mouse model based upon behavior but has given insight into the complexity of gene-environment interactions. We found evidence that both CPO and reelin cause sex specific differences within behaviors typically seen in ASD patients. The pairing of these two factors, environmental and genetic, was not additive as first hypothesized and followed a complex transient interaction between these variables. Given the fact that prenatal CPO alone

can cause a significant reduction of reelin, a different genetic mutation should be paired with prenatal CPO exposure to potentially push the animal to a more ASD-like behavioral phenotype.

Effects on brain morphology due to reelin deficiency and prenatal CPO exposure

Understanding molecular systems and cell populations that are affected in neuropsychiatric patients will allow researchers to investigate what causes the behavioral manifestations and how ultimately to alleviate their symptoms (Maloney et al., 2013). Reelin signaling is an established common molecular system shown to decrease expression within several developmental disorders; such as ASD, schizophrenia, bipolar, and major depressive disorders (Impagnatiello et al., 1998; Fatemi et al., 2000; Fatemi et al., 2002; Guidotti, et al 2000; Fatemi et al., 2005). In addition, a mutation in reelin affects many cell types and anatomical structures that are also affected in neurodevelopment disorders (Persico and Bourgeron, 2006). Importantly, reelin has been shown to have large influences in spine maturation and maintenance (Hertz and Chen, 2006). Both schizophrenia (SZ) and ASD are diseases of the synapse due to observed changes in dendritic spines and many reported molecular pathways suggested to influence synapse stability (Penzes et al., 2011).

Two theories of how these changes in dendritic spines influence pathology of ASD and SZ have arisen from fMRI and postmortem studies. Within ASD patients, post mortem assessment showed an increase in cortical dendritic spine densities and fMRI studies have demonstrated a decrease in functional communication between brain regions (Hustler and Zhang, 2010; Geschwind and Levitt, 2007). These two facts have contributed to a relatively new theory stating that individuals with ASD are characterized by increased connectivity within local circuits and decreased connectivity between distinct brain regions (Penzes et al., 2011). SZ patients, however, have over pruning of synaptic connections during adolescent years and a reduction in neuropil (Glantz and Lewis, 2000, Selemon and Goldman-Rakic, 1999). These studies helped to build the hypothesis that SZ results from an overall lack of communication

(Penzes et al. 2011). In our study, we demonstrated that prenatal CPO and reduced reelin expression generated few gross anatomical and morphological changes, but had a substantial impact on dendritic spine morphology.

We examined anatomical and morphological changes in three different experiments. First, using a Dab1 reporter mouse, which reveals cells that are normally responsive to reelin signaling, we examined cortical, hippocampal, cerebellar, and olfactory bulb organization in adolescent. Measurable changes were seen in the olfactory bulb and piriform cortex where reelin haploinsufficiency typically caused a compression of cellular layers. Prenatal CPO, on the other hand caused an expansion of the layers in those same structures. The combination of the two factors seemed to ameliorate the altered layer structure. This may be due to the increase in reelin production while CPO was present during critical times of neural development causing extra reelin signaling within *Reln*$^{+/+}$ animals and ameliorating the reelin deficiency in heterozygous animals. In addition to the lamination changes, we also noted ectopic expression patterns of the genetic Dab1 reporter, showing more abundant reelin-responsive cells in the molecular layer of the ansiform lobes of the cerebellum, oriens and alveus layers in the hippocampus, and laminae I of the piriform cortex. However, the specific cell types whose positions had changed were not identified; this is a topic for a future study.

Our second set of experiments addressed changes in a specific cell population, the GABAergic interneurons. These cells were selected for study because adult expression of reelin is confined to a subpopulation of these cells (Alcantara et al., 1998). Proper development of GABAergic interneurons requires them to tangentially migrate into the cortex and hippocampus during E11.5-E16.5 (Anderson et al., 2001). Despite the fact that reelin expression is reduced due to prenatal CPO exposure in adult tissue (see above) and that we introduced CPO into the system during a time of critical neurodevelopment (E13.5-E16.5) we saw no change in the density or the distribution of interneurons due to CPO exposure. Thus, we can conclude that the reduced reelin levels within adulthood is not caused by the loss of the

cells that produce the protein. This provides further evidence of a potential pharmaceutical cell targets to replenish reduced reelin levels.

Our third study examined dendritic spine organization. We found significant dendritic spine structure changes within hippocampal CA1 pyramidal cells. Reelin deficiency caused an overall reduction in the number of spines, confirming a prior report (Niu et al., 2008). We classified the specific spines that were reduced as stubby and mushroom spines. Prenatal CPO exposure also induced a reduction of stable spines but a concomitant increase in the number of immature spines. Both CPO and reelin haploinsufficiency decreased the mushroom spine cross sectional area. Reelin has been shown to influence spine maturation and to assist in long term potentiation (LTP) by recruiting NMDA receptors (Weeber et al., 2002; Niu et al., 2008; Chen et al., 2005). We show that prenatal CPO influences correct maturation of mushroom spines by showing a decrease in crosssectional area.

Cerebellar dendritic spines showed regional differences in their response to reelin reduction and CPO exposure. We showed more effects in posterior lobe dendritic spine formation. Lobule VI has been associated with language and working memory, whereas lobule VIII has been associated with language and sensorimotor systems (Stoodley et al., 2012). Cerebellar systems have been implicated in both ASD and schizophrenia (DiCicco-Bloom, 2006; Andreasen and Pierson, 2008). In our study, there were 3 general trends in stable spines. First, unlike the hippocampus, there were no changes to stable spine densities with respect to vehicle-treated $Reln^{+/+}$ animals in all but one condition – prenatal CPO exposure to $Reln^{+/+}$ animals increased the stable spine densities. Second, most stable Purkinje cell spines showed a decrease in cross sectional mushroom area similar to that within the hippocampus. Third, there was a drastic increase in mushroom cross sectional area in the posterior lobe (VI and VIII) compared to the anterior lobe (III and IV/V). Although, this increase was evident in each of the experimental conditions, all experimental groups' cross sectional spine areas remained significantly lower than the vehicle-treated *Reln*$^{+/+}$ animals. Purkinje cells' main

mechanism of learning occurs through long-term depression (LTD) (Ito, 2001). This mechanism of learning through LTD typically decreases the effectiveness that glutamate has on the postsynaptic PC. Future researchers would need to investigate what reelin's role is within maturation or manipulation of spines within the cerebellar circuit: 1) Reelin may still play a role in spine maturation and stabilization through influencing cytoskeleton proteins and recruiting gluatamatergic receptors and/or 2) reelin may assist in the learning process by down regulating these gluatamatergic receptors.

Two general trends were noted in the Purkinje cell immature spines. First, an overall decrease in thin spine densities was observed usually in the vehicle-treated animals. This decrease in thin spines could be due to two factors. 1) Reelin could be directly influencing the cytoskeletal infrastructure promoting more thin spines and/or 2) it could be a systemic problem due to the decrease in synaptic connectivity that is normally promoted by reelin. Second, there was a trend that prenatal CPO exposure increased filopodial spine formation. This was most evident within the $Reln^{+/+}$ CPO animals, where effects were seen in both lobes. However, within the $Reln^{rl/+}$ CPO animals there was an effect only within the posterior lobe. Prenatal CPO exposure caused an increase in filopodial spines, this characterization happens to be a phenotype that is typically seen within younger neurons (Ziv and Smith, 1996). This effect is not likely due to neuronal electrical activity, but more of an effect on spine motility based upon cytoskeleton regulation (Dunaevsky et al., 1999). Future studies would have to address the role that prenatal CPO has on regulations of the cytoskeletal systems.

In conclusion, this study looked at the environmental factor, Chlorpyrifos-oxon (CPO), and genetic factor, reelin haploinsufficiency; both of which potentially contribute to neuropsychiatric disorders. Our first study (Chapter 2) showed measurable effects due to reelin heterozygosity or early prenatal exposure to organophosphate pesticide; however, when the two

factors were combined within the same animals, the changes were typically ameliorated. In contrast, in the second study (Chapter 3) we do not see amelioration, but rather detrimental lasting changes to biochemical pathways and dendritic spines. Given the changes in dendritic spines and behaviors seen in these studies, both of these factors may play a role in neuropsychiatric diseases such as schizophrenia and autism.

References

Aldridge, J.E., Levin, E., Seidler, F., & and Slotkin, T. (2005). Developmental Exposure of Rats to Chlorpyrifos Leads to Behavioral Alterations in Adulthood, Involving Serotonergic Mechanisms and Resembling Animal Models of Depression. Environ. Health Perspectives , 113: 527-31.

Alcantara, S., Ruiz, M., D'Arcangelo, G.D., Ezan, F., de Lecea, L., Curran, T., Sotelo, C., Soriano, E. (1998) Regional and cellular patterns of reelin mRNA expression in the forebrain of developing and adult mouse. J. Neurosci. 18:7779-7799

Anderson, S.A., Marin, O., Horn, C., Jennings, K., Rubenstein, J.L.R. (2001) Distinct cortical migration from the medial and lateral ganglionic eminences. Development 128:353-363

Andreasen, N.C., Pierson, R. (2008) The role of the cerebellum in schizophrenia. Biol. Psychiatry 64:81-88

Chen, Y., Beffert, U., Ertunc, M., Tang, T.S., Kavalali, E. T., Bezprozvanny, I., Herz, J. (2005). Reelin modulates NMDA recetpor activity in cortical neurons. J. Neurosci. 25:8209-8217

Chow, M., Pramparo, T., Winn, M., Barnes, C., Li, H., Weiss, L., et al. (2012). Age-Dependent Brain Gene Expression and Copy Number Anomalies in Autism Suggest Distinct Pathological Processes at Young Versus Mature Ages. PLOS Genetics , 8:1-14.

Cole. T.B., Fisher, J.C., Burbacher, T.M., Costa, L.G., Furlong, C.E. Neurobehavioral assessment of mice following repeated postnatal exposure to chlorpyrifos-oxon. Neurotox. And Teratology 34:311-322

Deutsch, S., Urbano, M., Neumann, S., Burket, J., & Katz, E. (2010). Cholinergic Abnormalities in Autism: Is There a Rationale for Selective Nicotinic Agonist Interventions? Clinical Neuropharmacology , 33:114-120.

DiCocci-Bloom, E., Lord, C., Zwaigenbaum, L., Courchesne, E., Dager, S.R., Schmitz, C., Schultz, R.T., Crawley, J., Young, L.J. (2006) The developmental neurobiology of autism spectrum disorder. J. Neuroscience 26:6897-6906

Dunaevsky, A., Tashiro, A., Majewska, A., Mason, C., Yuste, R. (1999) Developmental regulation of spine motility in the mammalian central nervous system. PNAS 96:13438-13443

Fatemi, S. H., Earle, J. A., McMenomy T (2000) Reduction in reelin immunoreactivity in hippocampus of subjects with schizophrenia, bipolar disorder and major depression. Molecular Psychiatry 5: 654-663

Fatemi, S. H., Snow, A .V., Stary, J. M., Araghi-Niknam, M., Reutiman, T. J., Lee, S., Brooks, A. I., and Pearce, D. A. (2005). Reelin signaling is impaired in autism. Biol. Psychiat. 57:777-787.

Fatemi, S. H., Stary, J. M., and Egan, E. A. (2002). Reduced blood levels of reelin as a vulnerability factor in pathophysiology of autistic disorder. Cell. Mol. Neurobiol. 22:139-152.

Geschwind, D.H., Levitt, P. (2007) Autism spectrum disorders: developmental disconnection syndromes. Curr. Opin. Neurobiol. 17:103–111

Glantz, L.A., Lewis, D.A. (2000) Decreased dendritic spine density on prefrontal cortical pyramidal neurons in schizophrenia. Arch. Gen. Psychiatry 57:65–73

Grayson, D. R. and Guidotti, A. (2013) The dynamics of DNA methylation in Schizophrenia and related psychiatric disorders. Neuropsychopharmacology 38:138-166

Guidotti, A., Auta, J., Davis, J., Gerevini, V., Dwivedi, Y., Grayson, D., et al. (2000). Decrease in reelin and glutamic acid decarboxylase67 (GAD67) expression in schizophrenia and bipolar disorder. JAMA Psych , 57:1061-1069.

Heinrichs, M., Domes, G. (2008) Neuropeptides and social behaviour: effects of oxytocin and vasopressin in humans. Prog. Brain Research 170:337-350

Herz, J., Chen, Y. (2006) Reelin, lipoprotein receptors and synaptic plasticity. Nature Reviews 7:850-859

Hohmann, C.F., Berger-Sweeney, J. (1998) Cholinergic regulation of cortical development and plasticity. New twists to an old story. Perspect Dev Neurobiol 5:401-425

Hutsler, J., & Zhang, H. (2010). Increased dendritic spine densities on cortical projection neurons in autism spectrum disorders. Brain Research , 1309: 83-94.

Impagnatiello, F., Guidotti, A. R., Pescold, C., Dwivedi, Y., Caruncho, H., Pisu, M. G., Uzunov, D. P., Smalheier, N. R., Davis, J. M., Pandey, G. N., Pappas, G. D., Tueting, P., Sharma, R. P., Costa, E. (1998) A decrease of reelin expression as a putative vulnerability factor in schizophrenia. Proc. Natl. Acad. Sci. USA 95:15718-15723

Ito, M. (2001) Cerebellar long-term derpression: Characterization, signal transduction, and functional roles. Physio. Reviews 81:1143-195

Kemper, T.L., Bauman, M.L. (1993) The contribution of neuropathological studies to the understanding of autism. Neurol Clin. 11:175-187

Keller, F., and Persico, A. M. (2003). The neurobiological context of autism. Mol. Neurobiol. 28:1-22.

Laviola, G., Adriani, W., Gaudino, C., Marino, R., and Keller, F. (2006). Paradoxical effects of prenatal acetylcholinesterase blockade on neuro-behavioral development and drug-induced sterotypies in reeler mutant mice. Psychopharmacology 187: 331-344.

Lee, M., Marin-Ruiz, C., Graham, A., Court, J., Jaros, E., Perry, R. (2002). Nicotinic receptor abnormalities in the cerebellar cortex in autism. Brain 125:1483-1495

Liu, W., Pappas, G., & Carter, C. (2005). Oxytocin receptors in brain cortical regions are reduced in haploinsufficient (+/-) reeler mice. Neurol Res , 24:339-45.

Maloney, S., Rieger, M., & Dougherty, J. (2013). Identifying Essential Cell Types and Circuits in Autism Spectrum Disorders. Rev Neurobiol , 113: 61-96.

Mullen, B., Khialeeva, E., Hoffman, D., Ghiani, C., & Carpenter, E. (2013). Decreased reelin expression and organophosphate pesticide exposure alters mouse behaviour and brain morphology. ASN NEURO 5: 27-42.

Niu, S., Yabut, O., and D'Arcangelo, G. (2008). The reelin signaling pathway promotes dendritic spine development in hippocampal neurons. J. Neurosci. 28: 10339-10348.

Palmen, S.J.M.C., van Engeland, H., Hof, P.R., Schmitz (2004) Neuropathological findings in autism. Brain 127: 2572-2583

Penzes, P., Cahill, M., Jones, K., Van Leeuwen, J., & Woolfrey, K. (2011). Dendritic spine pathology in neuropsychiatric disorders. Nature Neurosci , 14:285-93.

Perry, E.K., Lee, M.L., Martin-Ruiz, C.M., Court, J.A., Volsen, S.G., Merrit, J., Folly, E., Iversen, P.E., Bauman, M.L., Perry, R.H., Wenk, G.L. (2001) Cholinergic activity in autism: abnormalities in the cerebtal cortex and basal forebrain. Am J Psychiatry 158:1058-1066

Persico, A. M., and Bourgeron, T. (2006). Searching for ways out of the autism maze: genetic, epigenetic, and environmental clues. Trends Neurosci. 29: 349-358.

Romano, E., Fuso, A., & Laviola, G. (2013). Nicotine Restores Wt-Like Levels of Reelin and GAD67 Gene Expression in Brain of Heterozygous Reeler Mice. Neurotox Res , 24: 205-15.

Salinger, W. L., Ladrow, P., Wheeler, C. (2003) Behavioral phenotype of the reeler mutant mouse: Effects of reln gene dosage and social isolation. Behav. Neurosci. 117:1257-1275

Schmahmann, J. D. (2013) Cerebellar cognitive affective syndrome and the neuropsychiatry of the cerebellum. In Manto, M., Schmahmann, J.D., Rossi, F., Gruol, D.L., Kiobuchi, N. (Ed.) Handbook of the cerebellum and cerebellar disorders. pp 1717-1751, New York, NY: Springer

Selemon, L.D., Goldman-Rakic, P.S. (1999) The reduced neuropil hypothesis: a circuit based model fo schizophrenia. Biol. Psychiatry 45:17-25

Shelton, J.F., Geraghty, E.M., Tancredi, D.J., Delwiche, L.D., Schmidt, R.J., Ritz, B., Hansesn, R.L., Hertz-Picciotto, I. (2014) Neurodevelopmental disorders and prenatal residential proximity to agricultural pesticides: the CHARGE study. Envrion Health Perspect 122:1103-1109

Shelton, J.F., Hertz-Picciotto, I., Pessah, I.N. (2012). Tipping the balance of Autism risk:

Potential mechanisms linking pesticides and autism. Environ Health Perspective 120: 994-951

Stoodley, C. J., Valera, E. M., Schmanhmann, J. D. (2012) Functional topography of the cerebellum for motor and cognitive tasks: An fMRI study. NeuroImage 59:1560-1570

Weeber, E. J., Beffert, U., Jones, C., Christian, J. M., Förster, E., Sweatt, J. D., Herz, J. (2002) Reelin and ApoE receptor cooperate to enhance hippocampal synaptic platicity and learning. J. Bio. Chem. 277:39944-39952

Ziv, N.E., Smith, S.J. Evidence for a role of dendritic filopodial in synaptogenesis and spine formation. Neuron 17:91-102